Direct Reprogramming of distinct cells into GABAergic motor neurons in *C. elegans*

Dissertation
zur Erlangung des akademischen Grades

Doctor rerum naturalium
(Dr. rer. nat.)

eingereicht an der
Lebenswissenschaftlichen Fakultät der Humboldt-Universität zu Berlin

von
Marlon Kazmierczak, M. Sc. Neurobiolgie und Verhalten

Präsidentin der Humboldt-Universität zu Berlin
Prof. Dr.-Ing. Dr. Sabine Kunst
Dekan der Lebenswissenschaftlichen Fakultät der Humboldt-Universität zu Berlin
Prof. Dr. Bernhard Grimm

Gutachter/innen:	Prof. Dr. Thomas Sommer
	Dr. Baris Tursun
	Prof. Dr. Ann Ehrenhofer-Murray
Tag der mündlichen Prüfung:	13. 12. 2018

Abstract

The knock down of genes by RNAi has been fundamental to identify inhibitors of induced cell transdifferentiation in *C. elegans* (Tursun et al., 2011). Bacteria strains expressing dsRNA that target specific genes can be fed to the worm allowing straightforward whole-genome RNAi screens of the 20,000 genes in the *C. elegans* genome. However, many biological processes are regulated by more than one gene raising the need for simultaneous knock down of two or more genes to more fully interrogate the regulation of complex biological processes Two approaches are currently available for double RNAi knockdown, – two bacteria strains expressing specific dsRNA can be mixed and grown together and fed simultaneously. Alternatively, a new bacterial clone can be generated carrying a plasmid on which two RNAi targets of interest are ′stitched′ together. We found that the results of double RNAi by mixing bacteria are highly variable. In contrast, the second approach of using stitched RNAi clones yield a high reproducibility of knockdown efficiency, but it is for obvious reasons not suitable for a whole-genome approach since it would require generating 20,000 new plasmids containing both targets on the same construct.

To address this challenge, we have developed a protocol using bacterial conjugation mediated by the ′Fertility Factor′ (F) Episome in order to combine two different RNAi plasmids in a single bacterium. The objective was to be able to transfer a single RNAi plasmid to a large number of bacterial cells carrying different RNAi clones in one step in a high-throughput manner for large scale ′double′ or even ′triple′ RNAi screens. To find enhancers of induced *unc-25::gfp* expression in the germ line enabled by the depletion of histone chaperone LIN-53 (RbAp46/48 in humans), double RNAi clones targeting *lin-53* and a total of 800 chromatin-related genes were generated and screened. We identified the Set1/MLL methyltransferase complex member RBBP-5 as a novel reprogramming barrier that putatively acts in a parallel pathway to LIN-53.

Double RNAi by conjugation permits to reliably knock down two genes simultaneously in order to study genetic interactions at a genome-wide level, thus further increasing the versatility of RNAi screens to investigate interconnected biological processes.

Zusammenfassung

Der Gen-Knock-down mittels RNAi hat sich als essentiel erwiesen, um Inhibitoren der induzierten Transdifferenzierung in *C. elegans* zu identifizieren (Tursun et al., 2011). Bakterienstämme, die dsRNA exprimieren, das die Expression spezifischer Gene mindert, können dem Wurm direkt zugefüttert werden, um einen genomweiten RNAi-screen der insgesamt 20.000 Gene in *C. elegans* durchzuführen. Allerdings werden die meisten biologischen Prozesse durch mehr als ein Gen reguliert, was den Bedarf nach einer Methode generiert, die es erlaubt, zwei oder mehr Gene gleichzeitig runter zu regulieren, um die Steuerung biologischer Prozesse studieren zu können. Derzeit gibt es zwei mögliche Herangehensweisen: Zwei verschiedene Bakterienstämme können vermischt und gleichzeitig an den Wurm verfüttert werden. Wir erzielten damit schlecht reproduzierbare Resultate. Alternativ kann ein neues Plasmid generiert werden, dass die Zielsequenzen zweier verschiedener Gene enthält. Der doppelte Gen-Knockdown damit ist sehr zuverlässig. Allerdings ist die Generierung dieser Plasmide zeitaufwendig und arbeitsintensiv und deshalb wenig geeignet, um genomweite Studien durchzuführen.
Um eine Methode zu entwickeln, die sowohl reproduzierbare Ergebnisse liefert als auch skalierbar ist, nutzen wir die bakterielle Konjugation, ermöglicht durch ein konjugatives Plasmid, um Bakterienzellen zu generieren, die zwei verschiedene RNAi-Plasmide enthalten. Das Ziel war es, modifiziere RNAi–Donor-Plasmide mittels bakterieller Konjugation an eine Vielzahl anderer Bakterienzellen zu übertragen, die bereits ein anderes RNAi-Plasmid enthalten und dies dann skalierbar im Hochdurchsatzverfahren durchführen zu können.
Um Enhancer induzierter Expression von *unc-25::gfp* in der Keimbahn, ermöglicht durch Knockdown des Histonchaperons LIN-53 (RbAp46/48 in Menschen), zu finden, wurden RNAi-Klone generiert, die gleichzeitig *lin-53* als auch eines von insgesamt 800 verschiedenen Chromatin-bezogenen Gene runter regulieren. Dabei identifizierten wir RBBP-5, Mitglied des Set1/MLL-Methyltransferase-Komplexes, als neuen Barrierefaktor zur induzierten Transdifferenzierung. RBBP-5 agiert dabei mutmaßlich parallel zu LIN-53.
Doppelte RNAi, ermöglicht durch bakterielle Konjugation, erlaubt den simultanen Knockdown zweier Gene, um genetische Interaktionen zu studieren und erweitert damit die Einsatzfähighkeit von RNAi-Screens, um untereinander verbundene biologische Prozesse zu studieren.

Contents

1. Introduction **1**

1.1. Cellular Reprogramming . . . 1
1.1.1. Reprogramming in general . . . 1
1.1.1.1. Induced pluripotent stem cells *in vitro* . . . 2
1.1.1.2. Direct reprogramming (transdifferentiation) . . . 3
1.1.2. The model system *C. elegans* . . . 4
1.1.2.1. Screens for cellular reprogramming in *C. elegans* . . . 5
1.1.2.2. Natural direct reprogramming . . . 5
1.1.2.2.1. The role of transcription factors in direct reprogramming . . . 7
1.1.2.3. ELT-7-induced reprogramming of gonad and pharyngeal cells into intestine-like cells . . . 8
1.1.2.4. Barrier factors to cell fate conversion . . . 9
1.2. Identifying Barrier Factors . . . 10
1.2.1. Identification of cell fate barriers *in vitro* . . . 10
1.2.2. RNAi-based genetic screens *in vivo* . . . 11
1.2.3. Multiple components required for Reprogramming . . . 12
1.2.3.1. Current methods for combinatorial RNAi screens *in vitro* and *in vivo* . . . 13
1.2.4. Other depletion methods . . . 14
1.2.4.1. Classical genetic screens . . . 14
1.2.4.2. CRISPR/Cas . . . 15
1.3. Aim of the study . . . 15

2. Results **17**

2.1. Part 1: MRG-1 and HSP-1 are reprogramming barriers . . . 17
2.1.1. MRG-1 is a safeguarding barrier protecting the germ line cell fate . . . 17
2.1.1.1. MRG-1 also barrier factor to GABAergic terminal transcription factor UNC-30 . . . 19
2.1.1.2. MRG-1 co-localizes only partly with LIN-53 . . . 19
2.1.1.3. Global histone modifications affected by knockdown of *mrg-1* . . . 21
2.1.2. HSP-1 is a barrier factor to the induction ASE neuron reporter *gcy-5* in epidermis . . . 22
2.1.2.1. Knockdown of *hsp-1* permits induction of intestine reporter *elt-2* but not GABA reporter *unc-25* . . . 23

2.1.2.2. *hsp-1* genetically interacts with *ogt-1* 23
2.1.2.3. HSP-1 interacts with histone acetyltransferase complex NSL 24
2.2. Part 2: : Double RNAi by bacterial conjugation 27
2.2.1. The principle of double RNAi by conjugation 27
2.2.2. The components of double RNAi by conjugation 28
2.2.3. Establishing the conjugation protocol 30
2.2.3.1. No conjugation using cultures at stationary growth phase in liquid medium 30
2.2.3.1.1. Conjugation successful on solid medium 30
2.2.3.1.2. No conjugation using cultures at exponential growth phase in liquid medium 32
2.2.3.2. On solid medium conjugative plasmid transfer at low efficiency 34
2.2.3.3. Conjugation efficiency slightly improved by using *E. coli* donor host strain HT115 34
2.2.3.4. Conjugation efficiency not improved at lower exponential growth phase and reduced concentration of antibiotics . . 35
2.2.3.5. Higher decrease of antibiotic concentration does not increase the succession rate of conjugation 36
2.2.3.6. An overabundance of donor cells improves conjugation efficiency 37
2.2.3.7. Addition of antibiotics diminishes conjugation success rate 37
2.2.3.8. No increase of conjugation efficiency upon dilution when using higher amount of donor cells 39
2.2.3.9. Functionality of conjugative F-plasmid not impaired by modification 40
2.2.3.10. Recombination deficient donor strain improves conjugation efficiency at different growth phases 41
2.2.3.11. Overnight cultures of donor and recipient strains adequate for conjugation 42
2.2.3.12. Conjugation success rate is not affected by growth phase 42
2.2.3.13. Translation of double RNAi by conjugation protocol to high-throughput approach 43
2.2.4. Proof-of-principle experiments 45
2.2.4.1. Proof-of-concept: Synthetic lethality 45
2.2.4.2. Proof-of-concept: Arrested oocyte maturation 46
2.2.4.3. Proof-of-concept: Induction of ectopical expression of pan-neuronal reporter 46
2.2.4.4. Proof-of-concept: Induced synthetic multivulva 49
2.2.5. Performing enhancer screen for *lin-53* RNAi mediated *unc-25::gfp* induction in germ line 50
2.2.5.1. Co-knockdown of *rbbp-5* and *lin-53* leads to increased expression rate of *unc-25::gfp* in germ line 50

2.2.5.2. *unc-25::gfp* positive germ cells also express Rab3a-interacting protein (RIM) . . . 53
2.2.6. Co-depletion of LIN-53 and members of the COMPASS complex does not increase reprogramming efficiency . . . 55
2.2.7. Triple RNAi by conjugation identifies no enhancer of *lin-53*; *rbbp-5* RNAi mediated induction of *unc-25::gfp* in the germ line . . . 57

3. Discussion **59**
3.1. Double RNAi allows investigation of genetic interactions of essential genes in large scale screens . . . 59
3.2. Establishment of double RNAi by conjugation . . . 60
3.2.1. Bacterial conjugation can occur at different stages of bacterial growth 60
3.2.2. Stable bacterial host strain EPI300 is crucial for reliable conjugation success rate . . . 60
3.2.3. Conjugation success rate unaffected by antibiotics in growth medium 61
3.2.4. Double RNAi bacteria able to deplete two genes simultaneously . . 61
3.3. Limitations of double RNAi by conjugation . . . 62
3.4. Double RNAi permits to study genetic interactions of essential genes in large-scale screens . . . 64
3.5. Simultaneous knockdown of *lin-53* and *rbbp-5* increases *unc-25::gfp* induction efficiency . . . 65
3.5.1. Converted germ cells start to express Rab3a-interacting protein (RIM) . . . 65
3.5.2. *lin-53* does not interact with the Set1/MLL methyltransferase complex . . . 66
3.5.3. *lin-53* and *rbbp-5* do not have common genetic interaction partners 66
3.5.4. *lin-53* and *rbbp-5* act in parallel pathways . . . 67
3.5.5. Low hit rate of RNAi enhancer screen potentially due to focus on chromatin-related genes . . . 68
3.6. MRG-1 is a barrier factor to UNC-30 induced direct reprogramming . . . 68
3.7. Depletion of HSP-1 is insufficient for UNC-30 to induce *unc-25::gfp* in the epidermis . . . 70
3.8. Transcription factor specificity of barrier factors HSP-1 and MRG-1 . . . 71
3.9. Outlook - testing results from iPSC studies in *C. elegans in vivo* . . . 72

4. Material and Methods **74**
4.1. Material . . . 74
4.1.1. Antibiotics . . . 74
4.1.2. Antibiodies . . . 74
4.1.3. Buffers, solutions, and media . . . 75
4.1.4. Bacterial strains . . . 77
4.1.5. *Caenorhabditic elegans* strains . . . 77
4.1.6. Enzymes . . . 78
4.1.7. Equipment . . . 78

4.1.8. Kits . . . 79
4.1.9. Plasmids . . . 79
4.1.10. Primers . . . 80
4.1.11. RNAi clones . . . 84
4.2. Methods . . . 85
4.2.1. Preparation of Plates . . . 85
4.2.1.1. Preparation of Nematode Growth Medium (NGM) Plates seeded with OP50 bacteria . . . 85
4.2.1.2. Preparation of 6-well RNAi plates seeded with RNAi bacteria . . . 85
4.2.2. Worm specific methods . . . 85
4.2.2.1. Maintenance and storage of *C. elegans* . . . 85
4.2.2.2. Worm lysis . . . 86
4.2.2.3. Harvesting worms . . . 86
4.2.2.4. Synchronizing worms . . . 86
4.2.2.5. Freezing worms for long term storage . . . 87
4.2.2.6. Transgenic crosses . . . 87
4.2.2.7. Genotyping . . . 87
4.2.2.8. Antibody stainings . . . 88
4.2.2.8.1. Antibody staining by reduction and oxidation method . . . 88
4.2.2.8.2. Antibody staining using slide crack method . . . 88
4.2.3. Molecular Biology Methods . . . 88
4.2.3.1. Polymerase Chain Reaction (PCR) . . . 88
4.2.3.1.1. NEB Taq Polymerase PCR (colony PCR) . . . 88
4.2.3.1.2. NEB Q5 Polymerase PCR (cloning) . . . 89
4.2.3.2. Colony PCR . . . 89
4.2.3.3. Gel electrophoresis . . . 89
4.2.3.4. DNA purification/Gel extraction . . . 90
4.2.3.5. Molecular cloning . . . 90
4.2.3.5.1. Cloning using Restriction Enzymes . . . 90
4.2.3.5.2. Gibson Cloning . . . 90
4.2.3.6. Transformation in *Escherichia coli* . . . 90
4.2.3.6.1. Chemical transformation . . . 91
4.2.3.6.2. Electroporation . . . 91
4.2.3.7. Plasmid isolation from *Escherichia coli* . . . 92
4.2.3.8. Bacterial Recombination . . . 92
4.2.4. Protein biochemical work . . . 92
4.2.4.1. SDS-page . . . 92
4.2.4.1.1. Preparation of polyacrylamid gels . . . 93
4.2.4.1.2. Electrophoresis . . . 93
4.2.4.2. Western blotting . . . 93
4.2.4.2.1. Wet transfer of proteins and blocking of membrane 94
4.2.4.2.2. Immunological detection . . . 94

4.2.5. RNAi interference 94
4.2.5.1. P0 RNAi-screen 95
4.2.5.2. F1 RNAi-screen 95
4.2.5.3. Fluorescent Microscopy 95

A. Appendix **113**

List of Tables

2.1. Conserved components of the COMPASS complex in *C. elegans*, yeast, and human. . . . 55
2.2. Known genetic interactors of *lin-53* and *rbbp-5* . . . 57

4.1. Used antibiotics . . . 74
4.2. Used antibodies . . . 74
4.3. Used buffers, solutions and media and their composition. . . . 75
4.4. Used bacterial strains . . . 77
4.5. *C. elegans* strains . . . 77
4.6. Used enzymes . . . 78
4.7. Used Equipment . . . 78
4.8. Used kits . . . 79
4.9. Used Plasmids . . . 80
4.10. Usesd Primers . . . 80
4.11. RNAi clones. Descriptions taken from wormbase.org . . . 84
4.15. Preparing SDS gels . . . 93

A.1. Conjugation in liquid medium in small tubes . . . 114
A.2. Conjugation in liquid medium in large tubes . . . 115
A.3. Confirmation of functionality of donor strain SW105(pRK24-kan; *hsp-1*) on solid medium . . . 115
A.4. Conjugation in liquid medium with donor and recipient strains at exponential growth phase . . . 116
A.5. Conjugation in liquid medium at higher total volume . . . 117
A.6. Conjugation on solid medium at late exponential phase . . . 118
A.7. Comparison of donor host strains HT115 vs SW105 . . . 118
A.8. Conjugation on solid LB agar with diluted mixtures . . . 119
A.9. Conjugation at higher dilutions . . . 119
A.10. Conjugation at different ratios of donor and recipient . . . 119
A.11. Conjugation on selective plates . . . 120
A.12. Increased dilution conjugation does not increase conjugation success rate . 120
A.13. Testing of proper function of F-plasmid in different donor strains. . . . 121
A.14. Conjugation of newly generated donor strain at different growth phases . . 121
A.15. Conjugation of overnight cultures . . . 121
A.16. Growth phase does not affect conjugation efficiency . . . 122
A.17. Optimization of conjugation in 96-well format . . . 122

List of Figures

1.1. Waddington's epinetic landscape . . . 1
1.2. Biomedical perspectives on direct reprogramming . . . 2
1.3. Two approaches to cell fate conversion . . . 3
1.4. Examples of direct reprogramming . . . 4
1.5. Life cycle of *C. elegans* . . . 5
1.6. Different tissues in *C. elegans* . . . 6
1.7. RNAi by feeding in *C. elegans* . . . 12
1.8. Double RNAi methods . . . 14
1.9. Generation of bacterial carrying two different RNAi plasmids by bacterial conjugation . . . 16

2.1. RNAi against *mrg-1* permits ectopic expression of *gcy-5::gfp* in the germ line . . . 18
2.2. Ectopic expresson in *mrg-1* (RNAi) animals overexpressing *unc-30* . . . 20
2.3. Immunostaining of wild-type young adult hermaphrodite with anti-MRG-1 and anti-LIN-53 antibody . . . 21
2.4. *mrg-1* RNAi-mediated changes of histone H3 modifications . . . 22
2.5. *hsp-1* RNAi-mediated ectopic induction of *elt-2::gfp* enhanced in *ogt-1* (ok430) mutant background . . . 23
2.6. *hsp-1* genetically interacts with the histone actetyltransferase complex NSL 25
2.7. Modification of Histone H4 acetylation in RNAi or *ogt-1* mutant background 26
2.8. Principle of double RNAi by conjugation . . . 27
2.9. Components of double RNAi by conjugation . . . 29
2.10. Conjugation in liquid medium without wash step . . . 31
2.11. Confirmation of functionality of donor strain SW105(pRK24-kan; *hsp-1*) on solid medium . . . 32
2.12. No conjugation in liquid medium at higher mating mixture volumes . . . 33
2.13. Conjugation on solid medium at late exponential phase at low efficiency . 34
2.14. Donor *E. coli* strain HT115 more efficient than donor strain SW105 . . . 35
2.15. Conjugation success rate not imrpoved of of donor and recipient cultures grown until exponential phase . . . 36
2.16. Conjugation success rate unaffected by reduced concentration of antibiotics 36
2.17. Overabundance of donor cells increases conjugation efficiency . . . 37
2.18. Addition of antibiotics to solid LB agar inhibits conjugation . . . 38
2.19. Reduced concentration of antibiotics does not increase conjugation success rate . . . 39

2.20. Modified F-plasmid pRK24-kan functional. 40
2.21. Improved conjugation using recombination deficient new donor strain EPI300 41
2.22. Conjugation efficiency unaffected by the usage of overnight cultures 42
2.23. Bacterial growth phase does not affect conjugation efficiency 43
2.24. Reduction of mating mixture volume increases conjugation efficiency in 96-well format 44
2.25. Double RNAi by conjugation against *rpn-10* and *rpn-12* leads to synthetic lethality 45
2.26. Arrested ooycyte development in *oma-1; oma-2* (RNAi) animals 47
2.27. Ectopic expression of pan-neuronal reporter *rab-3::tRFP* in the germ line in *gld-1; mex-3* (RNAi animals) 48
2.28. Combinatorial RNAi insufficient to inuduce SynMuv phenotype 49
2.29. Enhancer screen for *lin-53* RNAi-mediated ectopic induction of *unc-25::gfp* in the germ line 51
2.30. Results of chromatin library screen 52
2.31. Germ cells positive for *unc-25::gfp* also express active zone protein RIM . 54
2.32. *lin-53* does not genetically interact with members of the COMPASS complex 56
2.33. No identified enhancer of ectopic induction of *unc-25::gfp* in *lin-53*; *rbbp-5* (RNAi) animals 58

3.1. Modes of genetic interactions 63
3.2. *lin-53* and *rbbp-5* act in parallel pathways 67

4.1. Gibson Assembly Workflow 91

List of Abbreviations

Amp	Ampicillin
ANOVA	Analysis of variance
ASE	Amphid neurons (single celiated endings)
AWC	Amphid wing 'C' cells (sensory neurons)
bag-1	BAG1 (human) homolog, BAG family molecular chaperone regulator 1
BAT	Baris Tursun
bp	base pairs
BSA	Bovine serum albumin
°C	degrees Celsius
C52E2.4	C. elegans gene
C. elegans	*Caenorhabditis elegans*
C/EBP	Enhancer binding proteins, interact with the CCAAT box motif
Carb	Carbenicillin
Cam	Chloramphenicol
CGC	Caenorhabditis Genetics Center
che-1	abnormal CHEmotaxis
chp-1	CHORD protein, encodes a protein containing two CHORD domains
c-Myc	Myelocytomatosis viral oncogene homolog, encodes a nuclear phosphoprotein
DAPI	4,6-Diamidino-2-phenylindole
dBT	DNA Baris Tursun
ddH_2O	double distillied water
DNA	Deoxyribonucleic acid
dNTP	Desoxyribonukleosidtriphosphate
dsRNA	double stranded RNA
E. coli	Escherichia coli
EDTA	Ethylendiamintetraacetic acid
F1 generation	Filial 1 hybrid, first filial generation of offspring of distinctly different parental types
FWD	forward
g	gram
GABA	*gamma*-Aminobutyric acid
gcy-5	encodes a predicted guanylate cyclase
GFP	Green fluorescent protein

h	hour
H3	Histone 3
H3K4	Histone 3 Histone 3 Lysine (K) 4
H3K27	Histone 3 Lysine (K) 27
H3K9me3/ac	Histone 3 Lysine (K) 9 trimethylation/acetylation
H3K4me3	Histone 3 Lysine (K) 4 trimethylation
H4	histone 4
HAT	Histone acetyltransferase
H_20	water
hs	heat shock
hsp	heat shock promoter
HT115	competent E. coli strain
iPSC	induced pluripotent stem cells
IPTG	Isopropyl β-D-1-thiogalactopyranoside
Kan	Kanamycin
kV	kilovolt
l	liter
L1	larval stage 1
L4440	plasmid from Dr. A. FireâĂŹs lab
LB-Medium	Luria-Bertani-Medium
lin-53	lineage abnormal; histone-chaperone interacting with several epigenetic regulators in different tissues
M	Molar
MACH1	competent E. coli strain
mg	milligram
ml	milliliter
Âţg	microgram
µl	microliter
N2	wild type worms
NEB	New England Biolabs
NGM	Nematode growth medium
O/N	over night
oBT	oligo Baris Tursun
OP50	uracil auxotroph E. coli strain
P0	Parent generation
PBS	Phosphate buffered saline
PCR	Polymerase chain reaction
PRC2	Polycomb repressive complex 2
RE	Restriction enzyme
REV	reverse
RFP	Red fluorescent protein
RNA	Ribonucleic acid
RNAi	RNA interference

rpm	Revolutions per minute
RT	Room temperature
SDS	Sodium dodecyl sulfate
SDS-PAGE	SDS-polyacrylamide gel electrophoresis SEM
Standard error of the mean	
siRNA	small interfering RNA
TAE	Tris Acetat EDTA
Tet	Tetracycline
TF	Transcription factor
Tris	Tris (hydroxymethyl)-aminomethan
unc-25	UNCoordinated, encodes the C. elegans ortholog of the GABA neurotransmitter biosynthetic enzyme, glutamic acid decarboxylase
unc-30	UNCoordinated, encodes a homeodomain-containing protein that is orthologous to the Pitx family of homeodomain transcription factors
WT	wild type
µg	microgram
µm	micrometer

1. Introduction

1.1. Cellular Reprogramming

1.1.1. Reprogramming in general

In metazoan development only the zygote possesses totipotency and therefore has the capacity to form an entire organism. Beginning with the first series of zygotic divisions, totipotency is being gradually lost. Thus, the cellular capacity of cells to adapt to diverse cell fates is restricted and cells become specified for a particular cell type.

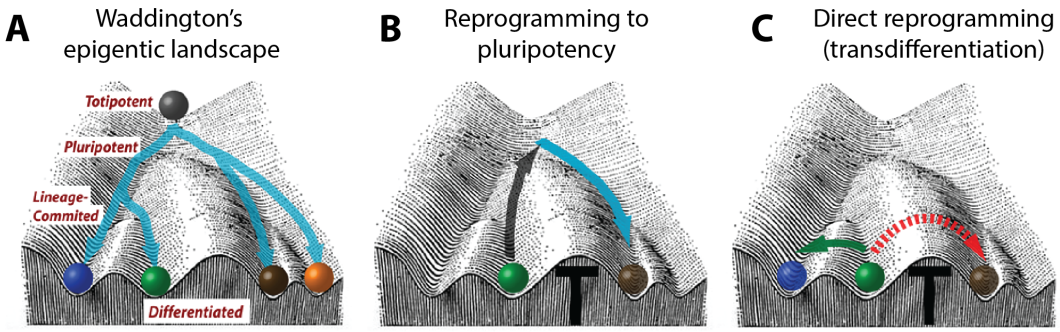

Figure 1.1.: **Waddington's epigenetic landscape and cell-fate conversion.** (A) During normal development beginning from a totipotent zygote, cells differentiate first to a pluripotent and later to a differentiated state while losing their cell fate potential. (B) Differentiated cells can be converted back into a pluripotent state from which they can be driven into a new cell type. (C) Cells can directly transdifferentiate into another cell fate without passing through a pluripotent state.

Originally it was assumed that the specified cell fate could not be altered as imagined by Waddington in his epigenetic landscapes (Waddington, 1957). However, by expression of cell-fate inducing transcription factors direct reprogramming can be induced in a permissive environment (Hanna et al., 2010). Humans possess adult stem cells that allow to regenerate most tissues such as the epithelium, while others such as neurons cannot be replaced. Diseases such as blindness caused by photoreceptor degeneration (Jayakody et al., 2015), Parkinson's caused by loss of dopaminergic neurons in certain parts of the midbrain (Jellinger, Bancher, 1998) or dysfunction of different kinds of neurons in selective areas of the brain leading to Alzheimer's disease (Jenner, Olanow, 1998) are all examples of diseases or permanent impairment due to damage of neuronal tissue .
Reprogramming of cells allows to model diseases, perform drug screening, and possibly

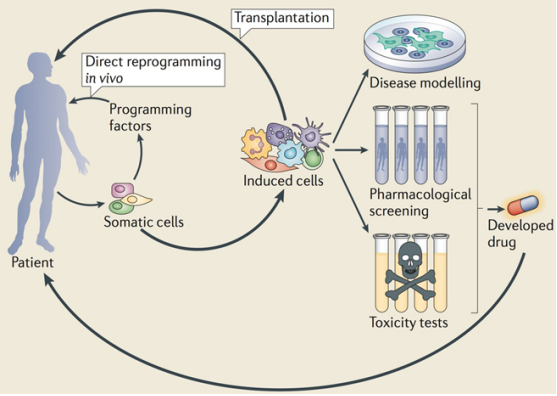

Figure 1.2.: **Biomedical perspectives on direct reprogramming.** Direct reprogramming could allow to replace non-regenerating cells, perform patient-specific disease modeling, drug screening etc. Modified from Ladewig et al. (2013)

replace dead neurons via conversion of neighboring astrocytes (reviewed in Gascón et al. (2017).

1.1.1.1. Induced pluripotent stem cells *in vitro*

Already in the 1960s fully differentiated cells could be converted back to an embryonic stem cell-like state by transplanting the nucleus of *Xenopus laevis* cells into an endonucleated oocyte, which then gave rise to a new organism (Gurdon, 1962). Gurdon (1962) could show that during nuclear transplantation the epigenome of a fully differentiated cell is completely reseted. This landmark study gave rise to a new era of experiments which culminated in the cloning of the sheep Dolly in 1997, demonstrating that erasing of the epigenetic information and reprogramming of a somatic cell is also possible in mammals (Wilmut et al., 1997).
Takahashi, Yamanaka (2006) showed that overexpressing four stem cell specific transcription factors, namely the octamer-binding transcription factor 4 (OCT4), sex determining region Y box 2 (SOX2). Krüppel-like factor (KLF4), and the avian myelocytomatosis viral oncogene homolog (c-MYC), is sufficient to induce reprogramming of mouse fibroblasts into induced pluripotent stem cells (iPSCs). Similar to embryonic stem cells (ESCs), iPSCs are able to generate all three germ layers, germ cells, proliferate and show self-renewal, and form teratomas (Takahashi, Yamanaka, 2006; Park et al., 2008). Using a combination of Sox2 and Oct3/4 with Klf4 and c-Myc or in combination with Lin28 and Nanog, human fibroblasts could be reprogrammed into iPSCs (Yu et al., 2007; Park et al., 2008). New paths in regenerative medicine were opened upon discovery of the return of the nucleus to pluripotency and the isolation of ESCs from mouse embryos (Evans, Kaufman, 1981) and then by the generation of ESCs from human embryos (Thomson et al., 1998).

Through differentiation of iPSCs a large number of cells can be generated and then transplanted into patients. However, these reprogrammed cells possess the capacity to develop teratomas, if they did not fully differentiate before transplantation (Yoshida, Yamanaka, 2010; Nasu et al., 2013). The generation of iPSCs can modify the genome of reprogrammed cells, induce a variation of copy numbers, chromosomal rearrangements or

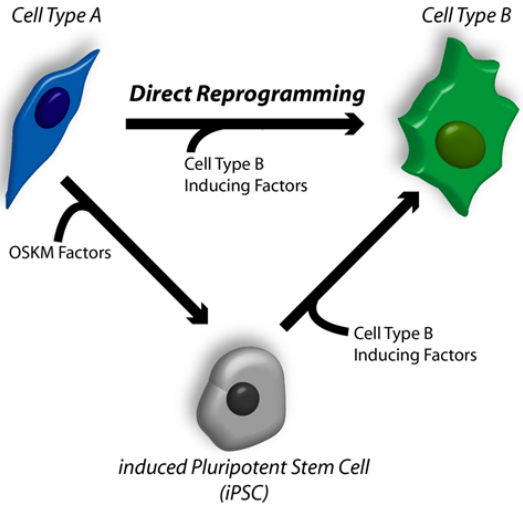

Figure 1.3.: **Two approaches to cell fate conversion** Indirect cellular reprogramming starts by overexpression of the OSKM factors to generate iPSCs by de-differentiation, followed by overexpression of a cell-fate inducing transcription factor. Direct reprogramming omits de-differentiation and the cell is directly converted into another cell type. OSKM factors: Oct3/4, Sox2, Klf4, and c-Myc. Picture: Tursun lab.

aberrant epigenetic signatures (Gore et al., 2011; Hussein et al., 2011; Pasi et al., 2011). To avoid the risk of teratoma formation, direct reprogramming could be an alternative for regenerative medicine.

1.1.1.2. Direct reprogramming (transdifferentiation)

Direct reprogramming describes the conversion of one cell type into another without passing through the stem or progenitor state. The overexpression of tissue-specific master or terminal regulator can be sufficient to induce cell fate conversion in a permissive environment. In 1987 Davis and his colleagues could show that upon overexpression of the muscle-specific master regulator MyoD fibroblasts could be transdifferentiated into muscle cells (Davis et al., 1987). Later it was demonstrated that B cells can be converted into macrophages by overexpressing C/EBPα or C/EBPβ (Xie et al., 2004) or cardiac fibroblasts into beating cardiomyocytes by overexpressing three factors, Tbx5, Mef2c, and Gata4 (Ieda et al., 2010).

Fig. 1.4 shows that direct reprogramming can be achieved even across different germ layers as demonstrated when murine fibroblasts (mesoderm) were converted into functional neurons (ectoderm)(Vierbuchen et al., 2010). It is important to note though that direct reprogramming is restricted by context, that is, whether the overexpression of a given transcription factor is sufficient to induce transdifferentiation is dependent on the origin of the cell type and the cell plasticity. Fibroblasts are amenable to be reprogrammed by overexpression of MyoD, whereas other cell types might either not respond to ectopical expression of MyoD or with lower efficiency (Weintraub et al., 1989; Choi et al., 1990).

The medical application of direct reprogramming avoids the main pitfall of iPSC generated tissue: the possible formation of teratomas. *In vivo* direct reprogramming was demonstrated in mice, where upon expression of the required mix of transcription fac-

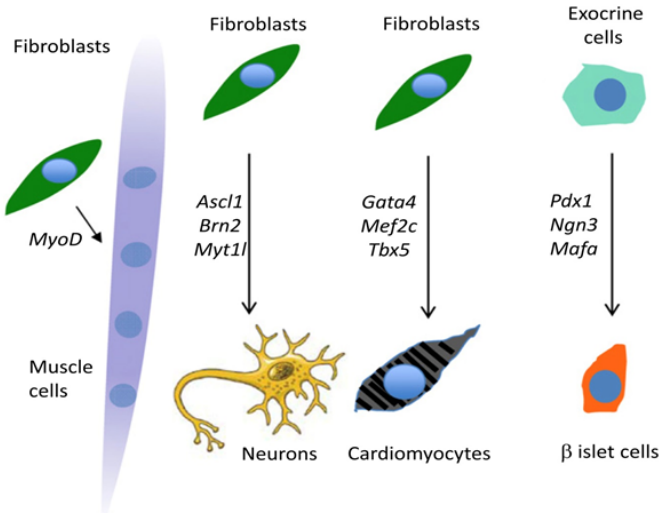

Figure 1.4.: **Examples of direct reprogramming** Direct reprogramming of fibroblasts into muscle cells (Davis et al., 1987), neurons (Vierbuchen et al., 2010), and cardiomyocytes (Ieda et al., 2010) *in vitro*. Zhou et al. (2008) showed the transdifferentiation of exocrine cells into insulin producing β islet cells *in vivo*.

tors exocrine cells could be converted into insulin-producing β islet cells (Ieda et al., 2010). However, our knowledge about the mechanisms that are responsible for cell fate conversion and the ones that restrict it are poorly understood. *C. elegans* is an ideal model organism to investigate direct reprogramming *in vivo* and help us to identify preventive mechanisms of cell fate conversion and thereby facilitate the application of direct reprogramming as a treatment method.

1.1.2. The model system *C. elegans*

C. elegans is perfectly suited for large-scale high-throughput genetic screens based on its size and the fact that it is self-maintaining. As adults worms reach about 1 millimeter in length and are found in two sexes: self-fertilizing hermaphrodites (XX) and males (X0). Hermaphrodites consist of exactly 959 cells, whereas males have 1,031 cells. Self-fertilizing hermaphrodites produce about 300 - 500 eggs of which only 0.1 - 0.2 % are males, arising from infrequent non-disjunction of the hermaphrodite's germ line (Ward, Carrel, 1979; Hodgkin, Doniach, 1997).
Sydney Brenner introduced *C. elegans* as a model organism for developmental biology originally in 1963 (Ankeny, 2001). One advantage for *C. elegans* as a model system is its short life span. Under optimal conditions the worm proceeds through all developmental stages within 3 days, including four larval stages (see fig. 1.5). A single worm, provided with sufficient amounts of food, lives two to three weeks. Under lab conditions, *E. coli* bacteria are fed to the worms. During starvation worms can go into the dauer stage and survive long periods of time. Additionally, worms can be frozen and stored for years.

Already in 1983 the complete cell lineage during embryogenesis and post-embryonic development had been mapped (Sulston, Horvitz, 1977; Kimble, Hirsh, 1979; Sulston et al., 1983), making *C. elegans* an excellent model organism to study cellular developmental biology. By 1998 the entire genome of *C. elegans* had been sequenced as the first

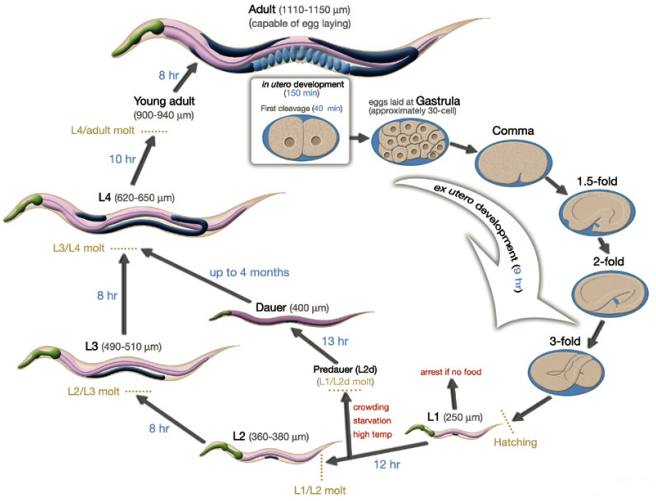

Figure 1.5.: **Life cycle of *C. elegans* at 22°C.** *C. elegans* passes within 3 days through four different larval stages (L1 to L4) and reaches adulthood. Under starvation worms can arrest at L1 or later become dauer larva at the L1/L2 molt as an alternative to survive long term stress conditions. Picture: http://www.wormatlas.org.

multicellular organism (*C. elegans* Sequencing Consortium 1998). The genome consists of five autosomal pairs of chromosomes and one pair of sex chromosomes (Hillier et al., 2005). Out of a total of 19,735 genes 40% of protein coding genes (Rubin et al., 2000; Hillier et al., 2005) and about 65% of disease associated genes have homologs within the human genome (Sonnhammer, Durbin, 1997). Additionally, molecular pathways implicated in human diseases such as Notch, Wnt, and insulin signaling are strongly conserved (Baumeister, Ge, 2002). Therefore *C. elegans* is an excellent model organism to investigate the function of genes related to pathways involved in epigenetics, aging, diseases, and cellular reprogramming.

1.1.2.1. Screens for cellular reprogramming in *C. elegans*

Despite its small size, *C. elegans* has several different types of tissues, such as epidermis, intestine, muscle, pharynx, and a complex nervous system consisting of 302 neurons that can be labeled with fluorescent proteins (see fig. 1.6). *C. elegans* has an invariant cell lineage and numerous cell types. The body of *C. elegans* is translucent throughout all its life stages, permitting to monitor morphological and molecular changes *in vivo* in the living animal by using differential interference contrast (DIC) microscopy or fluorescent microscopy to visualize proteins that were previously labeled with fluorescent reporter proteins such as Green Fluorescent Protein (Brenner, 1974; Chalfie et al., 1994).

1.1.2.2. Natural direct reprogramming

To identify and understand the mechanism of how barrier factor act against cell fate conversion it is crucial to increase efficiency and applicability of direct reprogramming. One approach to investigate barriers to transdifferentiation is to study natural events of cell fate conversion. The determined cell lineage (Sulston, Horvitz, 1977; Sulston et al., 1983) suggests that natural direct reprogramming occurs in *C. elegans* when the rectal cell 'Y' converts to a fully functioning motor neuron ('PDA'). Interestingly, no cell division is

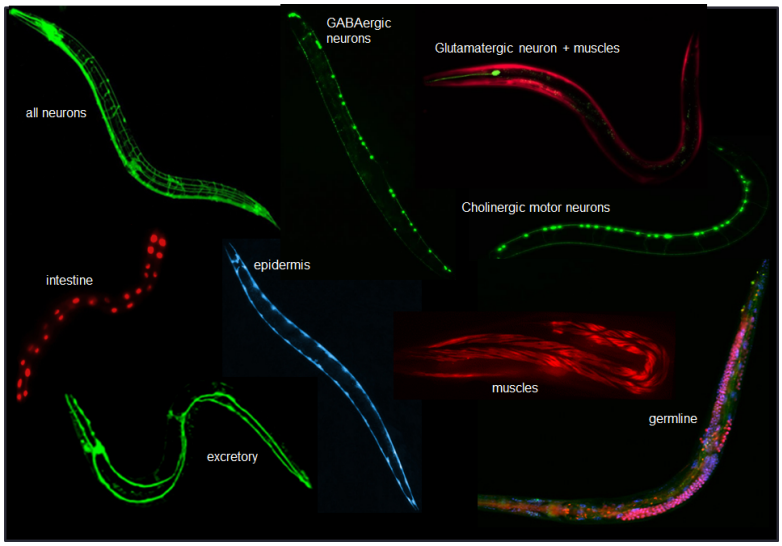

Figure 1.6.: **Different tissues in *C. elegans*.** *C. elegans* contains different tissues such as intestine, muscle, germ line, or GABAergic motor neurons that are labeled with fluorescence markers that allow to observe events of direct reprogramming *in vivo*. Picture: Tursun et al

required for the conversion of Y-to-PDA as it was shown by using live cell lineage tracing as well as DNA staining and quantification (Jarriault et al., 2008; Richard et al., 2011). Furthermore it could be demonstrated that the conversion of 'Y' to 'PDA' does not involve cell fusion or cell engulfment, and natural direct reprogramming is unaffected in mutant worms with defective engulfment or apoptosis machinery (Jarriault et al., 2008). By performing an EMS mutant screen 'Y' to 'PDA' conversion, Richard et al. (2011) identified a series of genetic mutations, which suggest that natural direct reprogramming occurs in multiple steps with no overlap of the original and the final cell fate.

Furthermore, none of the intermediaries can be converted into another identity by ectopic expression of cell fate inducing transcription factors that are able to induce conversion in early *C. elegans* blastomeres (Richard et al., 2011), indicating that de-differentiation does not necessarily coincide with a reversion into a pluripotent ground state or an increase of cellular potential. This reminds of the limb regeneration in axolotl, where regenerating cells that are produced from adult tissue do not de-differentiate into a pluripotent state, but instead possess a restricted potential, that is, in accordance with their tissue of origin (Kragl et al., 2009; T et al., 2014).
Thus, the natural direct reprogramming of Y into PDA has two distinct features: the identity change occurs in a stepwise process, in which first the initial identity is erased and only then the final identity is established without the reversion into a pluripotent ground state. In induced reprogramming events in mammals both of these features have been described and therefore appear to be conserved. For instance, no evidence for mixed identity intermediates was found when the C/EBPα-induced pre-B to macrophage cell conversion was analyzed using genome-wide transcriptomic data over a time course. Instead, first the transcriptomic program of the initial identity appears to be turned off before the program for the second identity was being turned on (Di Tullio et al., 2011). Additionally, no reversion to a pluripotent state was observed during transdifferentiation. This was also true when amniotic cells were converted into endothelial cells (Ginsberg

et al., 2015). Mutant studies further revealed that chromatin-modifying activities can promote Y-to-PDA direct reprogramming. Mutations affecting the H3K27 demethylase JMJD-3.1 and the SET1 complex with H3K4 methylase activity reduce the efficiency of conversion (Zuryn et al., 2014). Thus, it appears that their activity is crucial to ensure the deterministic Y-to-PDA conversion upon stress.

1.1.2.2.1. The role of transcription factors in direct reprogramming

A number of transcription factors are crucial to trigger direct cell fate conversion, either for directing cells towards a specific lineage or fate (Moody, 1998; Sindhu et al., 2012), or to maintain that fate over time (Holmberg, Perlmann, 2012; Deneris, Hobert, 2014). Transcription factors have a key role in the determination and expression of a specific cellular identity. Initially, studies *in vitro* demonstrated that the ectopic expression of GATA-1 (Kulessa et al., 1995), MyoD (Tapscott et al., 1988) or PPARγ plus C/EBPα (Hu et al., 1995) leads to cell type conversion. The Weintraub lab then showed that over-expression of the worm homologue of MyoD (*hlh-1*) in *C. elegans* embryo is sufficient to induce direct reprogramming of most cells in the embryo into muscle cells (Fukushige, Krause, 2005). Other studies in *C. elegans* have showed that upon ectopic expression of a single TF in blastomeres up unto the 8E stage is sufficient to convert the cell identity and that cells can adapt all three germ layers: UNC-30 (GABAergic neurons) (Jin et al., 1994), ELT-1 or ELT-3 (epidermis) (Gilleard, JD, 2001), END-1 (endoderm) (Zhu et al., 1998), ELT-2 (intestine) (Fukushige, Krause, 2005), PHA-4 (pharyngeal) (Kiefer et al., 2007; Horner et al., 1998) or LIN-26 (epithelial) (Quintin et al., 2001).
To initiate the conversion of Y cells *C. elegans* homologues of SOX2, OCT4 (CHE-6), SALL4 (SEM-4), and MTA1 (EGL-27) are crucial as mutations in either of these transcription factors repress the initiation of reprogramming. All these genes are expressed in the same rectal-epithelial cells. Co-immunoprecipitation experiments showed an association of SEM4/SALL4, OCT4/CEH-6, MTA1/EGL-27, and SOX2 (Kagias et al., 2012), suggesting that all these factors act through a multiproteic complex in the worm. These genes are not only conserved in mammals, but they also form the NODE complex (Liang et al., 2008). Interestingly, SOX2 and OCT4 are required as part of a cocktail of pluripotency inducing transcription factors to reprogram differentiated cells into iPSCs (Takahashi, Yamanaka, 2006) in mammals. In contrast to iPSC generation, Y cells lose their identity and pass through a de-differentiated state, in which the cells are not amenable to be reprogrammed into any other cell fate or gain pluripotency. Thus, the initial identity can be erased without reverting back to a pluripotent state. The conversion into a new cell type as well as the cellular potential are tightly regulated processes. Hence, the Y-to-PDA conversion in *C. elegans* is reminiscent of the lens regeneration of the newt. Cells from the pigmented iris that are de-differentiated express SOX2 early on, but convert only into lens cells, even if transplanted into another physiological environment (Maki et al., 2009; Bhavsar, Tsonis, 2014), suggesting that factors such as SOX2 either act as transcriptional repressors of the initial identity program or as transcriptional activators, inducing the expression of factors that in turn erase the initial (Y) identity

and lead to cell conversion. Alternatively, and depending on the co-factor, their function could be also both.

1.1.2.3. ELT-7-induced reprogramming of gonad and pharyngeal cells into intestine-like cells

As mentioned before, transcription factors can transdifferentiate most cells in blastomeres up to the 8E stage in *C. elegans* (Kiefer et al., 2007; Tocchini et al., 2014; Richard et al., 2011). At larval and adult stage, cells become refractory to direct reprogramming upon ectopic expression of a transcription factor with the exception of the GATA TF ELT-7. Differentiated adult pharyngeal cells start to express *elt-2* gene reporter in many cells throughout the body. The expression gradually fades of the course of 48 h in most cells, but persists in the proximal somatic gonad and the pharynx (muscular feeding organ). Interestingly most cells that showed intestinal features lose these characteristics 72 h after the initial brief expression of ELT-7 (Riddle et al., 2013), suggesting that terminally differentiated cells can be forced into adapting a new cell fate, but that it might depend on the cellular context.
In the endoderm regulatory network ELT-7 functions as the terminal component (Sommermann et al., 2010; Evans et al., 1994), downstream of END-1 GATA TF and is redundant with ELT-2 GATA TF. Both, ELT-7 and ELT-2, initiate gut differentiation during embryogenesis and maintain transcription of intestinal genes. Interestingly, the downstream END-1 cannot induce conversion. Other factors of the endoderm gene regulatory network, ELT-2 and END-3, which are also GATA type transcription factors, are capable of inducing transdifferentiation, albeit less efficiently than ELT-7 (Riddle et al., 2016). Perhaps the unusual small size of ELT-7 with only 198 amino acids or other structural characteristics permit it to access binding sites on promoters, which are otherwise inaccessible due to packed chromatin structure and therefore induce transdifferentiation. When ELT-7 is briefly expressed during mid-to-late larval development the somatic gonad converts into a well-formed intestine-like organ (Riddle et al., 2016). By activation of an intestine-specific intermediate filament protein (Riddle et al., 2016) that is normally expressed during terminal differentiation of the embryonic gut (Bossinger et al., 2004) an ectopic lumen-like structure is formed within the uterus. At the fine ultrastructural level the reprogrammed uterus is indistinguishable from the normal intestine, which includes intestine-like microvilli and terminal web, suggesting that the developing proximal gonad undergoes "transorganogenesis" into a morphological normal gut. Since order and timing are similar to normal embryonic gut development, it appears that the process of transorganogenesis redeploys the normal embryonic development program, but instead of beginning from naive, undifferentiated blastomeres, a fully formed organ is being reprogrammed. It remains to be seen whether a fully functioning intestine is formed. Gut development can only be induced in the gonad at L3-L4 stages of larval development. Prior to L3 the somatic primordium of the hermaphrodite is composed of 12 cells that appear to be refractory to induced direct reprogramming. By the end of L4 larval stage the window for gonad-to-intestine transorganogenesis closes. Hence, the developing uterus might be analogous to the early blastomere before the transition

to cell fate commitment. It is to note that neither expression of HLH-1 (muscle) or ELT-1 (epidermis) are able to reprogram developing uterine cells (Cinar et al., 2003). In addition, it could be shown that upon ectopically expressed ELT-7 fully differentiated pharyngeal cells lose their pharynx specific reporter expression and gain expression of intestine reporters. The ultrastructure also closely resembles that of the intestine indicating a complete transorganogenesis. In contrast to the somatic gonad is the pharynx amenable to be reprogrammed at any stage of development. This example shows that a single transcription factor can be sufficient to induce direct reprogramming in fully differentiated tissue without the removal of any other factor. A possible reason for the specific gonad-to-intestine and pharynx-to-intestine cell fate switch might be the *C. elegans* FoxA transcription factor homolog PHA-4, which is known to be expressed in pharynx, intestine, and developing somatic gonad and has been studied in the context of its existential role in pharynx organogenesis (Horner et al., 1998; Zhong et al., 2010; Chen, Riddle, 2008; Frederick et al., 2008; Mango et al., 1994). PHA-4 is required for the formation of the differentiated pharynx. Removal of PHA-4 during embryonic development suppresses the ability of ELT-7-induced transorganogenesis of pharynx-to-intestine, suggesting that PHA-4-dependent pharynx differentiation is a necessary pre-condition. A knockdown of PHA-4 at later stages that does prevent the formation of the pharynx does not inhibit the ELT-7-induced reprogramming (Riddle et al., 2016), suggesting that PHA-4 is not required during transorganogenesis of pharynx to gut, but to ensure pharynx differentiation as a pre-condition.
As shown above, direct reprogramming based on overexpression of ELT-7 is limited to certain tissues and time points. To overcome this limitation barrier factors to reprogramming have to be identified and removed.

1.1.2.4. Barrier factors to cell fate conversion

It has been thought that so called pioneer transcription factors are capable of binding their cognate DNA and thus initiating changes in chromatin structure even in chromatin that is compacted by linker histones (Cirillo et al., 1998, 2002). However, most transcription factors cannot induce direct reprogramming after the blastomere 8E stage indicating that a loss of plasticity occurs (Kiefer et al., 2007; Tocchini et al., 2014; Richard et al., 2011). When on the other hand the Polycomb repressor complex (PcG) or Notch signalling are eliminated, loss of plasticity can be postponed (Yuzyuk et al., 2009; Djabrayan et al., 2012). As such germ line-specific genes are being de-repressed in larval somatic cells, if Zn-finger protein MEP-1 and NurD complex subunit LET-418, that are both found in a complex with HDAC-1, are depleted (Unhavaithaya et al., 2002). In mutants of the retinoblastoma (Rb) pathway, that lead to a loss of chromatin remodeling, a somatic expression of germline specific P granules in the intestine was observed (Petrella et al., 2011). In mammals murine embryonic β cells transdifferentiate into glucagon producing α cells upon removal of DNA methyltransferase DNMT1 in (Dhawan et al., 2011). In all these examples already the removal of a barrier factor led to direct reprogramming.

In other cases the depletion of a barrier factor has to be combined with the ectopic

expression of a cell-fate inducing transcription factor. RNAi against *lin-53* (RBBP4 and 7 in humans) permits the transcription factors CHE-1 (ASE neurons), UNC-3 (cholinergic motor neurons), and UNC-30 (GABAergic motor neurons) to reprogram germ cells that lost their initial identity and express neuron-type specific and pan-neuronal reporters (Tursun et al., 2011). In addition, reprogrammed cells started to change their morphological shape and lose their characteristic fried egg-shaped nuclear and nucleolar morphology and assume a speckled neuronal nuclear morphology. The depletion of *lin-53* did not cause the formation of teratomas either, since expression of CHE-1 in *lin-53* (RNAi) animals did not lead to expression of other neuronal reporters, such as for GABA or cholinergic neurons, indicating that the reprogramming was specific to the expressed transcription factor. When CHE-1 is ectopically expressed in the larval stages or adult worm very few head neurons start to express the ASE-specific reporter *gcy-5::gfp* (Tursun et al., 2011), suggesting that the removal of LIN-53 is a necessary condition since otherwise germ cells are refractory to direct reprogramming upon cell fate inducing transcription factor expression.

1.2. Identifying Barrier Factors

1.2.1. Identification of cell fate barriers *in vitro*

Direct reprogramming in cell culture was initially described when it was shown that overexpression of the muscle-specifying transcription MyoD in fibroblasts is sufficient to reprogram them into muscle cells (Davis et al., 1987). Later it was demonstrated that fibroblasts can also be converted into cardiomyocytes (Ieda et al., 2010) and neurons (Vierbuchen et al., 2010) by expressing a single or mixture of different transcription factors. However, it turned out that the cell type mattered and that MyoD, for instance, is not sufficient to reprogram any cell into muscle cells (Weintraub et al., 1989), showing that reprogramming is restricted by cell context. Another issue of reprogramming is the low efficiency, in which a new cell fate is being induced. Recently it was demonstrated that a combination of transcription factors can reprogram somatic cells into induced pluripotent stem cells (iPSCs) (Takahashi, Yamanaka, 2006). However, only 1% of cells would be converted. Genes can be depleted by RNAi *in vitro*, which allowed to identify genes that antagonize reprogramming such as tumor suppressors (p53, INK4a/ARF, LATS2) (Kawamura et al., 2009; Qin et al., 2012; Zhao et al., 2008) and H3K9 methyltransferases (SETDB1, SUV39H, EHMT2) (Chen et al., 2013). In addition, focused RNAi screens identified the TGF-β signaling (Payman et al., 2010), H3K79 methylation by DOT1L (Onder et al., 2012), or protein ubiquitination (Buckley et al., 2012) act as a reprogramming barriers.

Genes can be selective depleted using either a pooled or an arrayed format. In the pooled format the RNAi reagent library in form of viral-encoded short hairpin RNA (shRNA) is introduced into cells en masse and at random. After transcription the RNA folds back on itself, forms small 4- to 8-nt loops. The resulting shRNA is recognized and cleaved by the Dicer complex to generate small interfering RNA (Brummelkamp et al.,

2002; T et al., 2002; Paddison et al., 2002). Each cell will on average receive one gene-specific shRNA. Afterwards, a specific selection might be applied followed by sequencing to identify the shRNA incorporated into the genome of the cell. There is some risk that the library might not be uniformly represented. More importantly, especially for time-sensitive assays, is the fact that the time in cell culture after introduction of the RNAi library may be in order of several days or weeks.
If shorter incubation times are required, such as when studying direct reprogramming induced in cells at a specific stage, an arrayed format is more practical, in which cells are being transfected with small interfering RNAs (siRNAs). Each well in a microtiter plate, such as a 96- or 384-well plate, contains a single or a mix of siRNA reagents. Typically, detection of the assay is done via measuring fluorescence, colorimetric, or luminescent response.

1.2.2. RNAi-based genetic screens *in vivo*

In vivo RNAi screens are mainly carried out in *Drosophila*, mice, and *C. elegans*. In *Drosophila* RNAi knockdown can be induced via injection or expression of dsRNAs and acts cell-autonomously, thereby facilitating tissue- and stage-specific studies (Roignant et al., 2003; Perrimon et al., 2010), which also allows to screen at adult stage, even when knockdowns in early stages are associated with lethality. *In vivo* RNAi in mice is performed by introducing pools of shRNA-transfected cells into mice, a process termed as *ex vivo* screening. This approach allows to combine the relative ease of introducing large pools of shRNA in cell culture with the advantages of placing the cells in an *in vivo* context. The *ex vivo* screening process has been proven to be particularly useful for cancer research, as it allows to study transduced cells for their ability to contribute to cancer formation (Meacham et al., 2009; Bric et al., 2009). Inducible constructs that are introduced into mice embryonic stem cells facilitating RNAi in ES cells or producing transgenic mice for *in vivo* RNAi are also available (Premsrirut et al., 2011; Katherine et al., 2011).

RNAi was originally identified in *C. elegans* when dsRNA was injected into worms, which led to the depletion of mRNA and started the revolution of *in vivo* RNAi (Fire et al., 1998). RNAi in *C. elegans* is both transitive and systemic, that is, injection or expression of dsRNA in one tissue can lead to gene knock down in other tissues (Fire et al., 1998; Winston et al., 2002). RNAi can be applied in worms simply by feeding (see fig. 1.7). The bacteria are digested in the gut and dsRNA is transported through specific transmembrane protein SID-1 into all cells with the exception of neurons (Feinberg, Hunter, 2003). RNAi in *C. elegans* is also transitive, whereby RNA-dependent RNA polymerase (RdRP) is involved in the amplification of RNAi. As a result, mRNA, which is targeted by siRNA, functions as a template for 5' to 3' synthesis of new dsRNAs (Alder et al., 2003).

dsRNA is spliced by Dicer into siRNAs and used as part of the RISC complex to identify concomitant mRNA sequences that are subsequently degraded. Due to its short life

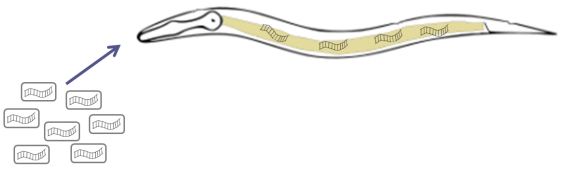

Figure 1.7.: **RNAi by feeding in *C. elegans*.** RNAi is being applied in *C. elegans* by feeding dsRNA expressing bacteria to the worm. The bacteria are digested in the gut and by the transmembrane protein SID-1 cellular uptake of dsRNA is conferred to cells (Feinberg, Hunter, 2003).

cycle, self-fertilization, invariable cell lineage, translucent body and the resulting ability to track the cell fate in the living organism, *C. elegans* is perfectly suited to conduct genetic screens. LIN-53 had been identified as a barrier to reprogramming of germ cells into ASE-neuron-like cells upon overexpression of *che-1* in a screen of chromatin related genes (Tursun et al., 2011). Later our lab performed a whole-genome RNAi screen to identify further barrier factors to reprogramming upon CHE-1 overexpression and identified the FACT complex (Ena Kolundzic et al., in revision). Since LIN-53 is part of the PRC2 complex and involved in chromatin regulation, a RNAi sublibrary, containing chromatin-related genes, was generated in our lab, and the following screen revealed that MRG-1 and HSP-1 are barrier factors to the induction of ASE neuron specific reporters upon che-1 overexpression (Hajduskova et al., submitted for publication).

1.2.3. Multiple components required for Reprogramming

Less than 50 % of *lin-53* RNAi animals show germ line conversion upon CHE-1 overexpression (Tursun et al., 2011), indicating that other factors protect the germ cell fate. When investing barrier genes to direct reprogramming it is important to study genetic interactions since neither a single process or a single gene prevent induced transdifferentiation. Combinatorial RNAi screens allow to identify redundancy in genetic networks (Boone et al., 2007). Large-scale pairwise RNAi screens in Drosophila cells have yielded insight into connectivity of conserved signal transduction pathways, demonstrating that combinatorial RNAi can reveal results that could not have been predicted based on single gene analyses (Horn et al., 2011). *In vitro* studies have already demonstrated the need for combinatorial RNAi screens in order to increase reprogramming efficiency and gain a better understanding of how reprogramming barriers function, as the following examples will show. The first protocol to re-differentiate mouse embryonic and adult fibroblast with a defined set of transcription factors had a very low efficiency (Takahashi, Yamanaka, 2006). Toh et al. (2016) performed a systemic genome-wide siRNA-mediated gene knockdown to identify reprogramming suppressors. The strongest identified reprogramming barriers were ZMYM2 (epigenetic modifier), SFRS11 (putative splicing factor), SAE1 (SUMO-activating enzyme), ESET(H3K9 methyltransferase), and SMAD3 (transforming growth factor β signal transducer), which all function in distinct pathways, suggesting that each factor is an independent reprogramming barrier. When depleting the five barrier genes simultaneously, the efficiency of iPSC generation was increased by several fold (Toh et al.,

2016).
In an earlier study Qin et al. (2014) had systematically analyzed reprogramming barriers to human iPSC generation and identified genes involved in chromatin-regulation, transcription, dephosphorylation, ubiquination, cell adhesion, and cellular transport. They found that RNAi against RNF40 affects other identified barrier genes by upregulating the expression of ADAM29, PTPN11, TTF2, TMF1, and MED19 and downregulating SLC174A5, PTPRJ, and CENPB. The transcriptional effects of RNF40 probably result from its role of regulating the levels of transcription factors, such as OCT4. Since the inhibition of one barrier factor could alter the expression of other barrier factors, RNF40 was simultaneously depleted with PTPN11, MED19, SLC174A5, and PTPRJ, leading to enhanced reprogramming efficiency, indicating that distinct barrier factors interact in dynamic feed forward loops (FFLs) that possibly stabilize cell types by providing response delay capabilities and noise filtering. FFLs can either be classified as coherent or incoherent. A coherent FFL stabilizes the cell against short-term or brief signals and can delay the response to genetic suppression. RNF40 positively regulates other barrier genes, namely SLC174A5 and PTPRJ. By depleting RNF40, the second barrier genes are depleted as well, but can still partially suppress reprogramming. Therefore, the combinatorial knock down of RNF40 as well as SLC174A5 and PTPRJ increases reprogramming efficiency. In an example of an incoherent feedback loops RNF40 represses the other barrier genes PTPN11 and MED19 so that RNAi against RNF40 leads to an upregulation of PTPN11 and MED19, which therefore functions as an additional line of defense against induced cell fate conversion. Depletion of RNF40 alone lowers only briefly the barrier for reprogramming as the secondary barrier genes PTPN11 and MED19 are subsequently upregulated. This effect can only be dampened by also depleting the secondary barrier factors. In addition to these feed forward loops, genes acting as barrier factors to cell conversion can interact in many more ways.
Barriers to reprogramming are found in many very distinct pathways, and it is imperative to study how they interact in order to understand underlying mechanisms and increase the efficiency of induced direct reprogramming.

1.2.3.1. Current methods for combinatorial RNAi screens *in vitro* and *in vivo*

In cell culture, combinatorial RNAi screens can be performed either in a pooled or arrayed format. The arrayed format permits to control beforehand which genes are depleted simultaneously and thereby testing for specific genetic interactions. Pooled shRNA screens, on the other hand, depend on a specific readout and/or selection with subsequent high-throughput screening to identify the incorporated shRNA sequences to identify the depleted gene afterwards.
Similarly to the arrayed format in cell culture, combinatorial RNAi in *C. elegans* can be performed by combining two bacteria strains expressing two different RNAi plasmids in one well (see fig. 1.8A). The ratio of delivered RNAi plasmids for each combination will vary substantially as bacteria strains containing different RNAi plasmids tend to grow at diverse rates, leading to highly varying amounts of each RNAi plasmids taken up by the animal and, as a consequence, a high rate of false-positive and false-negative results.

The reproducibility of mixed double RNAi experiments can be increased by adjusting the bacterial concentration before mixing the two strains. This step, however, is time-consuming and renders a large-scale high-throughput screen unfeasible.
Alternatively, two genes can be targeted by generating a single RNAi plasmid, containing sequences targeting both genes of interest (Min et al., 2010). Combinatorial RNAi experiments using so called 'stitched' double RNAi plasmids (see fig. 1.8B) are highly reliable, but to generate the double RNAi plasmids is very time consuming and as such also not suitable for large-scale high-throughput RNAi screens.

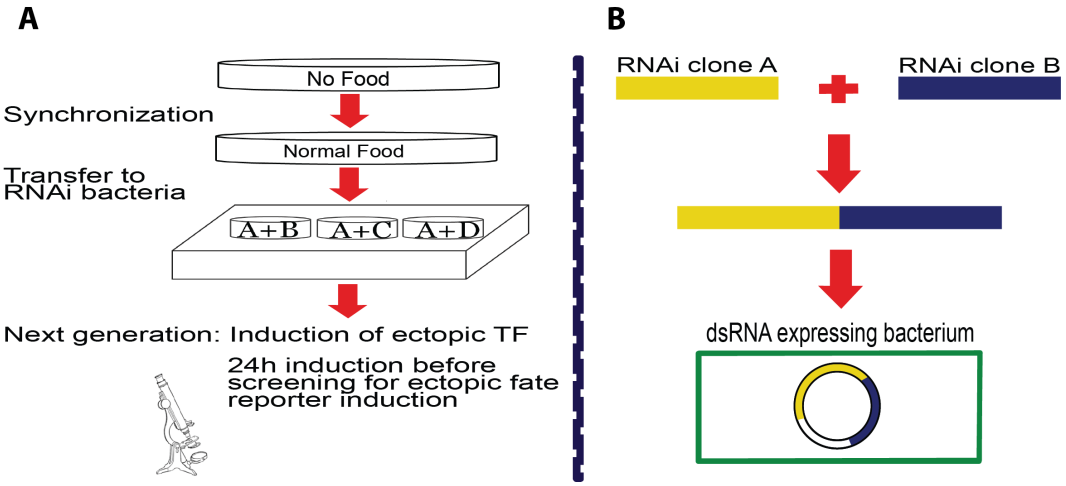

Figure 1.8.: **Two currently available approaches to perform double RNAi in *C. elegans*** (A) Double RNAi by mixing. Two bacteria strains expressing different dsRNAs are mixed in equal amounts to be then fed to worms. (B) Double RNAi by 'stitching' requires the generation of RNAi plasmids containing sequences targeting two different genes.

1.2.4. Other depletion methods

1.2.4.1. Classical genetic screens

In classical or forward genetic screens random mutations are induced by chemical treatment or radiation, and the cells or animals are then screened for the induction of a predefined phenotype. In contrast to RNAi screens, the locus of the mutation has to be determined afterwards, which is still a laborious process. Mutations usually affect a single gene and the mutation is heritable. They can lead to loss- or gain-of-function, which allows to study the regulatory mechanism. Mutations can be tissue-specific and point mutations allow to gain insights into the structure-function relationship. Theoretically every gene should be suitable for mutation, but mutations in essential genes and thus cannot be assayed for reprogramming. It also does not permit to knock out a given gene at a specific time point, instead it is permanently removed. In order to study genetic interactions a mutant strain with a specific phenotype can be screened to identify either

enhancing or suppressing mutations

1.2.4.2. CRISPR/Cas

Originally identified as the functional equivalent to an adaptive immune system in bacteria (Barrangou et al., 2007), the clustered regularly interspaced short palindromic repeats (CRISPR) pathway has been altered in order to engineer genomes highly efficiently (Cong et al., 2013; Mali et al., 2013; Hwang et al., 2013). The Cas9 nuclease, guided by a single-guide RNA (sgRNA), causes double strand breaks of matching target DNA sequences (Jinek et al., 2012). The target specificity is only dependent on the 20-base-pair sequence at the 5'-end of the sgRNA. Thus, knockout reagents are much easier to produce than it was possible with zinc-finger nucleases or transcription activator-like effector nucleases (TALENs). In contrast to RNAi, gene expression is not reduced but completely depleted. In cell culture large libraries of sgRNA can be screened using lentiviral delivery and subsequently analysed using high-throughput sequencing (Wang et al., 2014).
In *C. elegans* Norris et al. (2017) showed that by replacing the target gene with a heterologous GFP transgene through homology-directed repair double mutants are generated more easily. Independent mutants can be identified post-injection in F1 by following the introduced fluorescent reporter and mutants of two different genes can be crossed to generate double mutants, which are isolated by microscopy. While this makes it easier to identify mutants and has all advantages of a regular mutant, it is not suitable to perform large-scale high-throughput screens and does not allow to investigate the function of essential genes as reprogramming barriers.

1.3. Aim of the study

Direct reprogramming is a very promising approach to generate patient-specific disease models or to replace tissues, such as neurons, that do not regenerate (Ladewig et al., 2013). Studies *in vitro* and *in vivo* have shown that differentiated cells, such as fibroblasts, can be converted into muscle cells, cardiomyocytes or neurons (Davis et al., 1987; Ieda et al., 2010; Vierbuchen et al., 2010) by overexpressing cell-fate inducing transcription factors. However, they also revealed that there are protective mechanisms that prevent transdifferentiation, called barrier factors. Targeted genetic depletion by RNAi permits to identify barrier genes in large-scale high-throughput screens. Qin et al. (2014) have shown *in vitro* that barrier genes interact with each other, thereby increasing the robustness of the cell against external perturbations. In order to identify and investigate genetic interactions of barrier genes it is required to deplete two or more genes simultaneously. With its invariant cell lineage, translucent body, and the fact that RNAi is applied by feeding, *C. elegans* is perfectly suited as an *in vivo* model organism to study barrier genes to direct reprogramming by RNAi in large-scale high-throughput screens. In order to deplete two or more genes simultaneously, dsRNA expressing bacteria strains can either be mixed, resulting in a large number of false-positive and false-negative results, or knocked down by double RNAi plasmids ('stitching'), which have to be generated in a time-consuming process and which is therefore no appropriate for screening large

numbers of candidate genes. The aim of the study was to develop a method that allows to perform large-scale combinatorial RNAi screens *in vivo* in *C. elegans*, which is less time-consuming than double RNAi by stitching, but yielding much more reliable results than double RNAi by mixing. Our new method bases on bacterial conjugation (Lederberg, Tatum, 1946), in which a plasmid is transferred from a donor to a recipient cell.

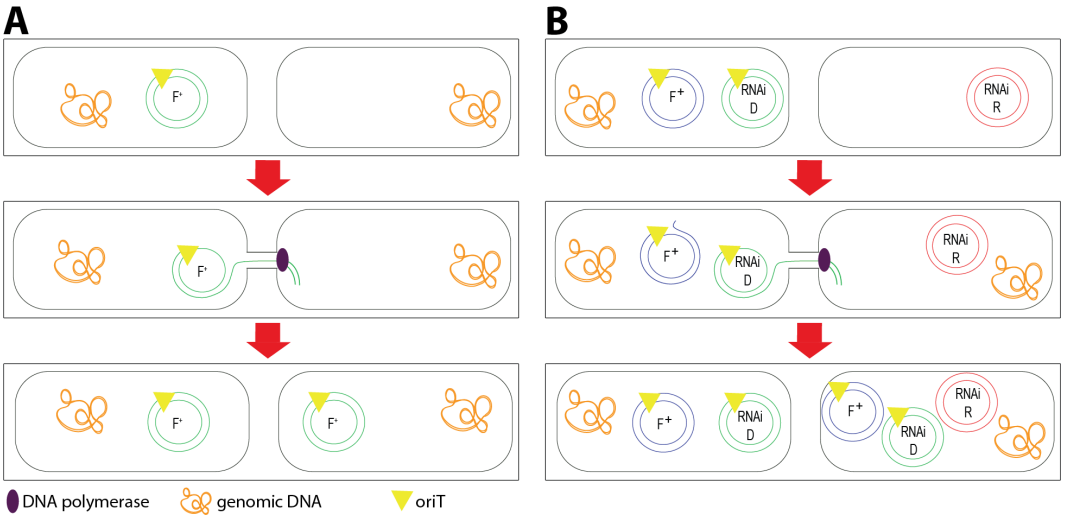

Figure 1.9.: **Generation of bacterial carrying two different RNAi plasmids by bacterial conjugation.** (A) During bacterial conjugation the donor cell transfers a conjugative plasmid to the recipient cell. (B) Double RNAi by conjugation uses bacterial conjugation to transfer in addition to the conjugative plasmid a RNAi plasmid modified with an oriT site to generate a single bacterial cell containing two different RNAi plasmids.

The donor cell carries a conjugative plasmid (F+ plasmid) that contains all genes required for the conjugation to occur, including a pilin gene to form a mechanical connection between the two cells, an origin of replication (oriV) as well as an origin of transfer (oriT) at which site the double stranded plasmid DNA is nicked. A single strand is then transfered from the donor to the recipient cell and complemented by DNA polymerase. The aim of the study was to develop a method in which a donor RNAi plasmids is modified by inserting an oriT site and to use the process of bacterial conjugation to combine two different RNAi plasmids in a single bacterial cell. Double RNAi by conjugation would allow to reliably deplete two genes simultaneously and perform large-scale high-throughput combinatorial RNAi screens to investigate interactions of barrier genes in *C. elegans in vivo*.

2. Results

2.1. Part 1: MRG-1 and HSP-1 are reprogramming barriers

2.1.1. MRG-1 is a safeguarding barrier protecting the germ line cell fate

To identify barrier genes that protect the cell fate from perturbation by cell fate inducing transcription factors (TF), genes were selectively knocked down by feeding the worm with dsRNA expressing bacteria.

MRG-1 was originally identified as a cell fate safeguarding barrier in a P0 RNAi screen done in our lab. Worms were transferred to RNAi plates after hatching (L1). At L4 the worms were subjected to a heat shock in order to induce the ectopic overexpression of ASE neuron transcription factor (TF) *che-1*. When subjected to ctrl RNAi, worms showed no ectopic expression of the ASE neuron fate reporter *gcy-5* in the germ line (GeCo), whereas knockdown of *mrg-1* permitted the induction *gcy-5::gfp*, resembling the phenotype observed in *lin-53* (RNAi) animals after overexpression of *che-1* (Hajduskova et al, submitted for publication).

MRG-1 is an orthologue of the mammalian chromodomain-containing MRG15 − a component of the NuA4 histone acetyltransferase (HAT) complex (Chen et al., 2009). Recently it had been shown that MRG-1 regulates the differentiation of germ cells in *C. elegans* (Gupta et al., 2015). Upon overexpression of *che-1* in *mrg-1* (RNAi) animals germ cells start to form neurite-like projections and *rab-3*, pan-neuronal reporter, is expressed (Hajduskova et al, submitted for publication).

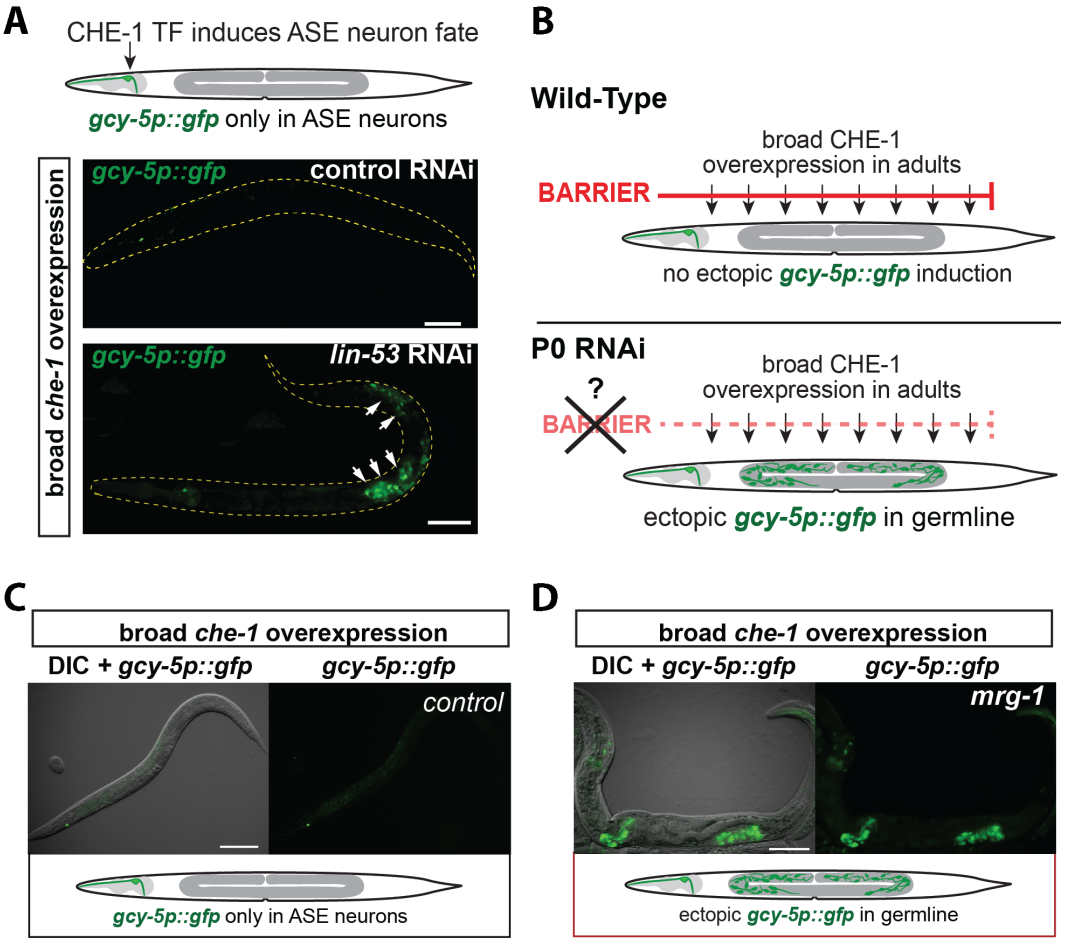

Figure 2.1.: **RNAi against *mrg-1* permits ectopic expression of *gcy-5::gfp* in the germ line.** (A) Control animals show *gcy-5::gfp* expression only in head neurons. RNAi mediated knock down of *lin-53* allows overexpressed *che-1* to induce *gcy-5::gfp* in the germ line. Modified after Tursun et al. (2011). (B) Overexpression of *che-1* in wild type adult worms ineffective in inducing *gcy-5::gfp* ectopically due to reprogramming. By RNAi barrier factors can be knocked down, thus allowing CHE-1 to induce direct reprogramming. (C) *che-1* overexpression in worms subjected to ctrl RNAi show no ectopical expression of ASE neuron fate reporter. (D) Depletion of *mrg-1* permits overexpressed *che-1* the induction of *gcy-5::gfp* expression in the germ line. Figures A to D modified after Hajduskova et. al (submitted for publication)

2.1.1.1. MRG-1 also barrier factor to GABAergic terminal transcription factor UNC-30

To address the question whether a safeguarding barrier factor is universal or specific to a certain cell type, they are assessed by overexpression of different cell-fate inducing transcription factors such as *elt-7* (gut) or *che-1* (ASE neurons).

To identify and test barrier genes that prevent somatic and germ cells from being converted into GABAergic neurons, new constructs containing the genomic DNA of the terminal transcription factor *unc-30* were generated. The transcription factor UNC-30 that is orthologous to the Pitx family of homeodomain transcription factors controls the terminal differentiation of all 19 type D GABA-ergic motor neurons. UNC-30 directly regulates the expression of UNC-25/GAD and UNC-47/VGAT, which regulate GABA formation and secretion (see fig. 2.2A on page 20). Regulatory sequences of transcription factors are often contained in the sequence of introns that cause the continuous expression of the transcription after initial induction, thereby allowing for a more stable expression of *unc-30*. The initial and time controlled induction was enabled by the usage of two different heat shock promoters (see fig. 2.2B. on page 20). *hsp-16.2* and *hsp-16.41* are both broadly expressed. However, *hsp-16.2* is predominantly expressed in neurons and hypodermal cells while *hsp-16.41* is stronger expressed in the intestine and pharyngeal tissue. Thus, by expressing *unc-30* under two separate heat shock promoters, *unc-30* is more broadly expressed upon heat shock driven induction.

The two constructs were injected into N2 wild type worms, and the expression of *unc-30* upon heat shock in generated transgenic worm lines was confirmed by Western blot. The specific GABAergic neuron fate reporter *unc-25p::gfp* and the pan-neuronal fate reporter *rab-3::tRFP* were crossed in to visualize induced direct reprogramming *in vivo*.

To test whether MRG-1 is a *che-1*-specific barrier, P0 RNAi and F1 RNAi was performed, using the newly generated transgenic strains carrying *hsp::unc-30*. When performing P0 RNAi against *mrg-1*, the increase of *unc-25::gfp* when compared to control, was not significant ($P \geq 0.5$, Student′s t-test ; see fig. 2.2D on page 20), potentially due to the high background levels of *unc-25::gfp* in ctrl RNAi. When the mothers (F1 RNAi) were already subjected to *mrg-1* RNAi a significantly increased percentage of their progeny showed expression of *unc-25::gfp* in the germ line ($P \leq 0.01$, Student′s t-test), but without the induction of morphological changes, resembling neurite-like structures or the expression of the pan-neuronal reporter *rab-3* (see fig. 2.2E on page 20). This indicates that MRG-1 is a common barrier factor to *che-1* and *unc-30* mediated cell fate conversion, but knockdown of additional factors would be required to permit UNC-30 the induction of morphological changes from germ line to neuron-like cell.

2.1.1.2. MRG-1 co-localizes only partly with LIN-53

To assess the localization of MRG-1, immunohistostaining was performed using a commercial anti-MRG-1 antibody. MRG-1 could be mainly detected in the germ line, but also in neurons in the head region, as well as in the gut (see fig. 2.2A on page 20)

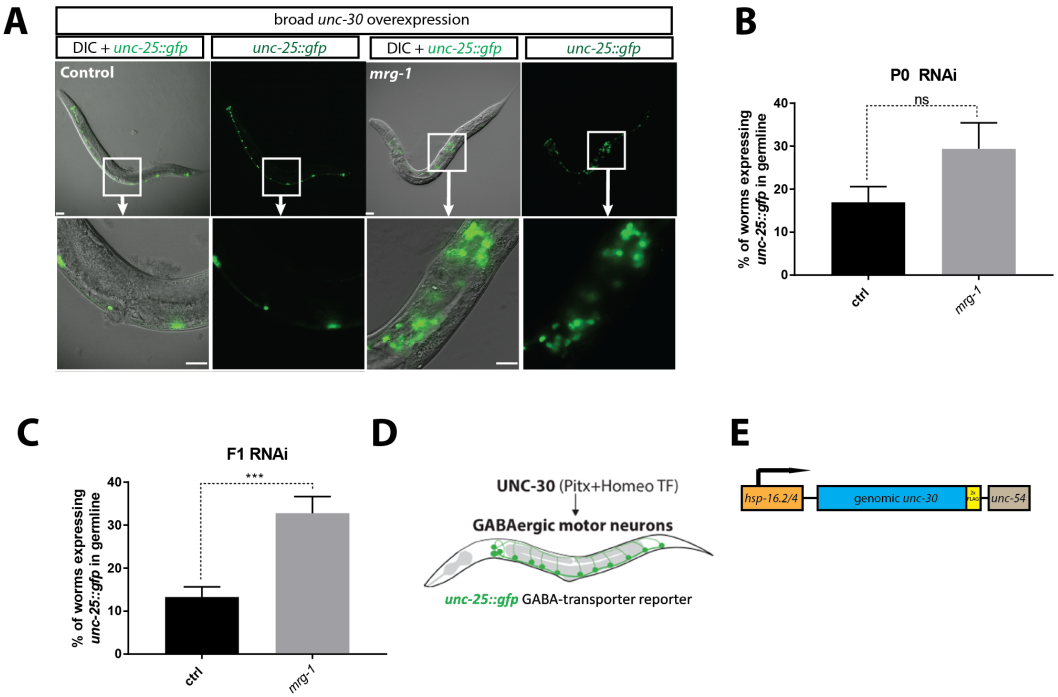

Figure 2.2.: **Ectopic expresson in *mrg-1* (RNAi) animals overexpressing *unc-30*.** (A) Control animals show expression of *unc-25::gfp* only in GABAergic neurons on the ventral side of the worm. F1 RNAi against *mrg-1* allows overexpressed *unc-30* to induce *unc-25::gfp* in the germ line. Magnification (white box) indicates that GFP-positive cells do not adapt neuronal morphology by showing axo-dendritic outgrowths of protrusions. Scale bar = 20 µm. (B) Quantification of animals that show *unc-25::gfp* in germ line when treated with *mrg-1* RNAi and *unc-30* overexpression. P-values were calculated using Student′s t-test (ns = $\geq$ 0.5). Error bars represent SEM from three independent RNAi experiments, n = 300 to 500 for each RNAi. (C) as in B, but as F1 RNAi. P-values were calculated using Student′s t-test (ns = P $\geq$ 0.5, ** = P $\leq$ 0.01). Error bars represent SEM from three independent RNAi experiments, n = 150 to 300 for each RNAi. (D) The *C. elegans* ortholog of mammalian Pitx-Homeo TF specifies the GABAergic motor neuron cell fate. (E) Newly generated constructs containing the genomic sequence of *unc-30* driven by *hsp-16.2* or *hsp-16.4* promoter.

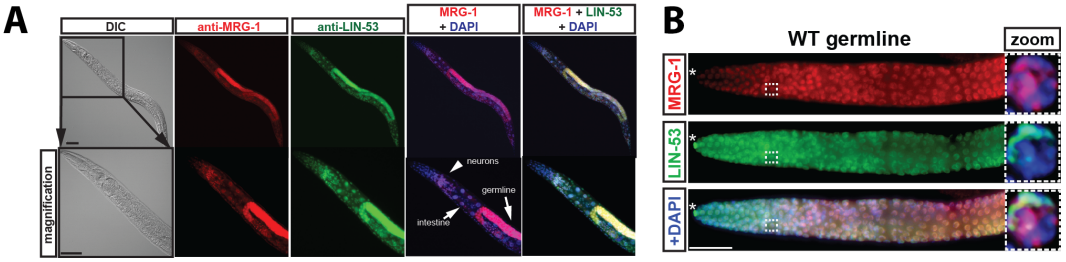

Figure 2.3.: **Immunostaining of wild-type young adult hermaphrodite with anti-MRG-1 and anti-LIN-53 antibody.** (A) MRG-1 proteins are detectable predominantly in the germ line and in neurons and the intestine. Co-staining for LIN-53. Scale bars = 20 µm. (B) Antibody staining of MRG-1 and LIN-53 proteins in the distal wild-type germ line of a young adult hermaphrodite. The magnified germ cell nucleus in the zoom is indicated with a white stipple-line box. Asterisk indicates distal tip of the gonad. Scale bar = 5 µm. Figures A and B modified after Hajduskova et al. (submitted for publication)

Interestingly, LIN-53 co-localizes only partially (see fig. 2.2B on page 21) in the germ line. Co-knockdown of *mrg-1* with members of the PRC2-complex *mes-3*, *lin-53*, or *mes-4*, while broadly overexpressing *che-1*, increases the germ cell reprogramming efficiency slightly but significantly when compared to RNAi against *mrg-1* alone (Hajduskova et al, submitted for publication). This non-synergistic increase of GeCo induction together with the observation that LIN-53 and MRG-1 proteins only partially co-localize might indicate that *mrg-1* has a PRC2 independent role in protecting germ cell fate.

2.1.1.3. Global histone modifications affected by knockdown of *mrg-1*

To investigate how *mrg-1* knockdown affects the chromatin structure, whole worm lysates of control and *mrg-1* RNAi animals were prepared and stained in Western blot with commercial antibodies against histone 3 modifications (see fig. 2.4A on page 22). When *lin-53* or other PRC2 complex units are knocked down, the heterochromatin mark H3K27me3 is globally lost in the germ line (Patel et al., 2012), whereas levels in *mrg-1* (RNAi) animals are unaffected. The histone modification H3K14ac is increased in *mrg-1* (RNAi) animals, whereas other euchromatin marks H3K9ac and H3K4me3 are not affected. In yeast, an increase of H3K14ac level has been associated with DNA damage (Wang et al., 2012).

Immunohistostainings were performed to assess the histone modification marks in germ line (see fig. 2.4B on page 22) and co-stained for LIN-53 to ensure consistent antibody penetration. In *mrg-1* (RNAi) animals neither levels of H3K27me3, nor those of H3K9me2 were decreased. Likewise, marks of open chromatin H3K9ac, H3K36me3, and H3K4me3 were unchanged. Confirming the results from whole worm western blot, H3K14ac levels are increased in germ line upon RNAi against *mrg-1*, suggesting that the

global histone modifications are distinctively affected by the knockdown of *mrg-1*.

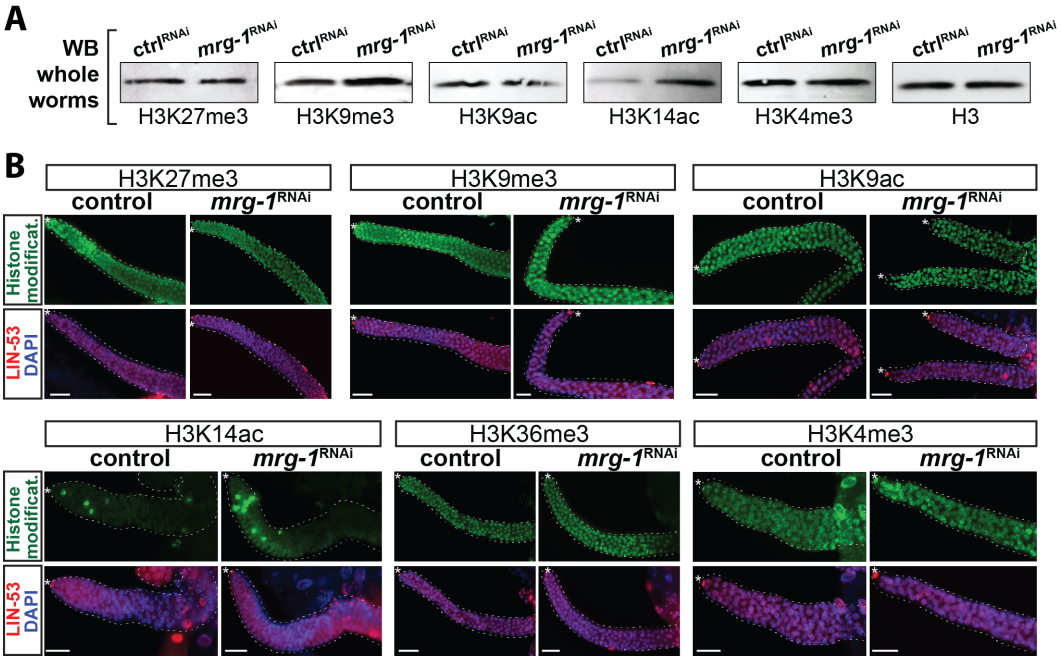

Figure 2.4.: ***mrg-1* RNAi-mediated changes of histone H3 modifications.** (A) Western Blot analysis of whole worm lysates, comparing control and *mrg-1* RNAi treated worms, using the indicated antibodies against specific histone modifications. Histone H3 detection serves as loading control. (B) Immunostaining of gonads from control and *mrg-1* RNAi treated worms, using the indicated antibodies against specific histone modifications. Staining for LIN-53 (shown as overlay with DAPI) serves as control for staining efficiency. Scale bar = 5 µm.

2.1.2. HSP-1 is a barrier factor to the induction ASE neuron reporter *gcy-5* in epidermis

During the same automated RNAi screen that identified MRG-1 another factor, HSP-1, was found. Depletion of *hsp-1* permits the induction of *gcy-5::gfp* upon misexpression of *che-1* in the epidermis (EpCo) (M. Hajduskova et al. unpublished). Using smFISH, it was also demonstrated that *hsp-1* knockdown permits the induction of other endogenous neuronal genes, such as *unc-10* (M. Hajduskova et al. unpublished). Hypodermal cells mis-expressing *gcy-5::gfp* do not show the formation of neuron-like structures, such as neurites. Therefore, it was tested, whether hypodermal cells lose their identity by knocking down *hsp-1* in animals expressing the hypodermal marker *dpy-7::mCherry*, which is lost when simultaneously *che-1* is overexpressed (M. Hajduskova et al. unpublished). However, at careful inspection, it was also noted that *che-1* overexpression alone independently suppresses the expression of *dpy-7::mCherry*, but it is further repressed when

hsp-1 is knocked down by RNAi (M. Hajduskova et al. unpublished).

2.1.2.1. Knockdown of *hsp-1* permits induction of intestine reporter *elt-2* but not GABA reporter *unc-25*

To test whether HSP-1 is a *che-1*-specific cell-fate barrier, the GATA transcription factor *elt-7* was overexpressed in animals on *hsp-1* RNAi, observing that the gut reporter *elt-2::gfp* is expressed in the epidermis, while the hypodermal marker *dpy-7::mCherry* is lost (M. Hajduskova et al. submitted to publication).
Interestingly, *hsp-1* RNAi did not permit the induction of*unc-25::gfp* in the epidermis upon overexpression of the terminal transcription factor *unc-30* (M. Hajduskova et al. submitted to publication).

2.1.2.2. *hsp-1* genetically interacts with *ogt-1*

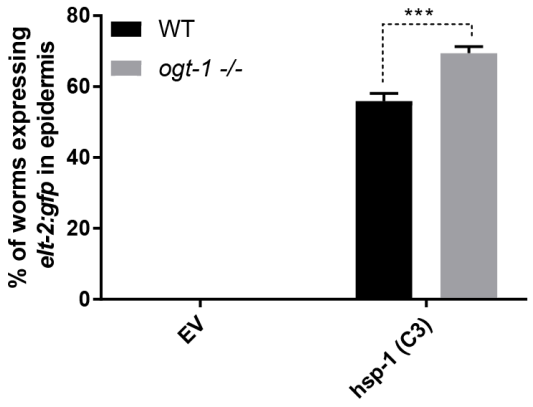

Figure 2.5.: ***hsp-1* RNAi-mediated ectopic induction of *elt-2::gfp* enhanced in *ogt-1* (ok430) mutant background.** Quantification of *hsp-1* RNAi-mediated induction of *elt-2::gfp* upon overexpression of *elt-7* in wild type and *ogt-1* (ok430) mutant background. P-values were calculated using Student′s t-test (ns = $P \geq 0.5$; *** = $P \leq 0.001$). Error bars represent SEM from three independent RNAi experiments, n = 300 to 700 for each RNAi.

hsp-1 is a member of the *hsp70* family that plays a role in proteostasis, raising the question, whether overexpressed CHE-1 might accumulate in *hsp-1* (RNAi) animals. Worm lysates were tested by Western Blot at 4h and 24h after heat shock induction and did not show an increase of HA-tagged CHE-1 in *hsp-1* RNAi lysates when compared to control, indicating that *hsp-1* RNAi increases the permissiveness for *gcy-5::gfp* expression by other means than increased protein level of CHE-1 (M. Hajduskova et al. unpublished). To test whether the inhibition of members of the protein degeneration pathway would allow the ectopic induction of *gcy-5::gfp* in epidermis, subunits of the proteasome were knocked down by RNAi, but without being able to phenocopy *hsp-1* RNAi (M. Hajduskova et al. unpublished).
To further decipher the mechanism of how *hsp-1* safeguards epidermal cells, while assuming that the chaperone function of HSP-1 is relevant, other known chaperone genes were knocked down with *hsp-1* using a double RNAi screen, to test for the enhancement of *gcy-5::gfp* induction efficiency in the epidermis. Moreover, of the two top candidate genes from the screen, *ogt-1* and *cdc-48.2*, mutants were tested to phenocopy the enhancement

observed in the double RNAi screen. Only in the *ogt-1* (ok430) mutant background had the permissiveness of epidermis cells significantly increased (M. Hajduskova et al. unpublished). Interestingly, neither in the *ogt-1* (ok430) mutant background, nor in *ogt-1* RNAi could the ectopic induction of *gcy-5::gfp* in the epidermis be observed in absence of *hsp-1* RNAi. The *ogt-1* (ok430) mutant, on the other hand, showed no obvious defect (Hanover et al., 2005).
As mentioned above, *hsp-1* is also a cell-fate safeguarding barrier for the induction of gut specific reporter *elt-2::gfp*. In *ogt-1* (ok430) mutants the *elt-2::gfp* induction efficiency is significantly increased when compared to WT on *hsp-1* RNAi ($P \leq 0.001$, Student′s t-test; see fig. 2.5 on page 23).

OGT-1 contains chaperone-characteristic tetratricopeptide repeat (TPR) domains. As a chaperon-function of OGT-1 itself could not be demonstrated, OGT-1 was therefore considered as a putative co-factor of chaperon-like proteins (Haslbeck et al., 2013). The human ortholog of OGT-1, the O-linked N-linked N-acetylglucosamine (O-GlcNAc) transferase OGT, has been suggested to be involved in insulin-signaling and aging, as well as nutrient signaling in *C. elegans* (Hanover et al., 2005; Mondoux et al., 2011; Love et al., 2010; Radermacher et al., 2014; Li et al., 2017). OGT-1 has also been implicated to be part of the MOF histone acetyltransferase-containing protein complex termed NSL (Hoe, Nicholas, 2014) (reviewed by Gambetta, Müller (2015), which suggests that removal of *ogt-1* could affect chromatin-regulation by NSL.

2.1.2.3. HSP-1 interacts with histone acetyltransferase complex NSL

The question arose whether impairment of the histone acetyltransferase (HAT) complex NSL could explain the enhancement of *hsp-1* RNAi-mediated induction of *gcy-5::gfp* expression in the epidermis upon removal of *ogt-1*. To investigate possible genetic interactions of *hsp-1* and members of the NSL HAT complex in *C. elegans* (Hoe, Nicholas, 2014)) (see fig. 2.6A on page 25) two knock down genes simultaneously double RNAi plasmids were generated, containing target sequences of *hsp-1*, as well as an NSL complex member (double RNAi by 'stitching'; see fig. 2.6B on page 25). When compared to *hsp-1* stitched with the control genes luciferase (rluc) or *unc-22*, an increased induction efficiency for *gcy-5::gfp*, as well as *elt-2::gfp* was observed upon simultaneous knockdown of *hsp-1* and the NSL genes *wdr-5.1*, *hcf-1*, *mys-2*, *smuv-1*, and *smuv-2* in transgenic lines carrying either *hsp::che-1* or *hsp::elt-7*. (see fig. 2.5C and D on page 23).

To assess the specificity of enhancement effects by 'stitched' double RNAi with NSL subunits HSP-1 was also co-depleted with additional chromatin regulators such as LIN-53 and HAT-1. Co-knockdown did not enhance the induction efficiency in *gcy-5::gfp* or *elt-2::gfp*. In *hsp-1 hat-1* (RNAi) animals the permissiveness of epidermis cells appears to be suppressed, implicating that *hat-1* might be required for the ectopic gene expression mediated by *hsp-1* knockdown (see fig. 2.6C and D on page 25).
The NSL HAT complex has been described to acetylate histone 4 lysine 5, 8, 16 (H4K5,8,16ac (Hoe, Nicholas, 2014). Therefore an immunohistostaining was performed using a commercial anti HAK5,8, 16ac antibody to test H4Kac levels upon RNAi against *hsp-1* and NSL subunits *smuv-1*, *mys-2* using WT and in *ogt-1* mutant animals. To ensure consis-

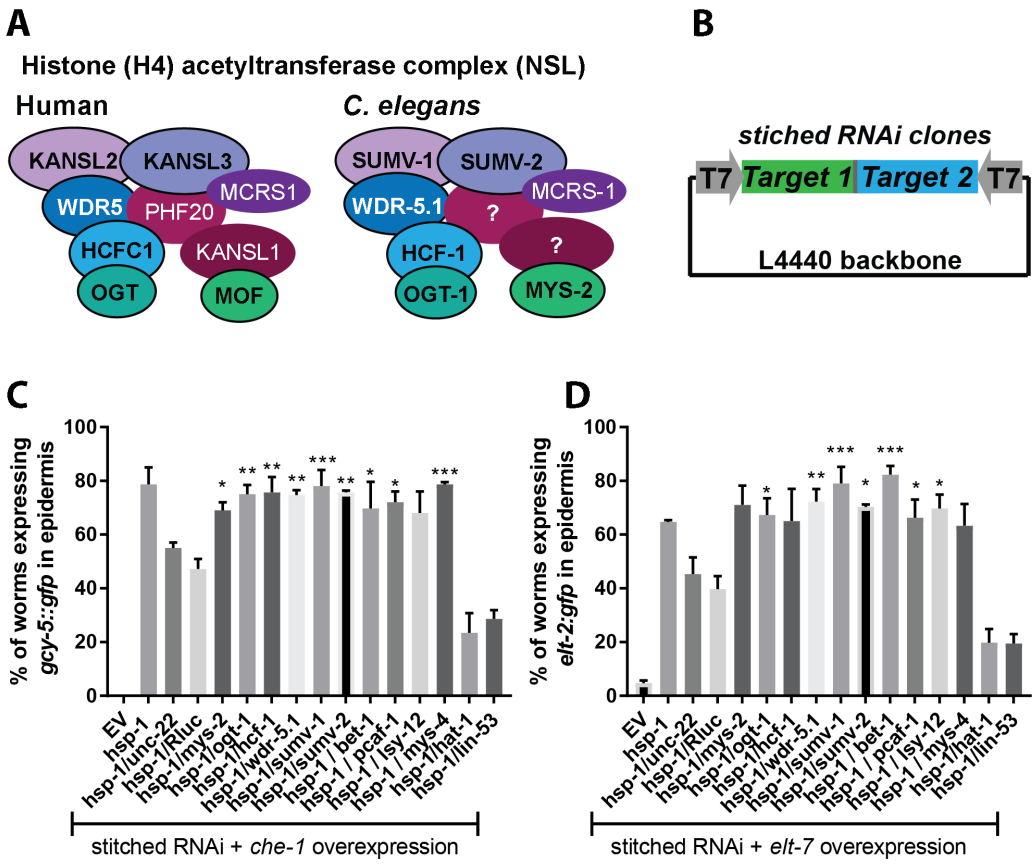

Figure 2.6.: ***hsp-1* genetically interacts with the histone actetyltransferase complex NSL.** (A) Overview of the NSL Histone 4 (H4) acetyltransferase complex NSL in humans and *C. elegans* modified after Hoe, Nicholas (2014). (B) Double RNAi by cloning (stitching) two RNAi clones together in the L4440 RNAi plasmid. In this experiment Target 1 is *hsp-1* and Target 2 are individual members of the NSL complex or as controls sequences of *unc-22* and Renilla Luciferase (Rluc). (C) Double RNAi using stitched RNAi clones in the *hsp::che-1*, *gcy-5p::gfp* transgenic background in order to test genetic interaction between *hsp-1* and the NSL complex. Stitched RNAi of *hsp-1* with *lin-53* or *hat-1* serve as additional controls for specificity of synergistic effects. P-values were calculated using one way ANOVA and Dunnett's multiple comparisons test comparing to *hsp-1*/Rluc. ns = $P \geq 0.05$, * = $P \leq 0.05$, ** = $P \leq 0.01$, *** = $P \leq 0.001$, and **** = $P \leq 0.0001$. Error bars represent SEM from three independent RNAi experiments, n = 300 to 650 for each RNAi. (D) As in (C) but using the *hsp::elt-7*, *elt-2p::NLS::gfp* transgenic background. P-values were calculated using one way ANOVA and Dunnett's multiple comparisons test comparing to *hsp-1*/Rluc. ns = $P \geq 0.05$, * = $P \leq 0.05$, ** = $P \leq 0.01$, *** = $P \leq 0.001$, and **** = $P \leq 0.0001$. Error bars represent SEM from three independent RNAi experiments, n = 350 to 700 for each RNAi. Figure A to D modified after Hajduskova et al. (submitted for publication)

tent antibody penetration anti myosin heavy chain (MHC) antibody was used.
Animals subjected to RNAi against *hsp-1*, *smuv-1*, and *mys-2* showed a decreased signal for H4Kac when compared to control animals in most cells, but neurons. Most *C. elegans* neurons are resistant to RNAi by feeding (Kamath et al., 2001; Timmons et al., 2001; Asikainen et al., 2005). In *ogt-1* (ok430) mutants H4Kac staining shows more global reduction, as compared to control (see fig. 2.7A and B on page 26). Taken together, the decrease of H4K5,8,12,16ac levels in animals depleted for HSP-1, *smuv-1*, *mys-2*, or *ogt-1* suggests that the NSL HAT complex indeed interacts with *hsp-1* as a barrier to the induction of ectopic gene expression in the epidermis, whereas *hat-1* is required for induced transdifferentiation (see fig. 2.7C on page 26).

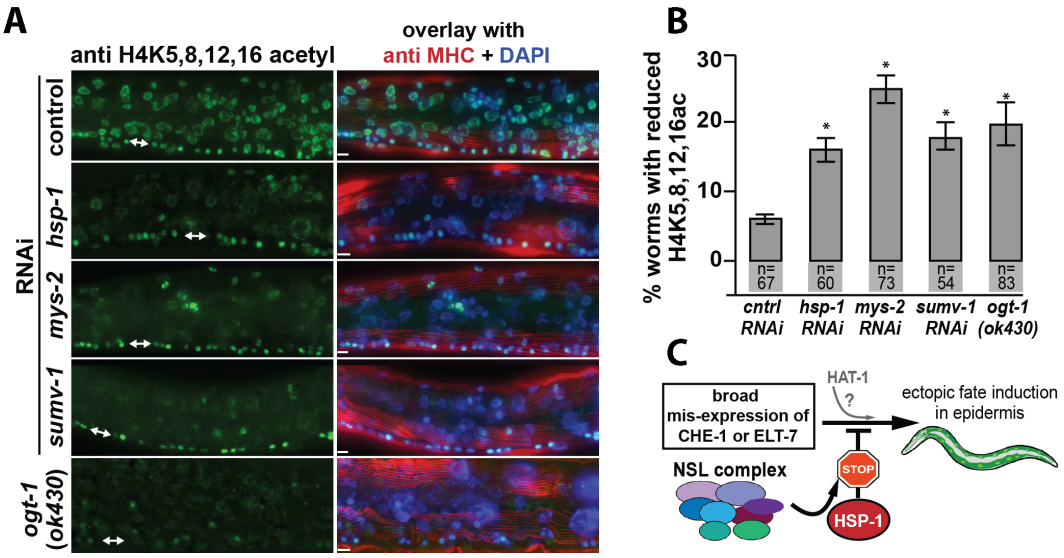

Figure 2.7.: **Modification of Histone H4 acetylation in RNAi or *ogt-1* mutant background.** (A) Immunostaining for Histone H4 acetylation on residues K5,8,12,16 (green channel) in RNAi or the *ogt-1* mutant background. Co-staining with myosin heavy chain (MHC) antibody (red channel) reflects general immunostaining efficiency. The white arrows indicate the ventral nerve cord (VNC). VNC neurons retain H4K5,8,12,16 acetylation in RNAi experiments because neuronal RNAi is inefficient. Scale bars represent 2 µm. (B) Quantification of animals with reduced H4K5,8,12,16ac staining as shown in A. Only animals with consistent MHC antibody and DAPI staining were counted to ensure even antibody penetration. p1 = 0,0369; p2 = 0,0136; p3 = 0,0541; p4 = 0,0497 based on Student′s t-test. Error bars represent STDEV. (C) Model: HSP-1 protects hypodermal cells from ectopic induction of neuronal or intestinal fates in collaboration with the NSL complex. HAT-1 might be required for promoting ectopic gene expression. Figures A to C modified after Hajduskova et. al (submitted for publication)

2.2. Part 2: : Double RNAi by bacterial conjugation

2.2.1. The principle of double RNAi by conjugation

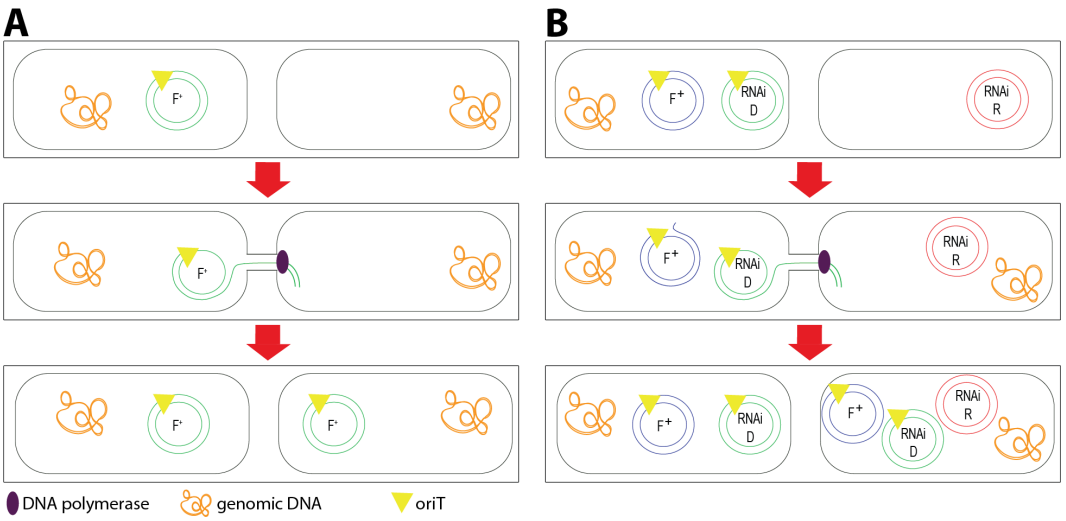

Figure 2.8.: **Principle of double RNAi by conjugation** (A) Schematic illustration of bacterial conjugation. The conjugative F-plasmid is being transferred during conjugation from the donor to the recipient cell. (B) Schematic illustration of double RNAi by conjugation. In addition to conjugative F-plasmid a RNAi donor plasmid is being transferred to the recipient cell.

Cells of *C. elegans* become refractory to direct reprogramming by overexpression of cell-fate inducing transcription factors (TF) after the 8E embryonic stage, suggesting that barrier factors protect the cell from conversion. Tursun et al. (2011) demonstrated that targeted knockdown of the histone chaperone *lin-53* permits the *che-1* mediated induction of ASE neuron-like fates in germ cells. Barrier factors can be found in different pathways and belong to separate mechanisms, as illustrated by research *in vitro*, converting human BJ fibroblasts to iPSCs (Qin et al., 2014). RNAi allows to specifically knock down targeted genes and thus to identify genes that protect the cell fate. In one study combinatorial RNAi against five different targets increased the reprogramming efficiency by several fold (Toh et al., 2016). In *C. elegans*, RNAi is being applied by feeding the worms with dsRNA expressing bacteria. Thus, the first and most direct approach to perform double RNAi is to mix two bacteria cultures, expressing different dsRNA, which is fast, but yields unreliable results. Alternatively, target sequences of two separate genes can be combined into one plasmid, thereby guaranteeing to knock down both targeted genes equally. However, this process is also laborious and thus not suitable for large scale screens.

Our double RNAi protocol relies on bacterial conjugation (Lederberg, Tatum, 1946) to generate double RNAi bacteria clones. The donor bacterial cell contains an F-plasmid that carries its own origin of replication (oriV), as well as an origin of transfer site (oriT),

at which the double stranded DNA is being nicked and single stranded DNA (ssDNA) is transferred to a recipient bacterial cell (see fig. 2.8A on page 27). The tra locus contains the pilin gene, as well as regulatory genes required to form a pilus that connects donor to recipient cell in order to transfer the ssDNA. DNA polymerase complements the transferred ssDNA in the recipient cell. The introduction of an oriT site to the RNAi plasmid allows it to be transferred together with the F-plasmid during conjugation with the end result of combining two different RNAi plasmids in a single bacterial cell (see fig. 2.8B on page 27). By feeding the generated double RNAi bacteria to worms, the genetic interaction of two or three genes can be investigated reliably in large scale high-throughput screens.

2.2.2. The components of double RNAi by conjugation

The transfer of ssDNA during conjugation is enabled by the F-plasmid pRK24 (see fig. 2.9A on page 29). Originally, the plasmid carries an Ampicillin resistance gene that has to be exchanged for Kanamycin in order to distinguish the F-plasmid by antibiotic selection from the RNAi plasmids contained in RNAi libraries. Due the large size of the F-plasmid (over 60 kb), it was required to use bacterial recombineering for which the F-plasmid was transferred to the *E. coli* strain SW105 that contains a temperature-sensitive λ-Red recombinase to generate pRK24-kan. Donor RNAi plasmid contains a Chloramphenicol resistance gene and an oriT site (see fig. 2.9B on page 29). A sequence targeting the gene of interest can be inserted in a one step mechanism. The donor RNAi plasmid was electroporated into the *E. coli* strain SW105, already containing the modified F-plasmid pRK24-kan.

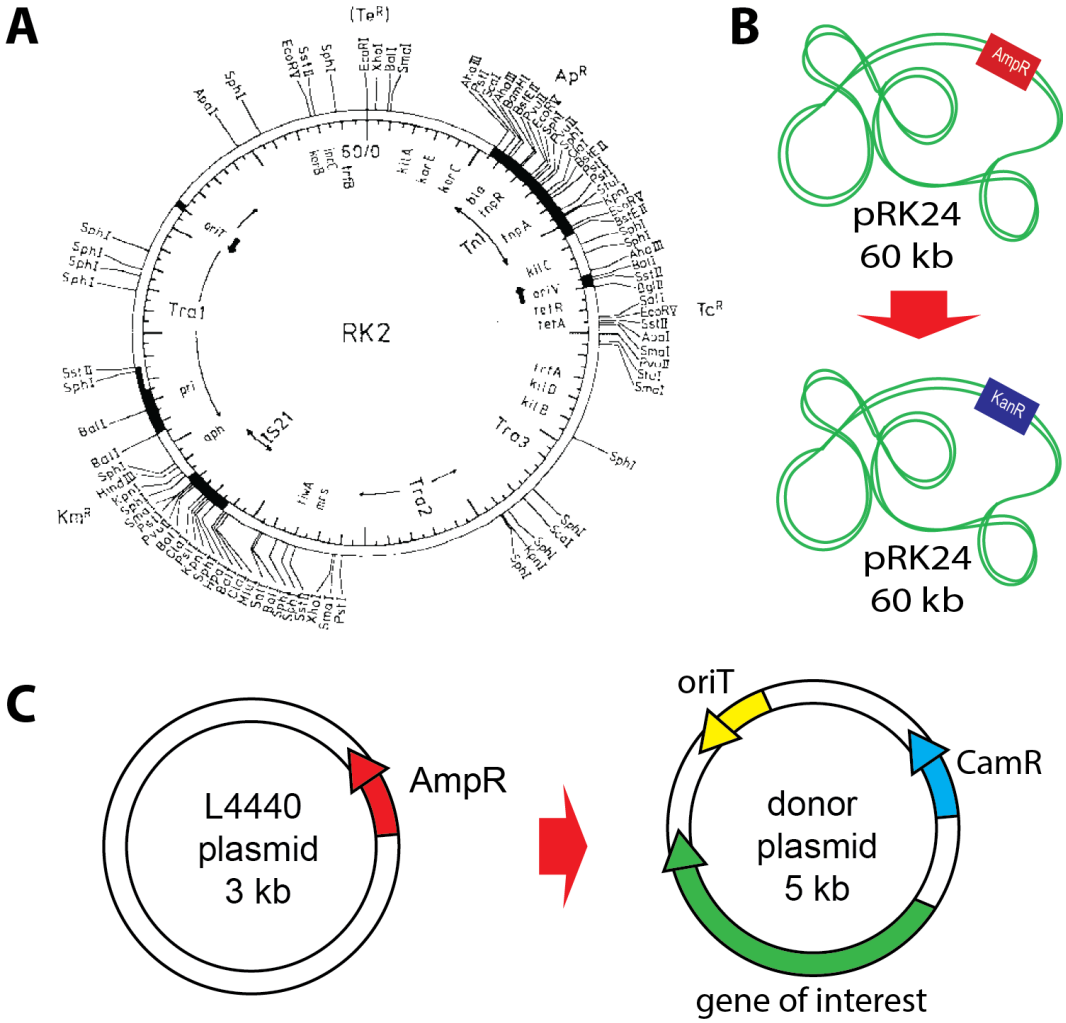

Figure 2.9.: **Components of double RNAi by conjugation.** (A) Graphical illustration of conjugative plasmid RK2. Modified after Thomas, Smith (1987). (B) Schematic illustration of replacing the Ampicillin resistance cassette with Kanamycin by bacterial recombineering in the conjugative F-plasmid pRK24 (C) Schematic illustration of the introduction of an oriT site as well as replacing Amipicillin resistance cassette with Chloramphenicol in order to be able to select for the donor and the recipient RNAi plasmid.

2.2.3. Establishing the conjugation protocol

2.2.3.1. No conjugation using cultures at stationary growth phase in liquid medium

Ma et al. (2014) used the F-plasmid pRK24 for their conjugation protocol (see fig 2.10A on page 31) that required several washing steps for bacterial cultures of donor and recipient, which were omitted in our protocol, as they would not be feasible in a large scale approach. Initially, conjugation was attempted in liquid medium, as it could be efficiently performed in high-throughput assays, since donor and recipient bacterial cultures could be directly pipetted together. To this end, donor and recipient cultures were grown O/N, then combined in 2 mL Eppendorf tubes and incubated at 32°C for 1h, 2h, or O/N. In order to minimize potential inhibitory effects of the containing antibiotics, mating mixtures of donor and recipient bacterial cultures were diluted with antibiotics-free medium. To determine the ideal relative amounts of donor and recipient, equal ratios of both as well as an overabundance of donor or recipient were tested. After incubation the mating mixtures were diluted at 10^{-1} or 10^{-2} and plated on selective $LB^{Amp+Tet+Chl}$ plates. The resulting colonies were streaked out on $LB^{Amp+Tet+Chl}$ plates as a second selection step. None of the streak outs grew after O/N incubation at 37°C, suggesting that colonies obtained after the first selection step were false-positives (see fig 2.10B on page 31). Based on the assumption that bacteria, if incubated O/N, require larger volumes of media to grow, 20 mL Falcon tubes were used instead of 2 mL Eppendorf tubes. Similar to before, various ratios of donor and recipient were tested and the mating mixtures were incubated at 32°C O/N. To minimize potential inhibitory effects by antibiotics contained in the growth media of donor and recipient cultures, the mating mixtures were diluted with increasing amounts of non-selective LB medium (see fig 2.10C). Most of the mating mixtures formed colonies on $LB^{Amp+Tet+Chl}$ plates in the first selection step, but failed to grow when streaked out on $LB^{Amp+Tet+Chl}$ plates, indicating that the colonies were false-positive and that a higher dilution would be required to effectively select for positive colonies.

Since bacteria cells tend to lose plasmids without selective pressure, a second set of mating mixtures were diluted with $LB^{Amp+Tet+Chl}$ medium. After incubation O/N at 32 °C, the bacteria were plated on selective plates. No bacterial colonies were observed the following day, indicating that the mating of donor and recipient bacterial cells is inhibited by added antibiotics.

2.2.3.1.1. Conjugation successful on solid medium

To test whether the donor strain SW105 (pRK24-kan; *hsp-1*) was functional, donor and recipient strains were mixed on a LB agar plates and incubated O/N at 32 °C.

The resulting colonies on $LB^{Amp+Tet+Cam}$ also grew when streaked out on selective media plates. Donor and recipient plasmids could be detected by PCR (see fig. 2.11 on page 32), illustrating the successful transfer of the donor RNAi plasmid during conjugation.

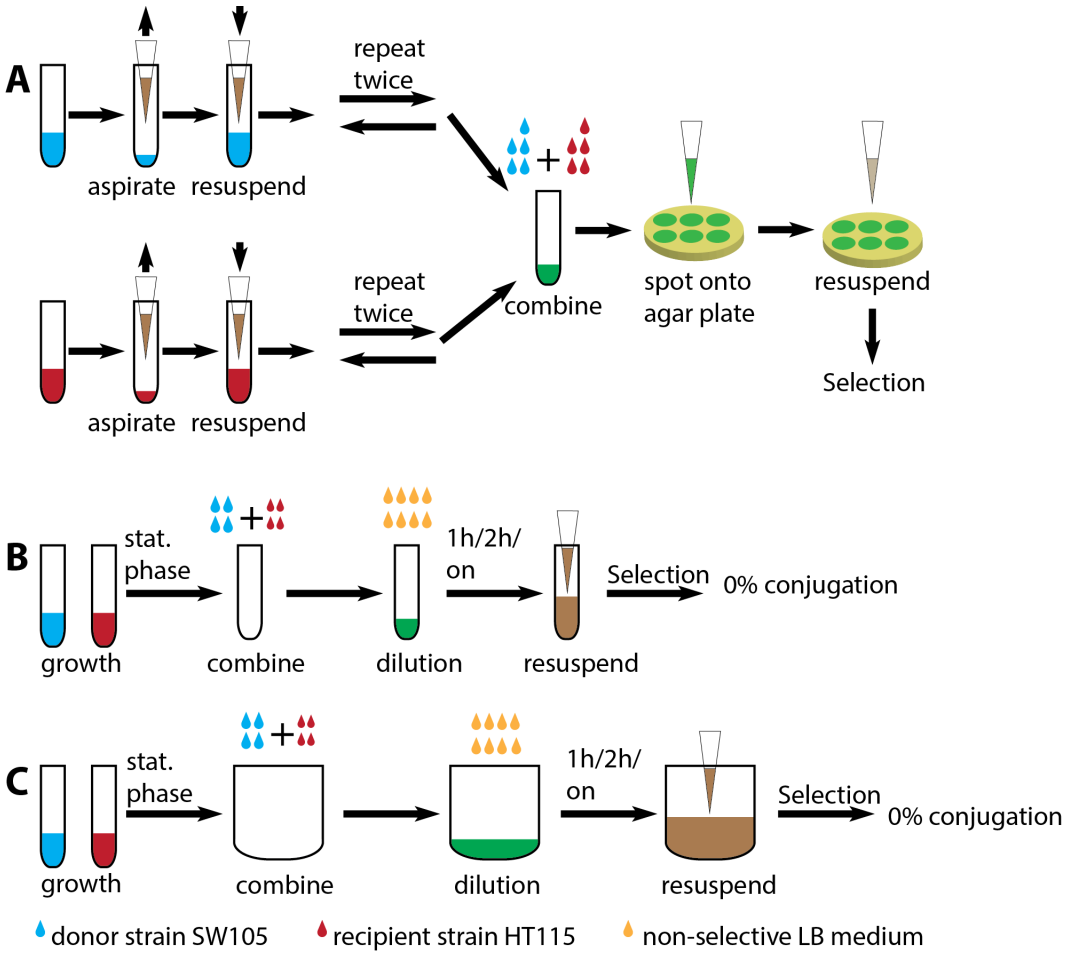

Figure 2.10.: **Conjugation in liquid medium without wash step.** (A) Conjugation on solid medium according to Ma et al. (2014). Two wash steps ensure the removal of antibiotics contained in growth media. (B) In contrast to the protocol of Ma et al. (2014), the washing steps of donor (blue) and recipient (red) culture are omitted. Instead antibiotics-free medium is being added. After incubation mating mixtures were plated on $LB^{Amp+Tet+Cam}$ plates. Colonies were subjected to a second selection on $LB^{Amp+Tet+Cam}$ plates and streaked out. All colonies were negative. See app. A.1 on page 114 for detailed results. (C) As in B, but instead of 1.5 mL Eppedendorf tubes, mating mixtures were incubated in 20 mL Falcon tubes. Conjugation did not occur. See app. A.2 on page 115 for detailed results.

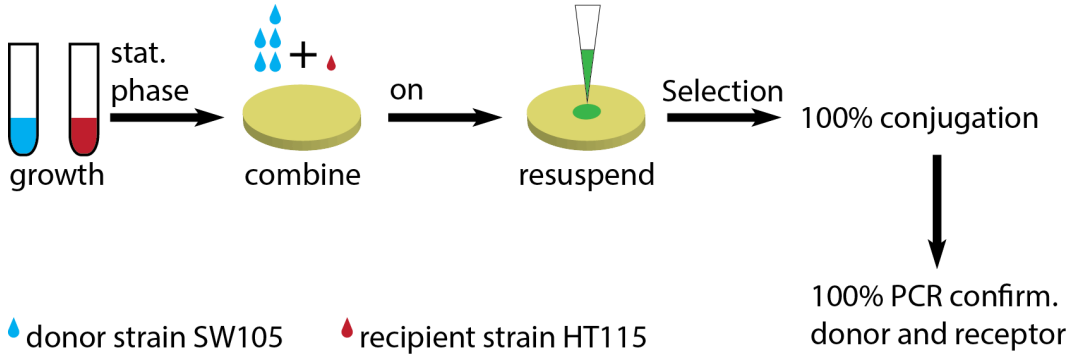

Figure 2.11.: **Confirmation of functionality of donor strain SW105(pRK24-kan; *hsp-1*) on solid medium.** Mating of donor strain SW105 (pRK24-kan; *hsp-1*) with HT115 (*ogt-1*) on solid LB agar plates, incubated O/N at 32 °C. Mating mixture resulted in colonies. Donor and recipient plasmid were detected by PCR. See app. A.3 on page 115 for detailed results.

2.2.3.1.2. No conjugation using cultures at exponential growth phase in liquid medium

The functionality of the donor strain had been demonstrated on solid agar, while conjugation attempts in liquid medium were negative, using bacteria cultures grown O/N. Since the stationary growth phase is characterized by the formation of inhibitory products, such as organic acid, and the depletion of essential nutrients, conjugation might be impaired at this stage. Instead bacteria cultures were grown until the exponential phase at an OD_{600} of 0.5, at which bacteria cells are actively dividing. Similarly to previous attempts, donor and recipient cultures were mixed in different ratios at equal amounts or an overabundance of donor or recipient strain. The total volume of the mating mixture was set to 50 µL and further diluted with LB or SOC medium in a 1:1 ratio and incubated for 2 to 8 h but not O/N in order to avoid the potential loss of plasmids in non-selective medium. For the first selection step post incubation, the mating mixtures were diluted at 10^{-1} and plated on $LB^{Amp+Tet+Chl}$ plates and incubated O/N at 37°C. A subset of colonies was streaked out on $LB^{Amp+Tet+Chl}$ plates. All tested colonies proved to be false-positives (see fig. 2.12A on page 33), suggesting that the bacterial growth phase did not affect conjugation performed in liquid medium.

To exclude the possibility that the small media volume negatively affected the conjugation, the total volume of donor and recipient mating mixture was increased to 100 µL, while testing equal amounts, as well as an overabundance of either donor or recipient bacterial cells, then incubating the mating mixtures at 32 °C for 2 to 8 h, but without adding LB or SOC medium. Following incubation mating mixtures were diluted at 10^{-1} and plated on $LB^{Amp+Tet+Chl}$ plates, incubated O/N at 37°C, and a subset of colonies was streaked out on $LB^{Amp+Tet+Chl}$ plates and incubated at 37°C O/N. The incubated selective plates did not show bacterial colony formation (see fig. 2.12B on page 33), suggesting that a larger mating mixture volume does not positively affect the conjugation.

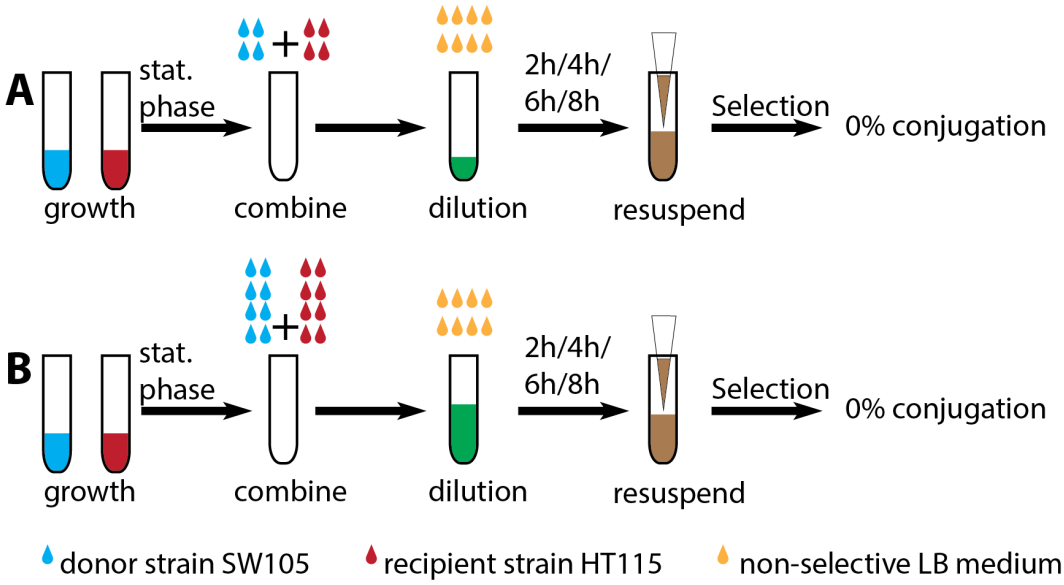

Figure 2.12.: **No conjugation in liquid medium at higher mating mixture volumes.** (A) Conjugation in liquid medium. Donor SW105 (pRK24-kan; *hsp-1*) and recipient HT115 (*ogt-1*) culture were grown until OD_{600} of 0.5, mixed in 1.5 mL Eppendorf tubes. The total volume of mating mixture (50 µL) was diluted in various ratios with either LB or SOC medium, incubated at 32 °C for 2 to 8h and subsequently plated and streaked out on $LB^{Amp+Tet+Cam}$ plates. See app. A.4 on page 116 for detailed results. (B) As in A, but with an increased mating mixture volume of 100 µL. See app. A.5 on page 117 for detailed results.

2.2.3.2. On solid medium conjugative plasmid transfer at low efficiency

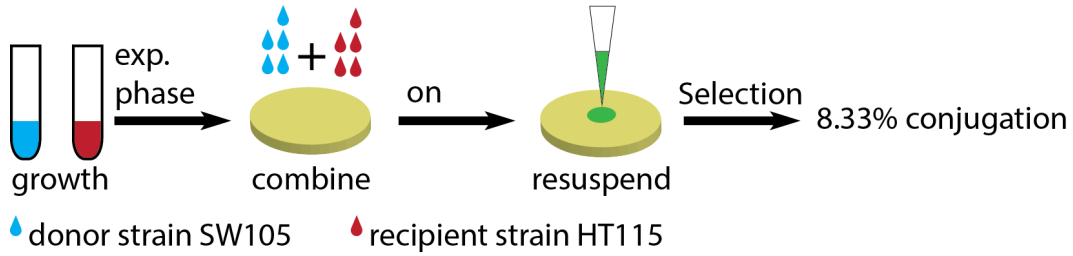

Figure 2.13.: **Conjugation on solid medium at late exponential phase at low efficiency.**
Donor strain SW105 (pRK24-kan; *hsp-1*) and recipient HT115 (*ogt-1*) were grown until late exponential phase and mixed at equal amounts on a LB agar plate, incubated at 32 °C O/N. Subsequently, the mating mixture was plated on $LB^{Amp+Cam+Tet}$ plates and resulting colonies were streaked out to select for containing both, donor and recipient plasmids. See app. A.6 on page 118 for detailed results.

Conjugation in liquid medium would be a more time efficient approach, but neither the dilution of the bacterial mating mixture, nor the manipulation of incubation time would enable the successful transfer of the donor RNAi plasmid to the recipient cell. However, a preliminary result had shown that conjugation did occur on solid medium, as shown previously (see fig. 2.11 on page 32), indicating that the donor strain was functional. Following the aforementioned protocol by Ma et al. (2014) (see fig. 2.10A on page 31), donor and recipient strains were mixed in equal amounts on LB agar plates containing no antibiotics. Bacteria cultures were grown until late exponential phase and mating mixtures were incubated at 32°C O/N and then subjected to antibiotic selection on $LB^{Amp+Cam+Tet}$ plates at dilutions of 10^{-1} and 10^{-2}. The first selection resulted in an overabundance of colonies, of which only a small subset grew when streaked out again on $LB^{Amp+Cam+Tet}$ (see fig. 2.13 on page 34), indicating the conjugation efficiency was low.

2.2.3.3. Conjugation efficiency slightly improved by using *E. coli* donor host strain HT115

To increase the conjugation success rate, a new host strain was generated using dsRNA expressing *E. coli* strain HT115. In previous experiments the *E. coli* strain SW105, which contains λ Red recombinase that might spontaneously modify the F-plasmid and thereby reduce conjugation efficiency, was used. In order to reduce potential inhibitory effects of antibiotics contained in donor and recipient cultures, the mating mixtures were diluted by the addition of LB medium in various ratios from 2:1 to 1:2 then incubated at 32°C O/N and subsequently subjected to antibiotic selection on $LB^{Amp+Tet+Chl}$ plates incubated O/N at 37°C. When using either *E. coli* strain SW105 or HT115, the number of formed colonies was positively correlated to added volume of LB medium. When streaked out on

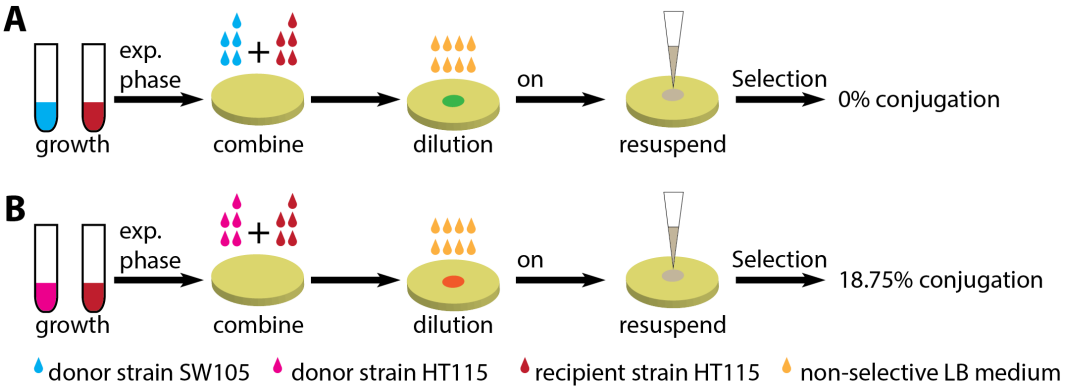

Figure 2.14.: **Donor *E. coli* strain HT115 more efficient than donor strain SW105.** Conjugation on solid LB agar using two different *E. coli* host strains, SW105 and HT115, both carrying pRK24-kan; *hsp-1* that are mixed at equal amounts with HT115 (*ogt-1*). Donor and recipient cultures were grown until the exponential phase. The mating mixture was diluted at various ratios with non-selective LB medium and incubated at 32 °C O/N. The next day mating mixtures were diluted and plated on $LB^{Amp+Tet+Cam}$ plates to select for containing both, donor and recipient plasmids. See app. A.7 on page 118 for detailed results.

$LB^{Amp+Tet+Chl}$ and incubated O/N at 37°C, all tested colonies for donor *E. coli* strain SW105 turned out to be false positives, whereas for the donor strain HT115 3 out of the 8 colonies selected grew on selective medium (see fig 2.14), suggesting that the usage of *E. coli* strain HT115 slightly increases the conjugation success rate, potentially due to the reduced risk of recombination.

2.2.3.4. Conjugation efficiency not improved at lower exponential growth phase and reduced concentration of antibiotics

Previous results indicated a possible benefit of diluting the mating mixture in order to decrease the concentration of antibiotics contained in the growth media of donor and recipient cultures. To further dilute the concentration of antibiotics, more LB medium was added to the mating mixture. Bacteria cultures were grown until the exponential phase to exclude any potential negative side effect of bacteria being depleted for nutrients. The conjugation was performed O/N at 32°C on LB agar plates using the *E. coli* donor host strain SW105. Positive clones were selected on $LB^{Amp+Tet+Chl}$ plates O/N at 37°C. Obtained colonies from the first selection step were streaked out on $LB^{Amp+Tet+Chl}$ plates to test for false positives. When the mating mixture was diluted at 1:2 and 1:5 with non-selective LB medium, 1 out of 8 tested colonies was a true positive (see fig. 2.15 on page 36), suggesting that the dilution of up to 1:5 did not increase conjugation efficiency.

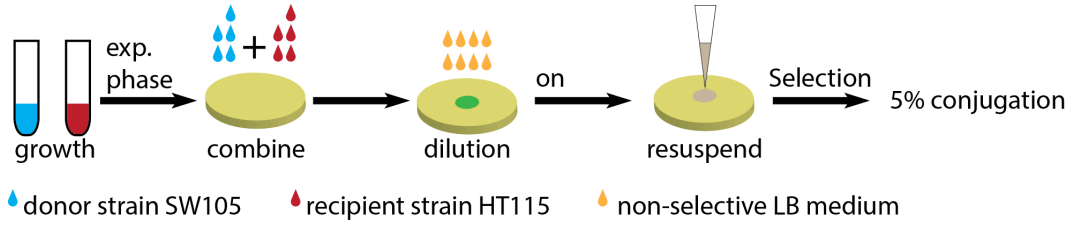

Figure 2.15.: **Conjugation success rate not improved of of donor and recipient cultures grown until exponential phase.** Mating of SW105 (pRK24-kan; *hsp-1*) and recipient HT115 (*ogt-1*) cultures, grown until exponential phase and mixed at equal amounts. The mating mixture was diluted in increasing volumes with non-selective LB-medium and incubated at 32 °C O/N,. The next day the mating mixture was plated on $LB^{Amp+Tet+Cam}$ plates and subsequently streaked out on $LB^{Amp+Tet+Cam}$ plates to select for containing both, donor and recipient plasmids. See app. A.8 on page 119 for detailed results.

2.2.3.5. Higher decrease of antibiotic concentration does not increase the succession rate of conjugation

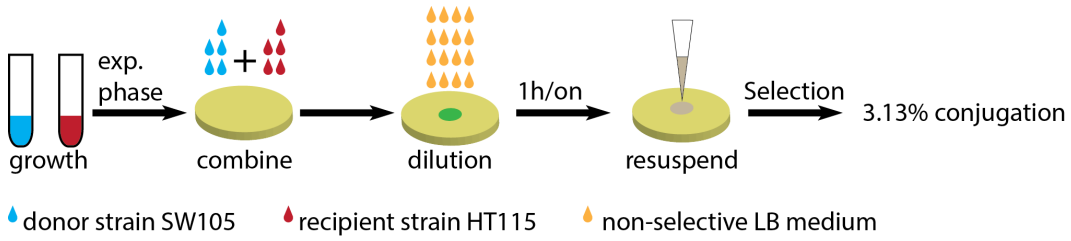

Figure 2.16.: **Conjugation success rate unaffected by reduced concentration of antibiotics.**
Mating on solid LB agar of donor strain SW105 (pRK24-kan; *hsp-1*) with HT115 (*ogt-1*). Donor and recipient culture were grown until exponential phase and mixed at equal amounts and diluted with higher volumes of non-selective LB medium. The mating mixtured was incubated at 32 °C O/N or for 1h and subsequently plated on $LB^{Amp+Tet+Cam}$ plates to select for containing both, donor and recipient plasmids. See app. A.9 on page 119 for detailed results.

Conjugation performed at a ratio of one volume mating mixture dilute with five volumes of non-selective LB medium did not increase the conjugation success rate. Thus, the question arose whether a higher dilution of the mating mixture and thereby a further decreased concentration of antibiotics contained in the growth media of donor and recipient strain could lead to increased conjugation efficiency.
The donor culture was grown until reaching the exponential phase, while the recipient strain was grown until the stationary phase. Donor and recipient cultures were mixed in equal amount, non-selective LB-medium was added at a range of ratios from 1:1 to

1:10 and incubated O/N or for 1h. Mating mixtures were distributed on $LB^{Amp+Tet+Chl}$ plates to select or double RNAi clones (see fig. 2.16 on page 36). Confirming a previous result, when streaking out colonies from mating mixtures diluted with LB medium in a ratio of 1:5, 1 out of 8 streaked out colonies grew on $LB^{Amp+Tet+Chl}$ plates. Higher dilutions did not increase the conjugation effectiveness. When the mating mixture was incubated for 1h instead of O/N, no colonies were observed on $LB^{Amp+Tet+Chl}$ plates, indicating that longer incubation times are required.

2.2.3.6. An overabundance of donor cells improves conjugation efficiency

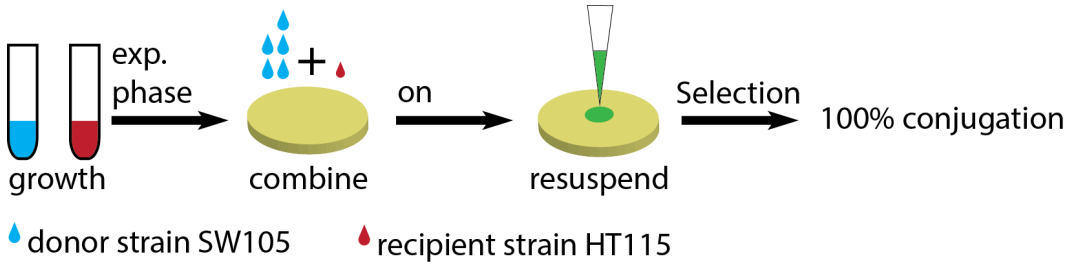

Figure 2.17.: **Overabundance of donor cells increases conjugation efficiency.** Mating of donor strain SW105 (pRK24-kan; *hsp-1*) with HT115(*ogt-1*) mixed at various ratios of donor or recipient cells. The mating mixture was incubated O/N at 32 °C, streaked on $LB^{Amp+Tet+Cam}$ plates to select for cells containing both, donor and recipient plasmids. See app. A.10 on page 119 for detailed results.

The dilution and thereby reduction of antibiotics in the mating mixture did not improve the conjugation success rate. Therefore, the ratio of donor to recipient was altered. Testing ratios of 1:10 and 1:5 of donor to receptor and vice versa showed that an overabundance of donor to recipient bacterial cells at a ratio of 5:1 yielded markedly improved conjugation efficiency (see fig. 2.17 on page 37). The total amount of colonies was very low (2), but both colonies were positive in the streak out test on $LB^{Amp+Tet+Chl}$ plates, indicating the importance of a surplus of donor cells in comparison to the recipient.

2.2.3.7. Addition of antibiotics diminishes conjugation success rate

The mating of donor and recipient strain was most efficient when the mating mixtures were incubated O/N and at an overabundance of the donor bacterial cells on non-selective LB agar plates.
To test whether due to the long incubation period and the absence of selective pressure, bacteria cells might lose plasmids, thereby impairing the total conjugation success rate, plates with reduced antibiotic concentrations were prepared for Ampicillin, Kanamycin, and Chloramphenicol. Kanamycin is used to select for the F-plasmid pRK24-kan and was the prime candidate to ensure a high conjugation efficiency. To reduce the antibiotic concentration originating from the growth media of donor and recipient cultures, the mating mixture was diluted by addition of non-selective LB medium at an equal amount.

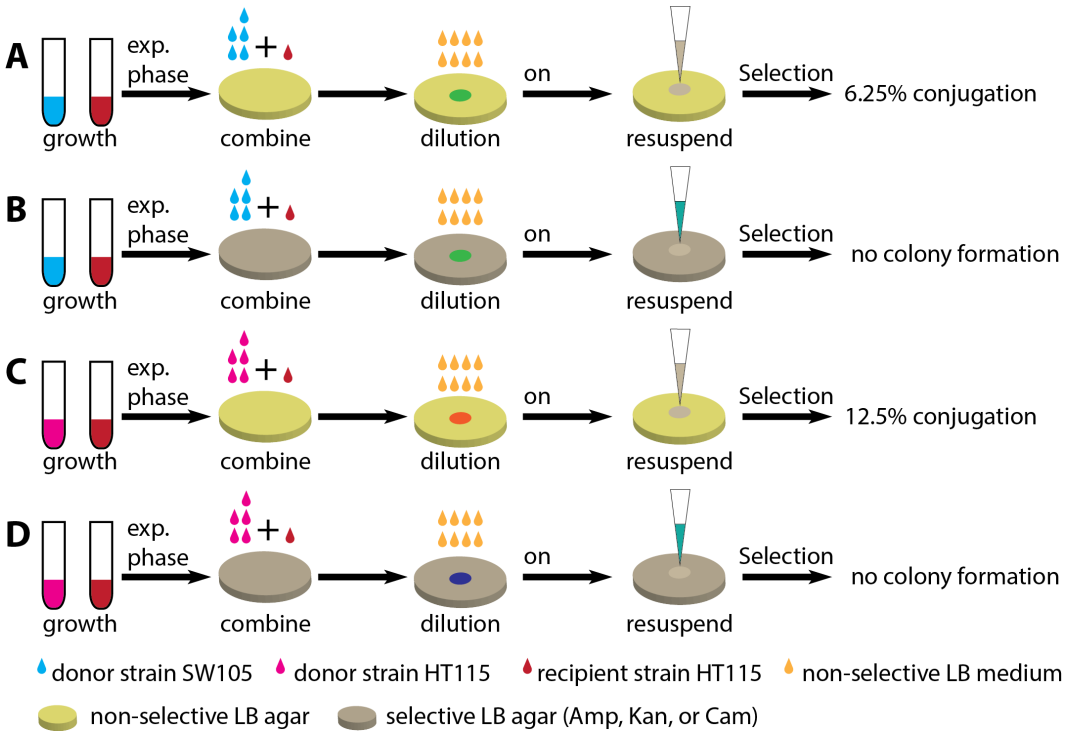

Figure 2.18.: **Addition of antibiotics to solid LB agar inhibits conjugation.** (A) Mating of donor strain SW105 (pRK24-kan; *hsp-1*) with recipient strain HT115(*ogt-1*) on LB agar plates. Donor and recipient cultures were combined at a ratio of 5:1, diluted with non-seletive LB medium and incubated O/N at 32 °C. The next day selection for cells containig both, donor and recipient plasmids on $LB^{Amp+Tet+Cam}$ plates. (B) as in A, but mating mixtures were incubated solid LB agar plates that contained either Ampicillin, Kanamycin, Chloramphenicol. (C) as in A, but using donor strain HT115 (pRK24-kan; *hsp-1*). (D) as in B, but using donor strain HT115 (pRK24-kan; *hsp-1*). See app. A.11 on page 120 for detailed results.

Based on our previous results, a surplus of donor cells, either *E. coli* strain SW105 or HT115, were used. As a direct comparison, mating mixtures were incubated on LB agar plates without antibiotics (see fig. 2.18 on page 38).
After incubation O/N at 32°C mating mixtures were diluted at 10^{-3} to reduce the number of false positive colonies and subjected to selection on $LB^{Amp+Tet+Chl}$ plates. Mating mixtures that were incubated on selective LB agar plates did not show colony formation, indicating the inhibitory effect of antibiotics in the LB agar plates. In the absence of selective pressure during conjugation, colonies were obtained on $LB^{Amp+Tet+Chl}$ plates, of which only a small subset were confirmed in the second selection step as true positive colonies, suggesting that dilution of the mating mixture of donor and recipient reduces the conjugation success rate.

2.2.3.8. No increase of conjugation efficiency upon dilution when using higher amount of donor cells

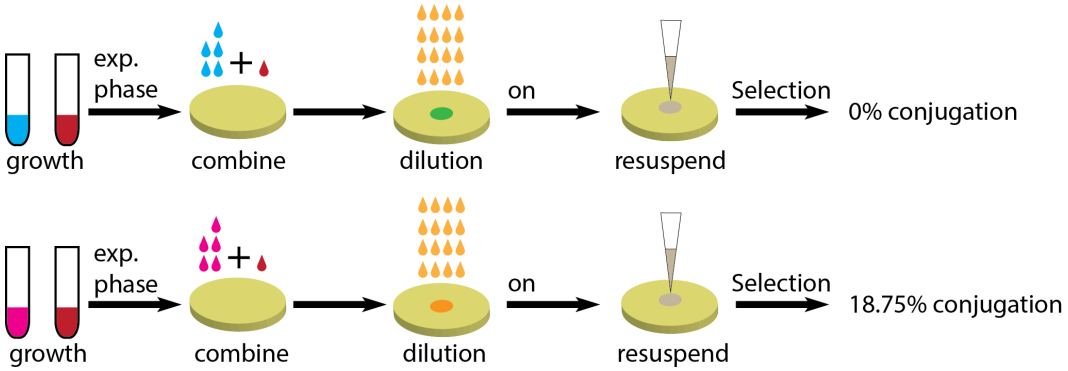

Figure 2.19.: **Reduced concentration of antibiotics does not increase conjugation success rate.** (A) Mating of donor strain SW105 (pRK24-kan; *hsp-1*) with recipient strain HT115(*ogt-1*) on LB agar plates. Donor and recipient cultures were combined at a ratio of 5:1, diluted with increased volumes of non-seletive LB medium and incubated O/N at 32 °C. The next day selection for cells containing both, donor and recipient plasmids on $LB^{Amp+Tet+Cam}$ plates. (B) as in A but using donor strain HT115 (pRK24-kan; *hsp-1*).
See app. A.12 on page 120 for detailed results.

An overabundance of donor cells compared to recipient cells improved the conjugation success rate, but very few colonies were obtained. Therefore, the conjugation efficiency was not sufficient to be used in high-throughput approaches. However, conjugation was inhibited when the mating mixture of donor and recipient was incubated on selective LB agar plates. Therefore higher amounts of non-selective LB medium was added to mitigate the potential inhibitory effects of antibiotics contained in the growth media (see fig. 2.19 on page 39). Contrary to what we had expected, very few colonies were formed on $LB^{Amp+Tet+Chl}$ plates at a dilution of 10^{-3}. Upon a second selection step only a small

subset of the colonies could be confirmed, irrespective of whether the *E. coli* donor strain SW105 or HT115 was used, indicating that neither strain is substantially more efficient than the other.

2.2.3.9. Functionality of conjugative F-plasmid not impaired by modification

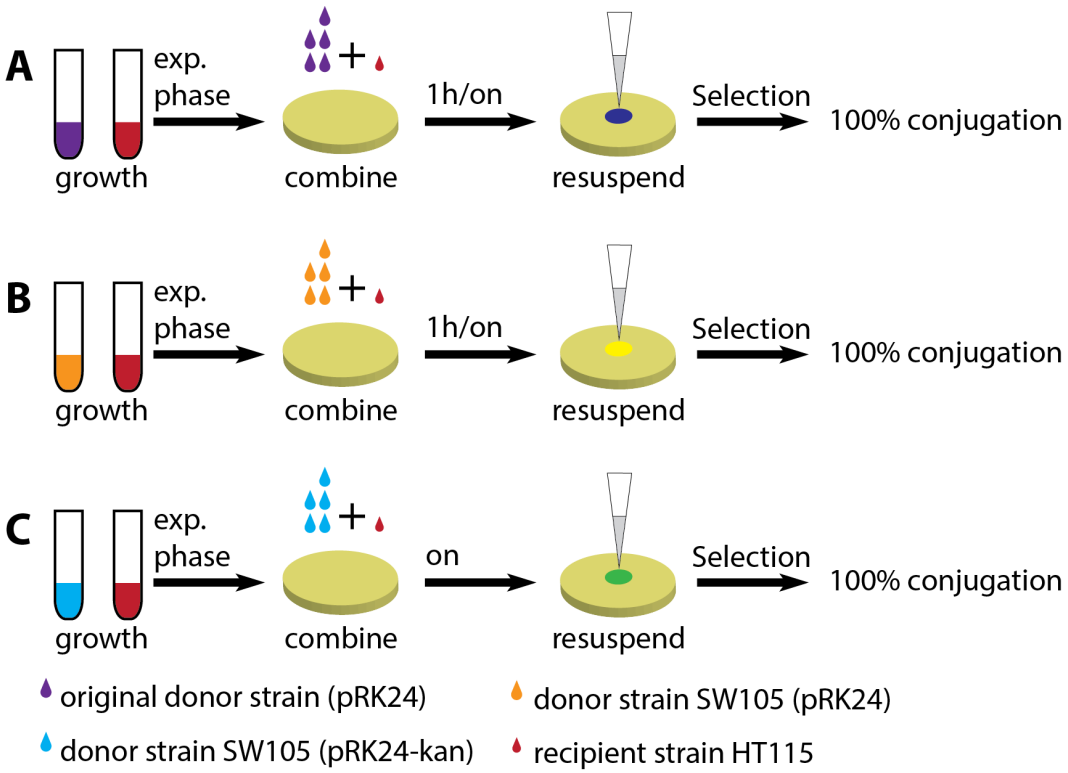

Figure 2.20.: **Modified F-plasmid pRK24-kan functional.** (A) Mating of original donor strain (ECNR2.δtolC.mutS:zeo) containing unmodified F-plasmid pRK24 with recipient strain HT115 (*ogt-1*). Donor and recipient cultures were combined at a ratio of 5:1, incubated at 32°C for 1h/ON. The next day selection for cells containing both, donor and recipient plasmids on $LB^{Amp+Tet+Cam}$ plates. (B) as in A but using donor strain SW105 carrying unmodified F-plasmid pRK24. (C) as in A but using donor strain SW105 carrying modified F-plasmid pRK24-kan.
See app. A.13 on page 121 for detailed results.

Donor RNAi plasmids could be transferred by conjugation, using the *E. coli* host strains SW105 or HT115, but at a low efficiency. This brought up the question whether the modified F-plasmid pRK24-kan functions properly after bacterial recombineering, during which the resistance gene had been exchanged. For this purpose the original F-plasmid (pRK24) in its original host strain (ECNR2.δtolC.mutS:zeo) was compared with unmodified pR24-Amp and pRK24-kan in *E. coli* strain SW105 (see fig. 2.20 on

page 40).

The mating mixtures were incubated either for 1h or O/N without the addition of non-selective LB medium. For the unmodified pRK24 plasmid in its original host strain (ECNR2.δtolC.mutS:zeo) or in *E. coli* SW105 affected the length of incubation not the conjugation success rate. In colonies streaked out on $LB^{Amp+Tet+Chl}$ in the secondary selection step were positive, suggesting that they were true-positives. Colonies obtained from the conjugation after incubating O/N using the modified pRK24-kan F-plasmid all streaked out colonies were positive as well, indicating that the functionality of the modified F-plasmid pRK24-kan is not impaired.

2.2.3.10. Recombination deficient donor strain improves conjugation efficiency at different growth phases

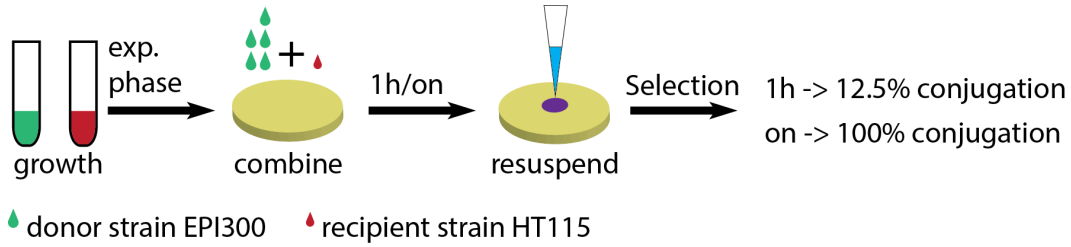

Figure 2.21.: **Improved conjugation using recombination deficient new donor strain EPI300.** Mating of recombination deficient donor strain EPI300 (pRK24-kan; *hsp-1*) with recipient strain HT115 (*ogt-1*). Donor and recipient culture were grown until exponential phase and mixed at a 5:1 ratio. The mating mixture was incubated at 37°C for 1h or O/N on LB agar plates. The next day selection for cells containing both, donor and recipient plasmids on $LB^{Amp+Tet+Cam}$ plates. See app. A.14 on page 121 for detailed results.

To improve the conjugation success rate a new donor strain was generated, using the recombination deficient *E. coli* strain EPI300(pRK24-kan; *hsp-1*). Using an overabundance of the donor strain, both, donor and recipient strain were combined and incubated at 37°O/N. The resulting colonies all grew when streaked out on $LB^{Amp+Tet+Chl}$. The growth phase of the donor culture did not affect the conjugation efficiency. In a second experiment, the donor culture was grown until the late exponential phase and the recipient culture was grown until the stationary phase. The mating mixture was incubated for 1h or O/N, followed by plating and subsequent streak out on $LB^{Amp+Tet+Chl}$ plates. When reducing the incubation time from O/N to 1h the conjugation success rate was drastically reduced from 100% to 12.5% (see fig. 2.21 on page 41), suggesting that incubation times longer than 1h are required.

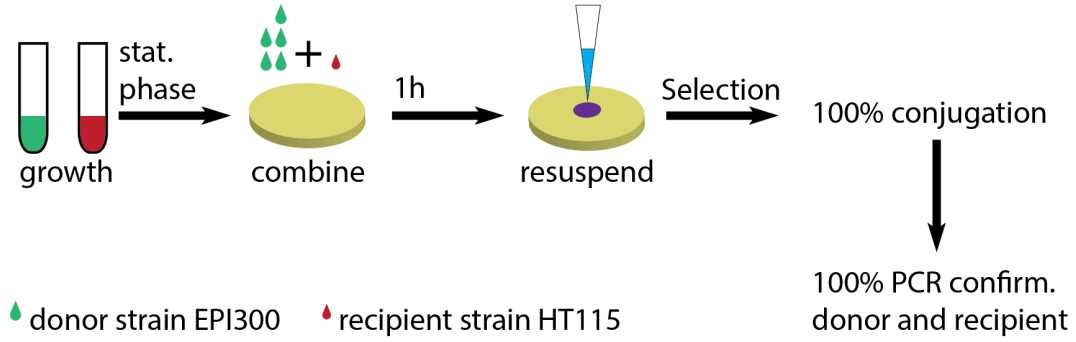

Figure 2.22.: **Conjugation efficiency unaffected by the usage of overnight cultures.**
Mating of donor strain EPI300 (pRK24-kan; *hsp-1*) with recipient strain HT115 (*ogt-1*) . Donor and recipient culture were grown O/N until stationary phase, combined at a ratio of 5:1 donor to recipient and incubated for 1h at 37°C non-selective LB agar plates. The next day selection for cells containing both, donor and recipient plasmids on $LB^{Amp+Tet+Cam}$ plates. See app. A.15 on page 121 for detailed results.

2.2.3.11. Overnight cultures of donor and recipient strains adequate for conjugation

Up to now bacterial cultures had been grown until reaching an OD_{600} of 0.8-1.2. Previous results have shown that using donor or recipient cultures in the stationary phase (OD_{600} > 1.0) does not affect the conjugation success rate. To simplify the protocol and make it applicable for high-throughput approaches it was tested, whether bacteria cultures grown O/N with an OD_{600} of > 1.5 could also be used.

Donor and recipient cultures were mated on non-selective LB agar plates for 1h at 37°C (see fig. 2.22 on page 42). Colonies from the conjugation were first streaked out on $LB^{Amp+Tet+Cam}$ plates. All colonies were positive, which could also be confirmed by colony PCR testing for donor and recipient plasmid. Thus, overnight cultures that are in stationary phase can mate with no reduction in conjugation efficiency.

2.2.3.12. Conjugation success rate is not affected by growth phase

After showing that bacterial cultures in late stationary phase mate without a reduction of efficiency, the question arose whether the growth phase did affect the conjugation success rate in any way. To test this, donor and recipient cultures were grown either until exponential or stationary phase, mated for 1h at 37°C and incubated O/N on selective medium (see fig. 2.23 on page 43). Colonies were streaked out on $LB^{Amp+Tet+Cam}$ plates and tested by PCR for donor and recipient plasmid. The conjugation success rate was at 100% independent of the growth phase, suggesting that mating is not affected by bacterial cultures being in the stationary or exponential growth phase.

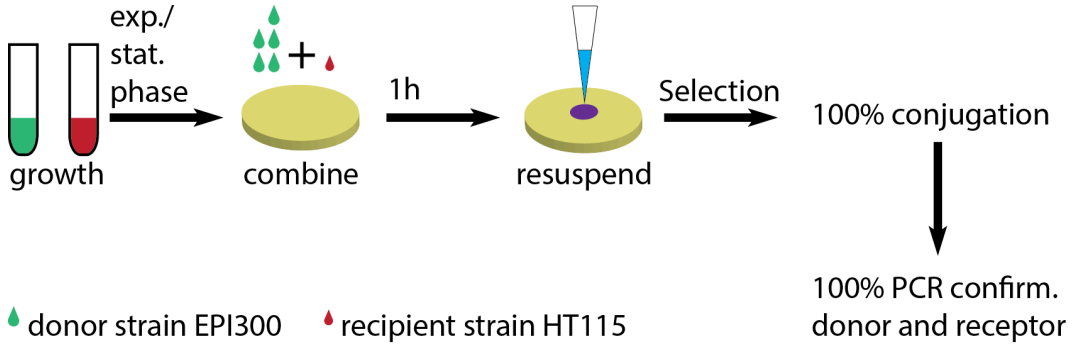

Figure 2.23.: **Bacterial growth phase does not affect conjugation efficiency.** Mating of donor strain EPI300 (pRK24-kan; *hsp-1*) with recipient strain HT115 (*ogt-1*) . Donor and recipient culture were grown either until exponential or stationary phase, combined at a ratio of 5:1 donor to recipient and incubated for 1h at 37°C non-selective LB agar plates. The next day selection for cells containing both, donor and recipient plasmids on $LB^{Amp+Tet+Cam}$ plates. See app. A.16 on page 122 for detailed results.

2.2.3.13. Translation of double RNAi by conjugation protocol to high-throughput approach

In order to transfer our conjugative plasmids to high-throughput with a large set of RNAi plasmid carrying bacteria, it was necessary to switch from 6 cm to 96-well LB agar plates. Each well was filled with 100 µL of LB agar and plates were left to dry O/N. Conjugation was performed with donor and recipient strains grown until stationary phase, then mated in a 5:1 ratio and incubated at 37 °C for 1h. Following incubation, the wells were washed off with LB and the resuspended media was incubated in $LB^{Amp+Tet+Cam}$ O/N. The overnight cultures were subjected to a secondary selection step in $LB^{Amp+Cam}$ O/N. First results showed a high variance of conjugation success rate after the second selection step ranging from 50 to 90 % (see).(see. fig. 2.24A on page 44)
From initial experiments it was known that conjugation did not occur in liquid medium. The total mating mixture volume of donor and recipient was 25 µL (20 µL donor culture and 5 µL recipient culture). The mating mixture would not dry in the well as it did on 6 cm agar plates. To reduce the total volume the concentration of the donor strain was increased by factor 4. Subsequently, 5 instead of 20µL of donor culture were mixed with 5 µL of recipient and the conjugation success rate increased up to over 90 % (see. fig. 2.24B on page 44)

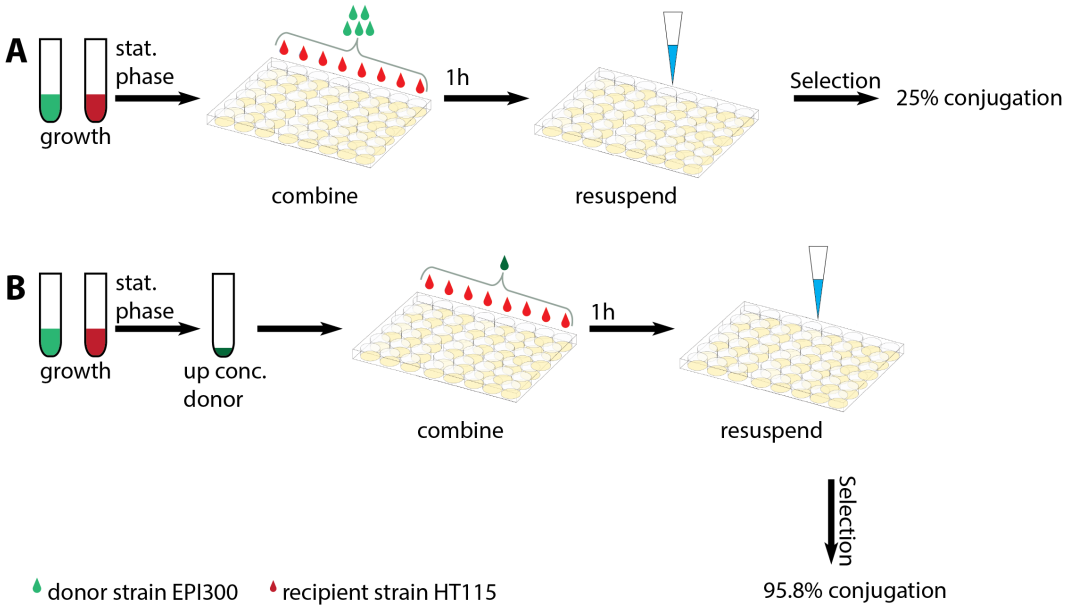

Figure 2.24.: **Reduction of mating mixture volume increases conjugation efficiency in 96-well format.** (A) Mating of donor strain EPI300 (pRK24-kan; *hsp-1*) with recipient strain HT115 (*ogt-1*). Donor and recipient cultures were grown until stationary phase, combined at a ratio of 5:1 donor to recipient and incubated for 1h at 37°C non-selective LB agar plates. The next day selection for cells containing both, donor and recipient plasmids on $LB^{Amp+Tet+Cam}$ plates. (B) as in A, but the donor culture was up concentrated to have an overabundance of donor cells in the mating mixture while simultaneously reducing the total volume of mixed donor and recipient cells.
See app. A.17 on page 122 for detailed results.

2.2.4. Proof-of-principle experiments

2.2.4.1. Proof-of-concept: Synthetic lethality

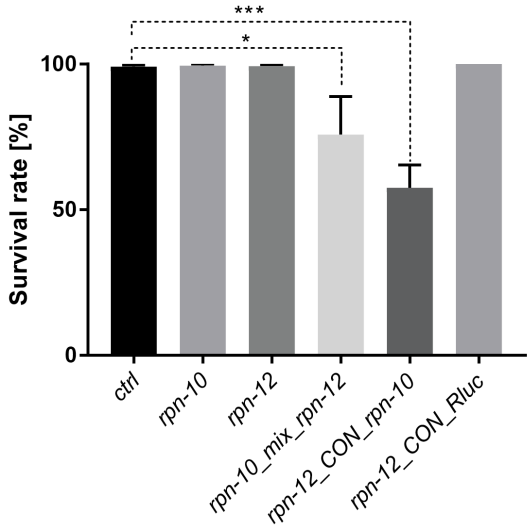

Figure 2.25.:
Co-knockdown of *rpn-10* and *rpn-12* is synthetically lethal. Relative quantification of survival rate of N2 animals on F1 RNAi by comparing number of layed eggs to L4 animals. P-values were calculated using one way ANOVA and Dunnett's multiple comparisons test comparing to ctrl RNAi (ns = $P \geq 0.5$, * = $P \leq 0.05$, *** = $P \leq 0.001$). Error bars represent SEM from three independent RNAi experiments, n = 120 to 300 for each RNAi.

Modified RNAi plasmids can be transferred by bacterial conjugation to generate bacterial cells, carrying two different RNAi plasmids, which could be demonstrated by antibiotic selection and subsequent detection by PCR. Following the demonstration of generating double RNAi clones that contain two differnt dsRNA plasmids, it was tested, whether the transferred RNAi plasmid was functional and able to be used as a template to knock down a target gene.
Takahashi et al. (2002) depleted 26S Proteasome subunits by RNAi and showed that a knock down of either *rpn-10* and *rpn-12* does not affect the survival rate, whereas the simultanoeus knockdown of *rpn-10* and *rpn-12* is synthetically lethal. A donor strain targeting *rpn-12* was created to generate *rpn-12*_CON_*rpn-10* as well as *rpn-12*_CON_Rluc to be used as a control. L4 animals were transferred on RNAi to lay eggs. The next day mother animals were taken off the plate and the eggs counted. The survival rate was calculated by comparing the number of laid eggs to the number of L4 animals. As figure 2.25 on page 45 shows, the RNAi knockdown of either *rpn-10* or *rpn-12* does not affect the survival rate of worms when compared to control RNAi. When rpn-10 and *rpn-12* containing RNAi bacteria are mixed in a well, the survival rate decreases by approximately 30 %. However, when *rpn-10* is combined with *rpn-12* via conjugation in a single bacterial cell, the survival rate is reduced by 50%, showing a trend of double RNAi by conjugation being more potent than the mixing of two RNAi bacteria strains. Conjugating *rpn-12* with control RNAi did not affect the survival rate, suggesting that the generated double RNAi clone *rpn-12*_CON_*rpn-10* simultaneously knocked down both targets and therefore induced synthetic lethality.

2.2.4.2. Proof-of-concept: Arrested oocyte maturation

During development oocyctes arrest at the prophase of the first meiotic division. The release from this prophase arrest is termed oocyte maturation. Detwiler et al. (2001) demonstrated in *C. elegans* that two TIS11 zinc finger-containing proteins, OMA-1 and OMA-2, are required for oocyte maturation. Both proteins share 64% identity throughout the entire amino acid sequence and are nearly identical in the two zinc fingers.
In wild type *C. elegans* hermaphrodites the reproductive system consists of two distal gonad arms, which are joined, and share a uterus (see fig. 2.26A on page 47). Both gonadal arms are filled with germ nuclei that proliferate mitotically before entering meiotic prophase I and initiating oogenesis. Oocytes grow in nuclear and cytoplasmic volumes after cellularization and late oogenesis. The fully grown oocytes remain in diakinesis of prophase I. If sperm is present, oocytes undergo maturation and are ovulated into the spermatheca where fertilization occurs and subsequently passed into the uterus. In wild type worms ovulation occurs in an assembly-line fashion. *oma-1; oma-2* (RNAi) animals produce sperm and oocytes, but not embryos and the uterus is empty. The gonadal arms in animals subjected to combinatorial RNAi againt *oma-1* and *oma-2* fill up with an abnormally large number of oocytes that accumulate even beyond the bend of the gonadal arm. In contrast, oocytes in wild type animals occupy less space. To recapitulate the induction of arrested oocyte maturation upon simultaneous knockdown of *oma-1* and *oma-2*, wild type N2 animals were subjected to RNAi and the progeny was scored at adult stage for arrested oocyte maturation by looking for the empty uterus and the accumulation of oocytes in the gonadal arms.

Figure 2.26B on page 47 shows that the oocyte development under control conditions, as well as when knocking down either *oma-1* or *oma-2*, by itself is not affected. However, animals on combinatorial RNAi generated by conjugation against *oma-1* and *oma-2* show a strongly increased onset of arrested oocyte development. Three different *oma-1*_CON_*oma-2* clones were compared, yielding similar results, indicating that double RNAi conjugation generates reliable combinatorial RNAi clones.

2.2.4.3. Proof-of-concept: Induction of ectopical expression of pan-neuronal reporter

Ciosk et al. (2006) demonstrated that MEX-3 and GLD-1 are essential for maintaining totipotency in the *C. elegans* germ line. Upon knockdown of *gld-1* and *mex-3*, germ cells transdifferentiate into somatic cell types such as neurons. GLD-1 belongs to a family of the signal transduction and activation RNA (STAR) family of KH-domain, RNA-binding proteins and is expressed primarily in the central gonad. MEX-3 is expressed complementary and contains two KH-domains, but is otherwise dissimilar to GLD-1. The double knockdown of *gld-1* and *mex-3* increases the percentage of gonads with somatic cells when compared to *gld-1* alone (Ciosk et al., 2006). A *gld-1* donor strain was generated and mated with *mex-3* RNAi containig bacteria, as well as *Rluc* as control. Worms carrying a *rab-3::tRFP* reporter construct were subjected to RNAi as L4 animals and the progeny was scored as late adult for the ectopic expression of *rab-3::tRFP* in the germ

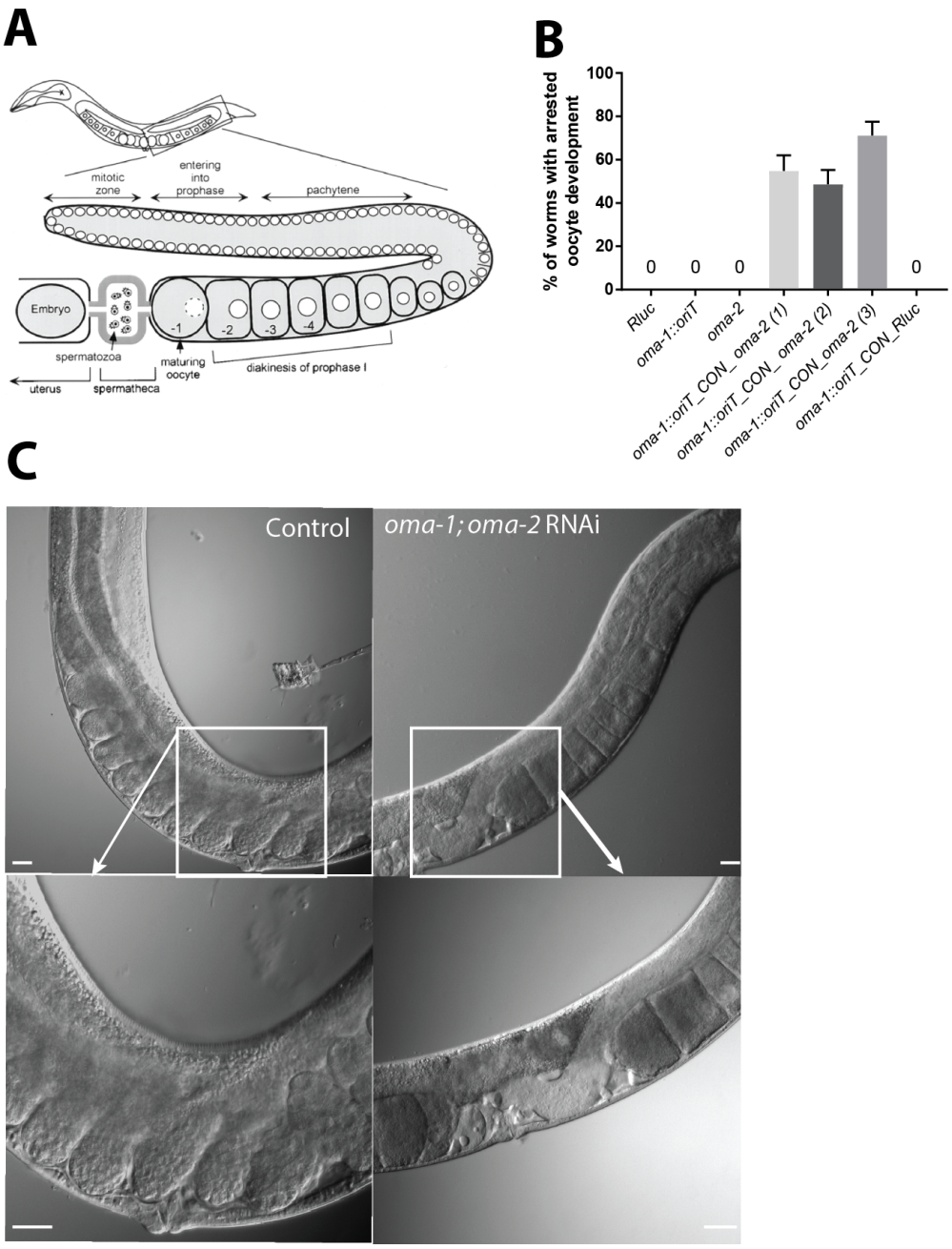

Figure 2.26.: **Arrested ooycyte development in *oma-1; oma-2* (RNAi) animals.** (A) Schematic depiction of a wild-type *C. elegans* adult hermaphrodite gonadal arm. In the distal region germ cells proliferate mitotically and then enter prophase of meiosis I before they form mature oocytes. Modified after Detwiler et al. (2001). (B) Quantification of animals that show arrested ooycyte development, comparing three separate clones. Error bars represent SEM from three independent RNAi experiments, n = 150 to 240 for each RNAi. (C) On control RNAi (left) the distal gonadal arm is empty of oocytes. Proximally oocytes mature and pass into the uterus. In animals subjected to *oma-1*; *oma-2* double RNAi oocytes arrest and accumulate even beyond the bend of the gonadal arm. The uterus is empty of oocytes.

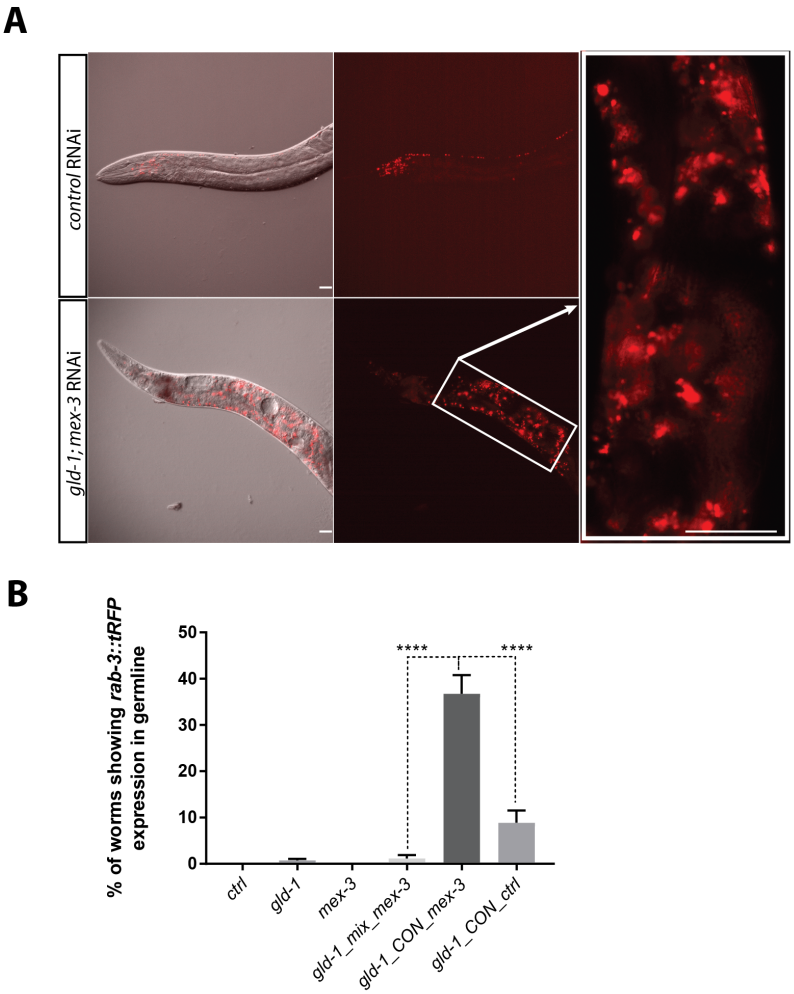

Figure 2.27.: **Ectopic expression of pan-neuronal reporter *rab-3::tRFP* in the germ line in *gld-1*; *mex-3* (RNAi animals).** (A) Worms expressed *rab-3::tRFP* in the germ line upon knockdown of *gld-1* and *mex-3*. Scale bar = 20 µm (B) Quantification of animals mis-expressing *rab-3::tRFP* in germ line. P-values were calculated using one way ANOVA and Tukey's multiple comparisons test (ns = $P \geq 0.5$, *** = $P \leq 0.001$). Error bars represent SEM from three independent RNAi experiments, n = 140 to 300 for each RNAi.

line.
Figure 2.27B on page 48 shows that in *gld-1* (RNAi) animals less than 5% of germ cells express the pan-neuronal reporter *rab-3*. Mixing of *gld-1* and *mex-3* RNAi containing bacteria did not result in the loss of germ cell totipotency, whereas animals subjected to *gld-1*_CON_*mex-3* RNAi showed a significantly increased amount of germ cells expressing *rab-3::tRFP* ($P \leq 0.001$, Dunnett's multiple comparisons test), suggesting that combinatorial RNAi by conjugation is more reliable than by mixing.

2.2.4.4. Proof-of-concept: Induced synthetic multivulva

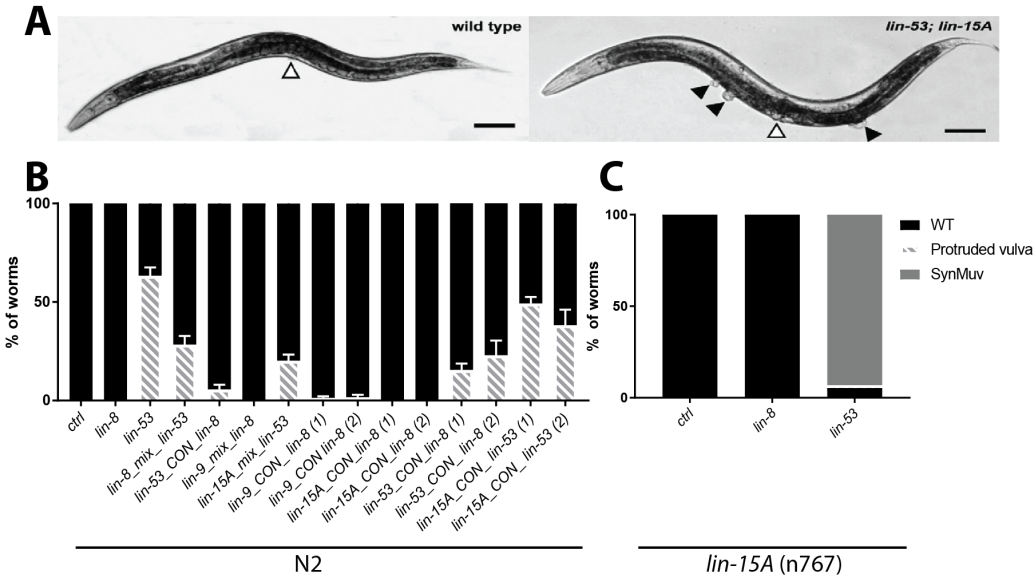

Figure 2.28.: **Combinatorial RNAi insufficient to induce SynMuv phenotype.** (A) Depiction of synmuv phenotype in *lin-53; lin-15A* double mutants. Figure modified after Andersen et al. (2006). (B) Quantification of N2 animals showing protruding vulva or synthetic multi vulva. Error bar represent SEM from two independent experiments, n = 160 to 240 for each RNAi. (C) As in B but using *lin-15A* -/- worms, n = 170 to 240 for each RNAi.

The synthetic multivulva (synmuv) phenotype is characterized by the formation of additional vulvas during development (see fig. 2.28A on page 49) and caused by two unlinked recessive mutations, neither of which is sufficient to cause the phenotype. Based on classical forward screens, genes were grouped into class A or B, whereby the simultaneous knockout of a gene from each class is required to induce the formation of synthetic multi vulvas (synmuv) during development (reviewed in Fay, Yochem (2007)).
Wild type worms at L4 were subjected to RNAi for knockdown of *lin-8*, *lin-53*, and *lin-8*_mix_*lin-53* (see figure 2.28C) and the progeny was scored at L4/YA stage for protruding and multivulva. In addition, donor strains for *lin-9*, *lin-15A*, and *lin-53* were generated. Synmuv class A gene *lin-15A* was mated with synmuv class B gene *lin-53*,

whereas *lin-53* and *lin-9* (class B) were mated with synmuv class A gene *lin-8*. The protruding vulva is caused by knockdown of *lin-53*, thus allowing to assess the effect of *lin-53* RNAi. Combinatorial RNAi by mixing was performed by combining bacteria containing RNAi against *lin-9*, *lin-15A*, and *lin-53* together with *lin-8* and *lin-53*, respectively. *lin-53* (RNAi) animals displayed the protruding vulva, thus confirming the proper function of the *lin-53* RNAi donor plasmids, whereas no worm showed the formation of synthetic multivulva (see fig. 2.28B on page 49), suggesting that combinatorial RNAi might be insufficient.
To test whether a knockout was required to induce the synthetic multivulva phenotype, *lin-15A* (n767) mutants were used. As a control *lin-15A* (n767) mutants were tested on ctrl RNAi as well as *lin-8* RNAi, which belongs to the same gene class as *lin-15A*, in which worms showed normal vulva development. *lin-15A* (n767) mutants subjected to *lin-53* RNAi (class B) resulted in over 90% of worms showing multivulva, indicating that combinatorial RNAi against *lin-15A* and *lin-53* is insufficient to induce the formation of additional vulvas.

2.2.5. Performing enhancer screen for *lin-53* RNAi mediated *unc-25::gfp* induction in germ line

Previously it was shown that LIN-53 acts as a barrier to the conversion of germ cells upon expression of the terminal transcription factor UNC-30 (Tursun et al. (2011)). Using the newly generated line, expressing *unc-30* under a heat shock promoter, these results could be confirmed. Less than 20% worms on *lin-53* RNAi while overexpressing UNC-30 show *unc-25::gfp* expression in the germ line(see fig. 2.30C on page 52). The aim of our screen was to increase the *unc-25::gfp* induction efficiency by identifying genetic interaction partners of *lin-53*. Synchronized L4 worms were transferred to RNAi plates. The progeny was subjected to a heat shock to activate the ectopic expression of *unc-30* and the worms would be scored on the following day (see fig. 2.29A on page 51).

Our lab has generated a RNAi sub-library containing about 800 chromatin-related genes, such as functions in chromatin structure, regulation of transcription or the modification of histones (see fig. 2.29B on page 51). LIN-53 is a histone chaperone (RbAp46/48 in humans) and its ortholog in various species have been found to be a component of several histone remodeling and modifying complexes such as HAT1 histone acetyltransferase complex, CAF1 chromatin assembly factor complex, Sin3 transcriptional repressor complex, PRC2 histone methyltransferase complex (Eitoku et al., 2008; Loyola, Almouzni, 2004). To identify potential interaction partner of *lin-53*, a *lin-53* donor strain was generated and mated with each RNAi clone of the Chromatin sub-library (see fig. 2.29C on page 51)

2.2.5.1. Co-knockdown of *rbbp-5* and *lin-53* leads to increased expression rate of *unc-25::gfp* in germ line

Candidates from the primary screen were re-tested in F1 RNAi (see fig. 2.30B on page 52). As a control *lin-53* was conjugated with Rluc. The co-knockdown of *lin-53* and

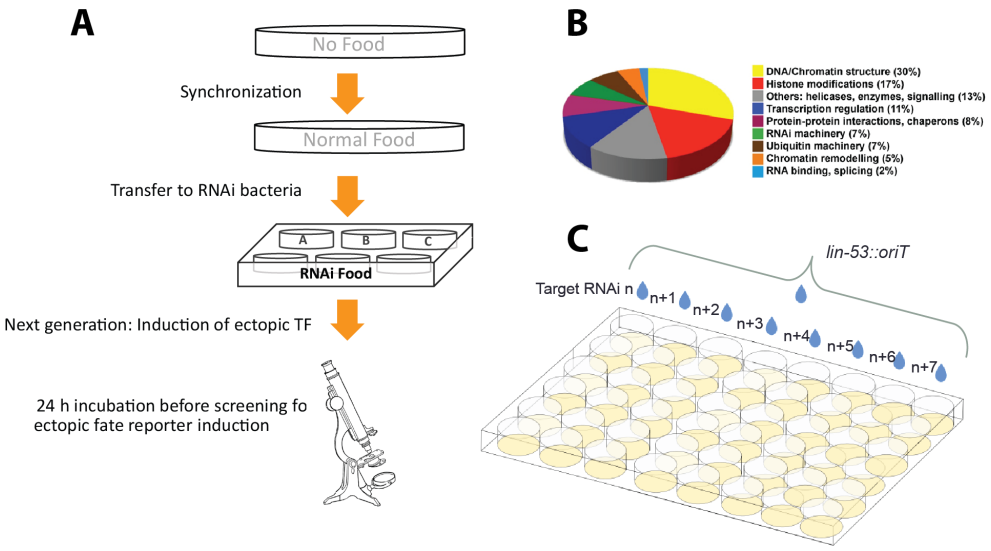

Figure 2.29.: **Enhancer screen for *lin-53* RNAi-mediated ectopic induction of *unc-25::gfp* in the germ line.** (A) For F1 RNAi experiments worms were synchronized by harvesting and transferred as L4 to RNAi bacteria. Ectopic expression of *unc-30* in F1 generation and quantification of ectopic induction of *unc-25::gfp* 24 h later. (B) A detailed breakdown of the targeted factors by the Chromatin RNAi sub-library 2.0 showing that targeted chromatin regulating factors are implicated in a variety of different biological processes. (C) Donor strain containing modified *lin-53* RNAi plasmid with oriT site was mated with every single RNAi clone from the Chromatin 2.0 sub-library by pipetting donor and recipient on 96-well plates together, incubation for 1h at 37°C. The next day mating mixtures were subjected antibiotic selection on $LB^{Amp+Tet+Cam}$ medium to select for clones that contain donor and recipient plasmid.

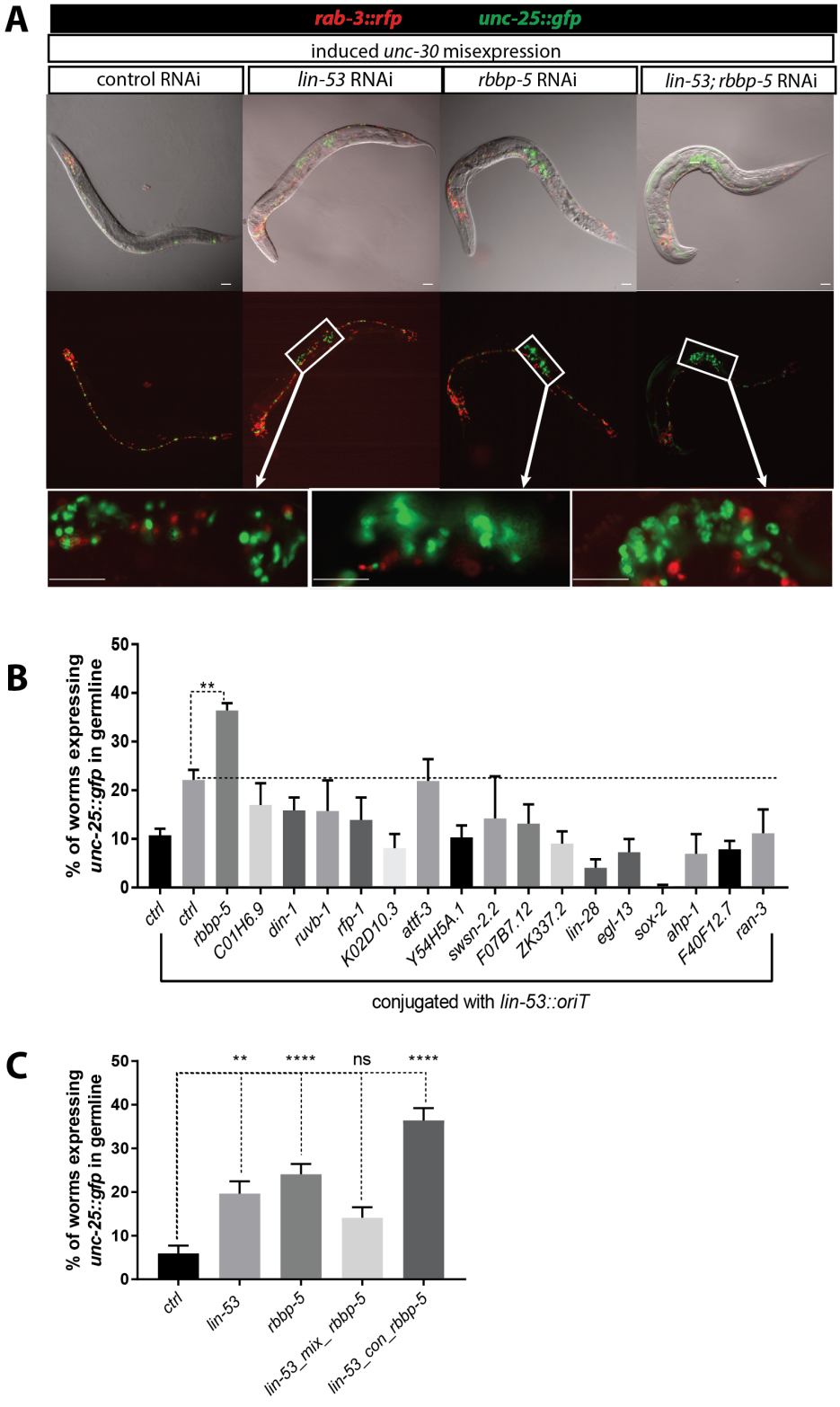
A
rab-3::rfp
unc-25::gfp
induced unc-30 misexpression
control RNAi
lin-53 RNAi
rbbp-5 RNAi
lin-53; rbbp-5 RNAi
B
% of worms expressing unc-25::gfp in germline
**
ctrl
ctrl
rbbp-5
C01H6.9
dlin-1
ruvb-1
rfp-1
K02D10.3
atff-3
Y54H5A.1
swsn-2.2
F07B7.12
ZK337.2
lin-28
egl-13
sox-2
ahp-1
F40F12.7
ran-3
conjugated with lin-53::oriT
C
% of worms expressing unc-25::gfp in germline
**
****
ns
****
ctrl
lin-53
rbbp-5
lin-53_mix_ rbbp-5
lin-53_con_rbbp-5

Figure 2.30.:

Figure 2.30.: **Increased *unc-25::gfp* induction efficiency upon RNAi against *lin-53* and *rbbp-5*.** (A) Transgenic background *hsp-16.2/4::unc-30*, *unc-25::gfp*, *rab-3::tRFP* was used for screening. Control animals show expression of *unc-25::gfp* in GABAergic neurons on the ventral side of the worm. F1 RNAi against *lin-53* and *rbbp-5* allows overexpressed *unc-30* to induce *unc-25::gfp* in the germ line. Magnification (white box) indicates that GFP-positive cells do not adapt neuronal morphology by showing axo-dendritic outgrowths of protrusions. Scale bar = 20 µm. (B) Quantification of animals expressing *unc-25::gfp* in the germ line upon overexpression of *unc-30*. Double RNAi using conjugated RNAi clones identified in primary screen testing for genetic interactions with *lin-53* P-values were calculated using one way ANOVA and Dunnett's multiple comparisons test (ns = $P \leq 0.05$, * = $P \leq 0.05$, ** = $P \leq 0.01$, *** = $P \leq 0.001$, and **** = $P \leq 0.0001$). Error bars represent SEM from three independent RNAi experiments, n = 300 to 500 for each RNAi. (C) Quantification of animals expressing *unc-25::gfp* in the germ line upon overexpression of *unc-30*. P-values were calculated using one way ANOVA and Dunnett's multiple comparisons test (ns = $P \leq 0.05$, * = $P \leq 0.05$, ** = $P \leq 0.01$, *** = $P \leq 0.001$, and **** = $P \leq 0.0001$). Error bars represent SEM from three independent RNAi experiments, n = 280 to 500 for each RNAi.

rbbp-5 significantly increased the *unc-25::gfp* expression efficiency ($P \leq 0.01$, Dunnett's multiple comparisons test). With the exception of LIN-53 co-depleted with ATTF-3 showed all other candidates a reduction of induced GABA fate reporter expression compared to *lin-53*_CON_Rluc.

To test whether *rbbp-5* and *lin-53* might genetically interact, RNAi against *rbbp-5* alone was performed showing that co-knockdown of *lin-53* and *rbbp-5* caused a significantly greater increase in *unc-25::gfp* induction efficiency when compared to *rbbp-5* alone ($P \leq 0.001$, Dunnett's multiple comparisons test). Surprisingly, mixing *lin-53* and *rbbp-5* RNAi did not permit a significant increase of ectopic GABA fate reporter induction when compared to control RNAi ($P \leq 0.05$, Dunnett's multiple comparisons test), indicating that the additive effect of co-depleting LIN-53 and RBBP-5 might not have been found in double RNAi by mixing.

2.2.5.2. *unc-25::gfp* positive germ cells also express Rab3a-interacting protein (RIM)

A typical characteristic of neurons is the process of neurotransmission by which neurotransmitters are released, bind to postsynaptic receptors and cause a change in the postsynaptic neuron. The site of neurotransmitter release is defined as the active zone that contains a highly interactive protein-rich web that is opposite to the postsynaptic density composed of neurotransmitter receptors (Harlow et al., 2001; Phillips et al., 2001). Using transgenic reporters, it also has been demonstrated that animals on *lin-53*_CON_*rbbp-5* RNAi start to express *unc-25*, which is the *C. elegans* ortholog of the GABA neurotransmitter biosynthetic enzyme, glutamine acid decarboxylase (GAD), in

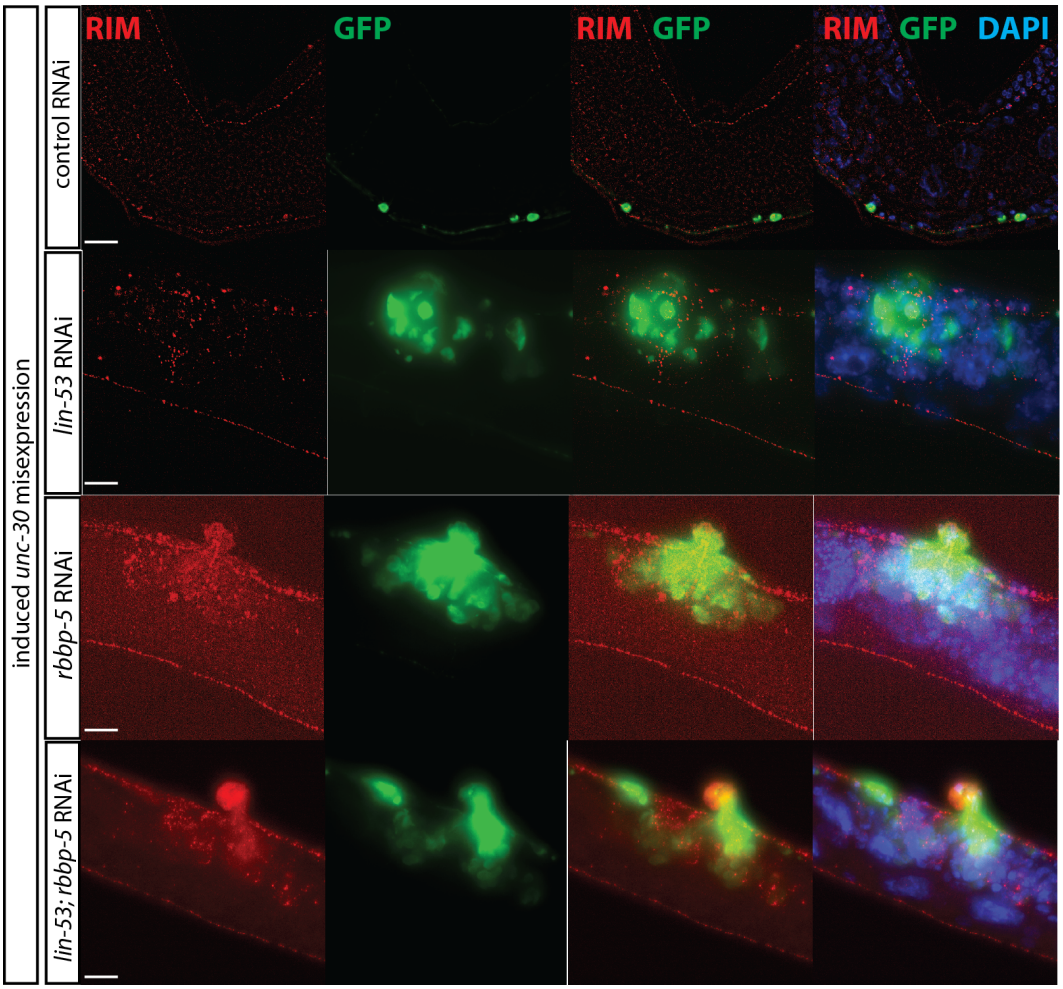

Figure 2.31.: **Germ cells positive for *unc-25::gfp* also express active zone protein RIM.** Antibody staining of RIM and GFP proteins in the germ line of young adult hermaphrodites. Transgenic background *hsp-16.2/4::unc-30*, *unc-25::gfp*, *rab-3::tRFP* was used for staining. Animals were subjected to RNAi and stained 24 h post heat shock. Scale bar = 20 µm.

Table 2.1.: Conserved components of the COMPASS complex in *C. elegans*, yeast, and human.

S. cerevisae	Human	*C. elegans*
	SET1	*set-2*
set1	MLL1	*set-16*
	MLL2	
	MLL3	
bre2	Ash2L	*ash-2*
swd1	RbBP5	*rbbp-5*
	WDR5	*wdr-5.1*
swd3		*wdr-5.2*
		wdr-5.3
spp1	CxxC1/Cfp1	*cfp-1*
swd2	WDR82	*wdr-82*
sdc1	hDPY30	*dpy-30*
shg1		

the germ line when additionally *unc-30* is overexpressed. To characterize the neuron-like cells further, worms were stained for the active zone specific Rab3a-interacting protein (RIM) (Dresbach et al., 2001; Rosenmund et al., 2003). Fig. 2.31 on page 54 shows that RIM proteins are co-localized with ectopic *unc-25::gfp* expression, indicating that they are indeed converting from germ cells to GABA neuron-like cells.

2.2.6. Co-depletion of LIN-53 and members of the COMPASS complex does not increase reprogramming efficiency

RBBP-5 is part of the Set-1/ML or COMPASS (Mixed Lineage Leukemia/Complex Proteins Associated with Set1) complex that is responsible for the methylation of lysine 4 of histone 3 and also found in humans (see tab. 2.1 on page 55). The complex contains seven subunits that are all present in *C. elegans*, including RBBP-5, three WDR5-like proteins (WDR-5.1, .2, and .3), ASH-2, CFP-1, two histone methyltransferases (SET-2 and SET-16), as well as either WDR-82 or DPY-30 (Li, Kelly, 2011). Various components of the COMPASS complex are involved in aging (Greener et al 2010), dosage compensation (Pferdehirt, 2011), vulval development (Fisher et al 2010) and neuronal development (Poole 2011).

To test for further genetic interactions of *lin-53* with the COMPASS complex, double RNAi bacteria were generated by conjugation with the *lin-53* donor strain. The *unc-25::gfp* induction efficiency was compared to *lin-53*_CON_Rluc. With the exception of *rbbp-5*, none of the tested simultaneously knocked down COMPASS complex members showed a significant increase in induction efficiency ($P \leq 0.05$, Dunnett's multiple comparisons test). On the contrary, most showed a strong decrease of ectopic GABA reporter induction when compared to *lin-53*_CON_Rluc. This suggests that if *lin-53* and *rbbp-5* genetically interact, it is independently of the COMPASS complex. Further-

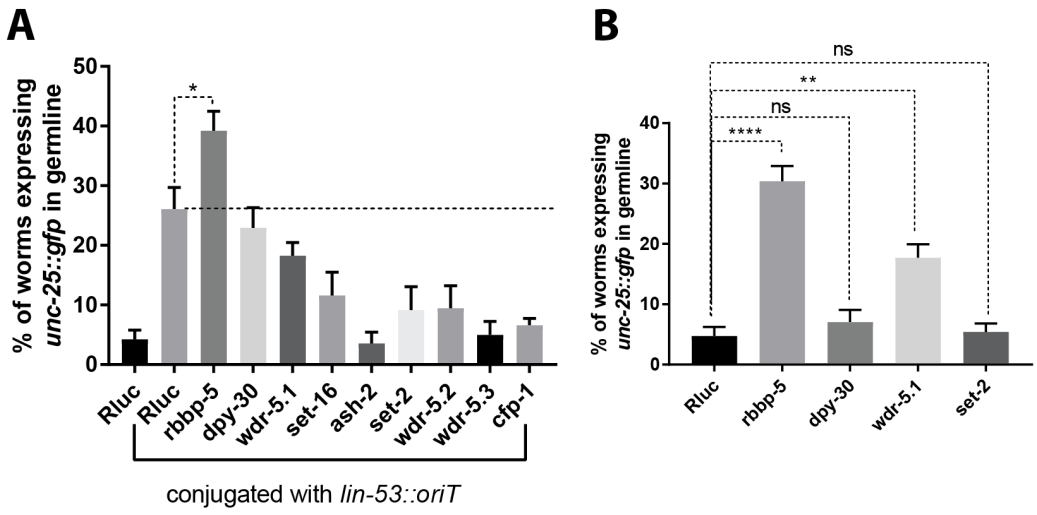

Figure 2.32.: ***lin-53* does not genetically interact with members of the COMPASS complex.** (A) Transgenic background *hsp-16.2/4::unc-30*, *unc-25::gfp*, *rab-3::tRFP* was used for RNAi experiments. Double RNAi clones of members of the MLL/COMPASS complex and *lin-53* were generated by conjugation. Quantification of worms that express *unc-25::gfp* in the germ line after induced overexpression of *unc-30*. P-values were calculated using one way ANOVA and Dunnett's multiple comparisons test (ns = $P \leq 0.05$, * = $P \leq 0.05$, ** = $P \leq 0.01$, *** = $P \leq 0.001$, and **** = $P \leq 0.0001$). Error bars represent SEM from three independent RNAi experiments, n = 190 to 300 for each RNAi. (B) as in A, but performing single RNAi against selected members of the MLL/COMPASS complex. Error bars represent SEM from three independent RNAi experiments, n = 200 to 400 for each RNAi.

Table 2.2.: Known genetic interactors of *lin-53* and *rbbp-5*

lin-53 *interactors*			***rbbp-5*** *interactors*
lin-53	*lin-40*	*xnp-1*	*wdr-5.1*
chaf-1	*egl-27*	*fit-1*	*C31C9.2*
chaf-2	*rba-1*	*nurf-1*	*ctf-4*
mes-6	*lin-61*	*isw-1*	*gap-1*
lin-9	*dcp-66*	*pyp-1*	*mtq-2*
lin-35	*hda-1*	*mes-2*	*rad-50*
lin-37	*hda-2*	*mes-3*	*rnr-2*
lin-52	*hda-3*	*mes-6*	*swd-2.2*
lin-54	*chd-3*	*sin-3*	*ubp-1*
dpl-1	*let-418*	*C16C10.4*	*dpy-30*
hat-1	*mep-1*	*mbd-2*	*ash-2*

more, it indicates that the COMPASS complex is not a barrier to reprogramming, but actually required for UNC-30 to be able to induce the expression of *unc-25::gfp* in the LIN-53 depleted germ line.

2.2.7. Triple RNAi by conjugation identifies no enhancer of *lin-53*; *rbbp-5* RNAi mediated induction of *unc-25::gfp* in the germ line

Having demonstrated that *lin-53* does not genetically interact with the COMPASS complex via conjugation and subsequent co-knockdown, the question arose whether *lin-53* and *rbbp-5* have common genetic interaction partners. To test of enhancement of the induction efficiency observed upon simultaneous depletion of LIN-53 and RBBP-5 and overexpression of *unc-30*, a new donor strain was generated, containing target sequences for *rbbp-5* and *lin-53* (see. fig. 2.33A on page 58). The newly generated *lin-53*::*rbbp-5* donor strain was conjugated with a set of 36 known genetic interactors of *lin-53* and 11 of *rbbp-5* (see tab. 2.2 on page 57) to test for enhancement of *unc-25::gfp* induction efficiency when compared to *lin-53::rbbp-5*_CON_*Rluc*. For none of the 47 newly generated triple RNAi clones could an increase of induced *unc-25::gfp* expression in the germ line of worms be observed, indicating that *lin-53* and *rbbp-5* do not share common genetic interactors.

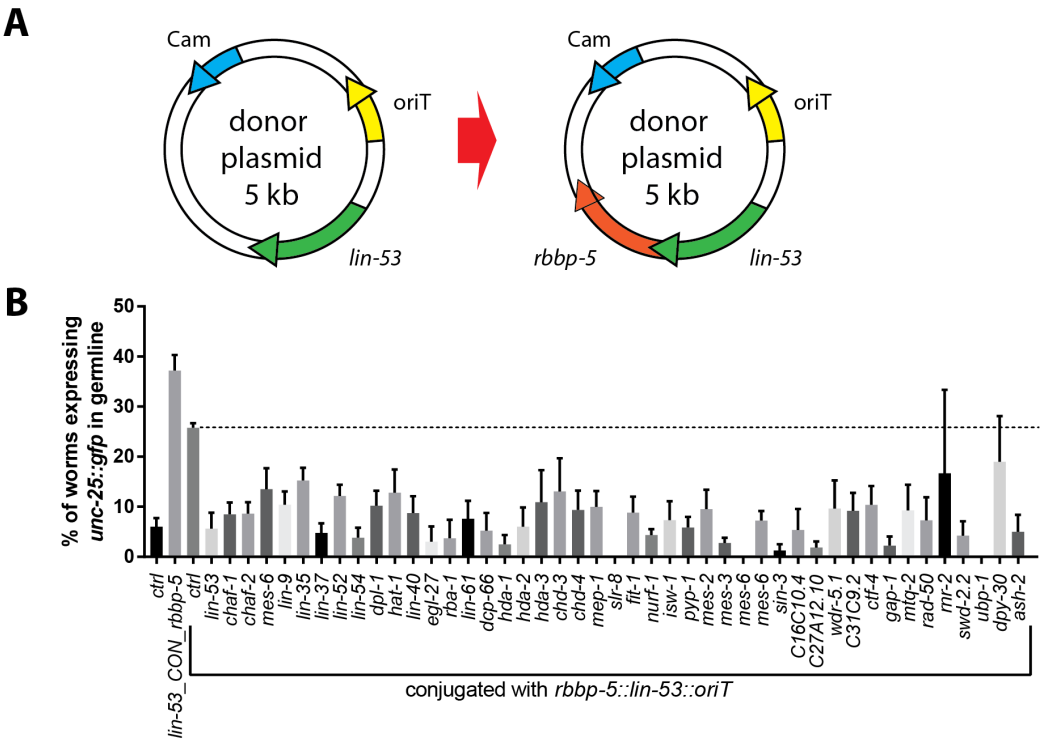

Figure 2.33.: **No identified enhancer of ectopic induction of *unc-25::gfp* in *lin-53*; *rbbp-5* (RNAi) animals.** (A) Schematic illustration of triple RNAi by conjugation. By generating a 'stitched' double RNAi donor plasmid, three genes can be selective knocked down. (B) Transgenic background *hsp-16.2/4::unc-30*, *unc-25::gfp*, *rab-3::tRFP* was used for RNAi experiments. Triple RNAi clones of known genetic interactors of either *lin-53* or *rbbp-5* and *rbbp-5::lin-53* were generated by conjugation. Quantification of worms that express *unc-25::gfp* in the germ line after induced overexpression of *unc-30*. Error bars represent SEM from three independent RNAi experiments, n = 30 to 100 for each RNAi.

3. Discussion

3.1. Double RNAi allows investigation of genetic interactions of essential genes in large scale screens

Originally it was assumed that differentiated cells are unable to adapt a new cell fate (Waddington, 1957). With the discovery of induced direct reprogramming a door opened for the development of new *in vitro* disease models, as well as the replacement of lost neuronal tissue in patients with neurodegenerative diseases (Gascón et al., 2017).

Shortly after the initial observation that overexpression of the transcription factor (TF) MyoD is sufficient to reprogram fibroblasts into muscle cells (Davis et al., 1987) it became apparent that other cell types were refractory to transdifferentiation into muscle cells (Weintraub et al., 1989), indicating that cell-type specific barrier factors prevent cell-fate conversion. The model organism *C. elegans* is perfectly suited to study direct reprogramming *in vivo* with its short life span, translucent body, and invariant cell lineage. Developing cells after the blastomere 8E stage in *C. elegans* become refractory to induced reprogramming upon overexpression of cell-fate inducing transcription factors, suggesting that the cells lose their plasticity (Yuzyuk et al., 2009).

Thus, the depletion of barrier factors is required in addition to overexpression of cell-fate inducing TFs to convert differentiated cells, which was demonstray by Tursun et al. (2011). They showed that the targeted depletion of LIN-53 by RNAi is required to convert germ cells into ASE neuron-like cells. However, only a subset of *lin-53* (RNAi) animals expressed the ASE fate marker *gcy-5::gfp* upon overexpression of the TF CHE-1, suggesting that other barrier factors act as additional protective mechanisms. In order to identify genetic interactors of *lin-53*, it has to be co-depleted together with other genes. Currently, two approaches are available in *C. elegans* to achieve simultaneous knock down of two genes. First, *lin-53* RNAi can be mixed with other dsRNA expressing bacteria strains. This method, however, has a high false-negative rate, since bacteria containing different RNAi plasmids grow at varying speeds, leading to disproportionate depletion of one gene over the other. Alternatively, a new RNAi plasmid containing the *lin-53* target sequence combined with other genes could be generated. This approach results in a reliable knock down of the target genes. The cloning process is, however, laborious and therefore inapplicable for large-scale high-throughput screens. The fate of differentiated cells is maintained and protected by a complex interplay of many genes, as demonstrated by *in vitro* studies that resulted in improved efficiency of iPSC generation (Qin et al., 2014; Toh et al., 2016). The systematic investigation of genetic interactions between barrier genes in *C. elegans* thus requires the application of large scale and effective

combinatorial RNAi. The aim of this study was therefore to develop a new method based on bacterial conjugation (Lederberg, Tatum, 1946) that allows combination of two distinct RNAi plasmids in a single bacterial cell in a high-throughput approach to study the genetic interactions of the reprogramming barrier factor *lin-53* with other chromatin-related genes in a large scale screen.

3.2. Establishment of double RNAi by conjugation

3.2.1. Bacterial conjugation can occur at different stages of bacterial growth

Bacterial cells undergo several growth phases, beginning at the lag phase, in which the bacterial cell matures and is thus unable to divide. This phase is followed by the exponential phase, characterized by cell doubling. After the depletion of essential nutrients or formation of inhibitory products, such as organic acids, bacteria cells stop dividing and enter starvation. During this phase mutations can occur. Bridges et al. (2001) demonstrated that DNA damage is responsible for many of the mutations.
To establish the protocol for double RNAi by conjugation, donor and recipient bacterial cultures grown until the exponential phase were used. However, later experiments demonstrated that the conjugation efficiency is not affected by the stage of bacterial cultures. This is crucial, as it makes the protocol more suited to be used in large-scale approaches, because, although all RNAi plasmids are contained in the same *E. coli* host strain (HT115) that expresses dsRNA, the growth rate varies substantially, rendering it very difficult to grow a large set of bacterial cultures to a similar concentration. Additionally, the growth phase would have to be determined by measuring the optical density of at least a subset of bacterial cultures, thereby making the protocol cumbersome and impractical for high-throughput approaches. Since bacterial conjugation occurs also in the stationary phase, it is possible to use overnight cultures for generating double RNAi clones, thereby simplifying the protocol substantially.

3.2.2. Stable bacterial host strain EPI300 is crucial for reliable conjugation success rate

The original F-plasmid pRK24 contained an Ampicillin cassette similar to RNAi plasmids in the recipient strains. In order to select for pRK24 specifically, Ampicillin, carried by recipient RNAi plasmids, was replaced with Kanamycin. Due to the large size of the F-plasmid pRK24 (over 60 kb), it had to be transferred into the *E. coli* strain SW105 in order to exchange the antibiotic resistance cassette via recombineering. Subsequently, the RNAi donor plasmid was added by electroporation to generate the first donor strain. This donor strain exhibited low and inconsistent conjugation success rates, possibly due to the fact that *E. coli* SW105 contains a temperature-sensitive λ-Red recombinase that might interfere with the integrity of the F-plasmid pRK24. Therefore, the dsRNA expressing *E. coli* strain HT115, which does not contain a recombinase, was tested as a donor strain. However, only small differences in conjugation efficiency were observed. The usage of

the stable *E. coli* host strain EPI300, which is recombination deficient, allowed for very reliable conjugation, suggesting that the reduction of unwanted recombination was instrumental to maintain the functionality of the modified F-plasmid pRK24.

3.2.3. Conjugation success rate unaffected by antibiotics in growth medium

Presence of antibiotics contained in the growth media of donor and recipient culture did not seem to affect the bacterial conjugation when performed on non-selective LB agar plates. These antibiotics included Ampicillin that inhibits the enzyme transpeptidase required for formation of bacterial cell walls and Chloramphenicol that inhibits peptidyl transferase to prevent protein chain elongation. Ma et al. (2014) used the same F-plasmid pRK24 and performed two washing steps of the donor and recipient cultures, which were omitted in this protocol, since they would render a high-throughput approach impractical. Initially, the mixtures of donor and recipient strains were diluted, which did not affect the outcome of conjugation attempts on solid agar.
In addition to the presence of antibiotics in the growth medium, the probability of donor and recipient bacteria encountering each other also appear to influence the conjugation success rate. This hypothesis is supported by the notion that upon transfer of bacterial conjugation from 6 cm agar plates to 96-well plates the conjugation success rate was strongly reduced. In the initial attempts many wells did not dry out completely in the given incubation time in 96-well plates, in contrast to bacterial mixtures on 6 cm plates. However, up concentration of the donor culture to reduce the total volume of bacterial mixture, resulted in reliable conjugation rates. This suggests that the likelihood of donor and recipient strain to encounter each other affected the outcome. Interestingly, addition of either Ampicillin, Kanamycin, or Chloramphenicol to the solid agar plate prevented any conjugation, suggesting that non-selective LB agar plates diluted down antibiotic concentrations, such that they would not affect the conjugation success rate. Thus, the lower probability of donor and recipient cell encountering each other as well as the residual antibiotic concentration in the mixture might explain why the initial attempts of conjugation in liquid medium had failed. In contrast, by performing bacterial conjugation on non-selective solid agar, the likelihood of donor-recipient interaction is increased, resulting in enhanced conjugation. Furthermore, omission of washing steps improved the time efficiency of the protocol.

3.2.4. Double RNAi bacteria able to deplete two genes simultaneously

One aim of developing a reliable and fast double RNAi method is being able to investigate redundantly or synergistically functioning genes that would be not identified in single RNAi screens. Takahashi et al. (2002) had shown that RNAi against either one of proteasome subunits *rpn-10* or *rpn-12* alone does not affect the survival rate of *C. elegans* larvae, whereas the simultaneous depletion of *rpn-10* and *rpn-12* leads to synthetic lethality This result could be recapitulated using double RNAi clones of *rpn-12*_CON_*rpn-10*, demonstrating that the donor RNAi plasmid is still functional after

being transferred to the recipient cell during conjugation.
Removal of the redundantly functioning TIS11 zinc-finger-containing proteins OMA-1 and OMA-2 leads to arrested oocyte maturation (Detwiler et al., 2001). As a consequence, oocytes cannot proceed to the uterus and fill up the gonadal arms of the animal. The phenotype could be observed in animals subjected to *oma-1*_CON_*oma-2* double RNAi, indicating the ability of our newly developed method to identify redundantly functioning genes that would otherwise be missed in single RNAi screens.
Furthermore, Ciosk et al. (2006) showed that by knockdown of *gld-1* and *mex-3*, germ cells lose their totipotency and transdifferentiate into somatic cells. It could be demonstrated that worms on *gld-1*_CON_*mex-3* double RNAi generated by conjugation ectopically express the pan neuronal reporter *rab-3::tRFP* in the germ line. Only a small fraction of *gld-1* depleted animals showed ectopic expression of *rab-3::tRFP*. Combinatorial RNAi against *gld-1* and *mex-3* by mixing did not lead to an increase of the phenotype, suggesting that double RNAi clones generated by conjugation are more reliable in causing the depletion of *gld-1* and *mex-3* than mixing of the two single RNAi clones.
Thus, double RNAi by conjugation allows to deplete two genes simultaneously and effectively in order to study genetic interactions in *C. elegans in vivo*.

3.3. Limitations of double RNAi by conjugation

Double RNAi by conjugation subjecting animals to *lin-53*_CON_*lin-15A* did not induce the formation of additional synthetic vulvas during development, as it has been described for *lin-15A* (n767) *lin-53* (n833) double mutants (Andersen et al., 2006). Subjecting *lin-15A* (n767) mutants to *lin-53* RNAi this result could be replicated, suggesting that low levels of LIN-15A are sufficient for normal vulva development. Double RNAi permits to study genetic interaction by knocking down two genes simultaneously. This in turn also means that residual levels of the depleted proteins still will be found in the cell, which can be even larger, depending on the half-life of targeted proteins. Thus, double RNAi based on conjugation provides reliable knock-downs of two genes simultaneously, but phenotypes that require combinatorial knock-outs cannot be replicated.
RNAi in general is further known to causing off-target effects (Fedorov et al., 2006; Jackson, Linsley, 2010) that can lead to artificial side effects of the RNAi machinery. To exclude that the observed phenotype is not due to an off-target effect, a mutant of the targeted gene can be used to confirm the result.
Furthermore, double RNAi by conjugation permits to interrogate the function of a gene only based on the observed phenotypes upon its depletion. There are no equivalents to gain-of-function or point mutations. The latter can give insight into the structure-function relationship. In forward genetic screens tissue-specific alleles can be recovered, whereas RNAi in *C. elegans* affects the whole worm with the exception of neurons that are generally refractory to RNAi (Kamath et al., 2001; Timmons et al., 2001; Asikainen et al., 2005). The usage of hypersensitive strains to circumvent this shortcoming often negatively affects the physiology of the animal (Asikainen et al., 2005; Calixto et al., 2010; Firnhaber, Hammerlund, 2013; Sieburth et al., 2005).

The interpretation of synthetic phenotypes is more difficult on RNAi since gene activity is reduced but not removed (Kamath, Ahringer, 2003). Whether two genes act in the same or in different pathways, can generally be determined by performing classical epistasis experiments (Avery, Wasserman, 1992; **?**), which is difficult using RNAi. The phenotypic penetrance in RNAi experiments varies from experiment to experiment, since RNAi is administered by feeding, which does not allow to control the applied dosage per worm. This in turn makes it more difficult to determine whether two genes act in the same pathway, in parallel pathways, or synergistically. Additionally, RNAi clones containing the same plasmid can differ in their efficiency, probably due to variations in their plasmid copy number.
Thus, double RNAi permits to study the effects of a knock down of the expression of targeted genes upon systemic depletion. However, residual levels of the respective proteins can still be found in the cell, potential off-target effects have to be accounted for, and neurons are generally refractory to RNAi. Furthermore, the ability to infer how two genes interact from data generated by double RNAi is limited. Nevertheless, one big advantage of RNAi is that it allows to investigate essential genes, which otherwise cause lethality when completely removed.

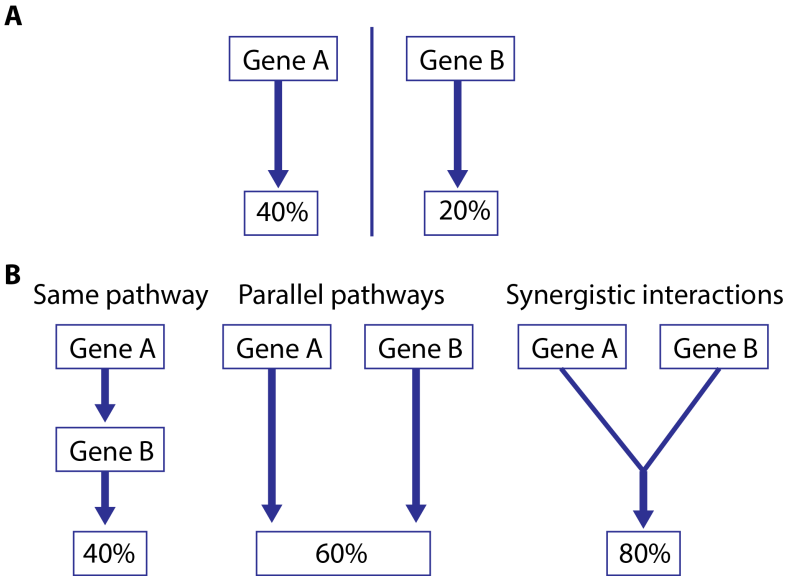

Figure 3.1.: **Modes of genetic interactions** (A) Knockdown of either gene A and B cause varying phenotypic penetrance. (B) Gene A and B act in the same pathway if the phenotypic penetrance is equal to either gene A or gene B. If they act in parallel pathways, the phenotypic penetrance is the sum of the knockdown of both genes combined. If upon double knockdown of gene A and B the phenotypic penetrance is larger than the sum of both, it is assumed they act synergistically.

3.4. Double RNAi permits to study genetic interactions of essential genes in large-scale screens

Double RNAi by conjugation allows to perform a large-scale high-throughput screen to identify genetic interactions of essential genes that are required during development and whose knockout is lethal. Mutants of such genes are either not available or they have to be balanced, for example *lin-53* (n3368), and are therefore unsuitable for genetic screens.

lin-53 (RNAi) animals overexpressing *unc-30* show a 20% penetrance of ectopically expressed *unc-25::gfp* in the germ line. In order to identify genetic enhancers, a *lin-53* (RNAi) donor strain was generated to obtain double RNAi bacterial clones by conjugation. The alternative of mixing *lin-53* RNAi bacteria with other RNAi containing bacteria tends to yield poor results (Min et al., 2010). In contrast to randomly mutate every gene in the genome, double RNAi by conjugation allowed to study the interaction of *lin-53*, which is part of the PRC2 complex and involved in chromatin regulation, with 800 chromatin-related genes. The focus on a pre-defined subset of genes further increases the likelihood of identifying weak phenotypes that might be overlooked in a whole-genome approach, in which strong phenotypes tend to dominate. By using CRISPR/Cas (Jinek et al., 2012) genes can be specifically targeted and new and improved approaches allow the generation of double mutants more easily in *C. elegans* (Norris et al., 2017). However, they are cumbersome and can thus only be applied on a small set of candidate genes, whereas double RNAi by conjugation is suitable for large-scale screens. Furthermore, double RNAi permits to deplete genes transiently at defined time points of development, which is crucial for the study of essential genes, in contrast to gene deletion, which is permanent.
Double RNAi clones containing a *lin-53* RNAi plasmid as well as one of in total 800 chromatin-related RNAi plasmids could be generated by conjugation in 96-well format in a high-throughput approach and could be used within two days. In contrast to classical genetics, gene sequence of positive screen hits in forward screens is known and does not require the laborious and time-consuming process of mutant allele identification (Doitsidou et al., 2010). Additionally, the donor RNAi plasmid can be easily modified to contain the target sequences of two genes to further explore their genetic interaction network and gain insight into the phenotype causing mechanism.
Thus, by reliably and effectively depleting two targeted genes simultaneously and at defined time points during development, double RNAi by conjugation enables studying the genetic interaction of a gene of interest with a pre-defined set of candidate genes and can be performed at large-scale in a high-throughput approach. This allows bypassing the time-consuming process of mutant-allele identification and, more importantly, allows the investigation of essential genes.

3.5. Simultaneous knockdown of *lin-53* and *rbbp-5* increases *unc-25::gfp* induction efficiency

LIN-53 had been previously identified as a barrier for germ cell conversion (Tursun et al., 2011).To identify potential enhancers of the *lin-53* RNAi-mediated cell conversion phenotype, *lin-53* was co-depleted one by one with 800 chromatin related genes using double RNAi by conjugation. Co-knockdown of *lin-53* together with *rbbp-5* while overexpressing the GABAergic fate inducing transcription factor UNC-30 led to ectopically expressed *unc-25::gfp* in the germ line (GeCo) in 36% of the animals ($P \leq 0.0001$, Dunnett's multiple comparisons test). In contrast, worms subjected to single RNAi against either *rbbp-5* or *lin-53* showed a phenotype penetrance of 24% and 19.6% GeCo, respectively ($P \leq 0.01$ and $P \leq 0.0001$, Dunnett's multiple comparisons test). Interestingly, the *unc-25::gfp* induction efficiency was not significantly increased in worms on *lin-53*_mix_*rbbp-5* RNAi at around 14% when compared to ctrl RNAi ($p \leq 0.05$, Dunnett's multiple comparisons test), showing that by using double RNAi by mixing the enhancement of the *lin-53* RNAi mediated phenotype might not have been detected. Double RNAi by conjugation thus allowed co-knockdown of the known reprogramming barrier *lin-53* with 800 chromatin-related genes and identification of RBBP-5 as a novel barrier factor. In contrast, combinatorial RNAi by mixing against *lin-53* and *rbbp-5* did not lead to an increased *unc-25::gfp* induction efficiency, suggesting that double RNAi clones generated through conjugation cause a more reliable double knock down than combinatorial RNAi achieved by mixing and are therefore better suited for large-scale double RNAi screens to investigate genetic interactions.

3.5.1. Converted germ cells start to express Rab3a-interacting protein (RIM)

The overexpression of *unc-30* while depleting either *lin-53*, *rbbp-5*, or both genes simultaneously permitted the induction of the GABA reporter *unc-25::gfp* in the germ line. Germ cells positive for the GABA reporter, however, neither express the pan-neuronal reporter *rab-3::gfp* nor show the formation of axo-dendritic extensions typical for neurons. In contrast, these characteristics were observed in animals subjected to *lin-53* RNAi in *gcy-5::gfp* positive germ cells after overexpression of ASE neuron TF CHE-1. This suggests that *unc-25::gfp* positive cells do not convert to the same quality as *gcy-5::pfp* positive germ cells. To further assess the degree of germ cell to neuron conversion, antibody staining was performed on animals subjected to *lin-53*, *rbbp-5*, or *lin-53*_CON_*rbbp-5* RNAi showing ectopic *unc-25::gfp* expression in the germ line. It could be demonstrated that Rab3a-interacting protein (RIM), which is found in active zones of neural synapses, is co-localized with *unc-25::gfp* in all three conditions, suggesting that the converted cells start to form synapses. Further characterization of the observed phenotype would require the usage of additional reporter strains, such as *unc-47::RFP* (transmembrane vesicular GABA transporter) or *ttr-39::mCherry* (TransThyretin-Related family domain; enriched in GABAergic neurons), as well as smFISH probes to detect neuron-relevant mRNA sequences in *unc-25::gfp* positive cells.

The absence of axo-dendritic formation shows that the co-knockdown of *lin-53* and *rbbp-5* increases the *unc-25::gfp* induction efficiency, but does not influence the degree of conversion from germ cell to GABAergic neuron, suggesting that further barrier factors have to be identified and depleted to improve the extent of conversion. This underlines the utility of the newly developed system to study genetic interactions in large-scale high-throughput approaches.

3.5.2. *lin-53* does not interact with the Set1/MLL methyltransferase complex

rbbp-5 encodes a WD40 repeat containing protein that is the *C. elegans* homolog of mammalian RbBP5 (Retinoblastoma binding protein 5) and a part of the Set1/MLL methyltransferase complex (Li, Kelly, 2011). Double RNAi clones of *lin-53* combined with members of the Set1/MLL methyltransferase complex were generated by conjugation. Co-knockdown of *lin-53* with Set1/MLL methyltransferase complex members other than *rbbp-5* did not result in increased *unc-25::gfp* induction in the germ line when compared to *lin-53*_CON_*Rluc* ($P \leq 0.05$, Dunnett's multiple comparisons test), suggesting that *lin-53* does not genetically interact as a barrier factor with the Set1/MLL methyltransferase complex.
Single RNAi against a subset of Set1/MLL methyltransferase complex members showed that knockdown of *wdr-5.1* allowed significant increase in the induction of GABAergic fate reporter *unc-25* ($P \leq 0.01$, Dunnett's multiple comparisons test), whereas depletion of *dpy-30* or *set-2* did not when compared to ctrl ($P \leq 0.05$, Dunnett's multiple comparisons test). RNAi. Li, Kelly (2011) demonstrated that RNAi against *set-2*, *wdr-5.1*, or *rbbp-5*, but not *dpy-30*, led to a reduction of 90% of H3K4me3 in the most distal part of the gonadal arm in adult animals and about 50% in the meiotic zone. H3K4me2 is only affected upon depletion of *rbbp-5* and *wdr-5.1*, but not *set-2* or *dpy-30*, indicating that H3K4me2 and H3K4me3 may require different histone methyl transferases that rely on the same core complex containing at least RBBP-5 and WDR-5.1 (Li, Kelly, 2011). Hörmanseder et al. (2017) demonstrated that H3K4me3 is a major epigenetic roadblock that limits transcriptional reprogramming and efficient nuclear transfer. However, neither single RNAi against *set-2* nor *lin-53*_CON_*set-2* permitted the induction of ectopic *unc-25::gfp* expression, suggesting that H3K4 methylation is not the main reprogramming barrier to UNC-30 induced conversion of germ cells.
Thus, the enhancement observed upon simultaneous knockdown of *lin-53* together with *rbbp-5* cannot be explained by a reduction of H3K4 methylation levels. In addition, double RNAi by conjugation revealed that *lin-53* does not genetically interact with the Set1/MLL methyltransferase complex as a reprogramming barrier.

3.5.3. *lin-53* and *rbbp-5* do not have common genetic interaction partners

Co-knockdown of *lin-53* and *rbbp-5* increases the *unc-25::gfp* induction efficiency in the germ line upon simultaneous overexpression of *unc-30*. The next aim was to identify shared genetic interaction partners of *lin-53* and *rbbp-5*. The double RNAi by conjuga-

tion protocol was modified to achieve a triple depletion and thereby gain insight into the mechanism of how *lin-53* and *rbbp-5* protect the germ cell fate.
A donor RNAi plasmid was generated that contained target sequences of *lin-53* and *rbbp-5*. The newly generated donor was conjugated with previously known interaction partners of either *lin-53* or *rbbp-5*. No triple knock down resulted in an enhancement of *unc-25::gfp* induction efficiency in the germ line when compared to *rbbp-5::lin-53* _CON _*Rluc*, suggesting that *lin-53* and *rbbp-5* do not have common genetic interactors in their function as barrier factors.
Thus, although the simultaneous depletion of *lin-53::rbbp-5* with members of the HAT, CAF-1, Sin3, PRC2, NURF, Mi-2/NURD, or the DRM complexes did not increase the GABA reporter induction efficiency, it demonstrated the versatility of the newly developed double (or triple) RNAi by conjugation method that allows the investigation of genetic interactions in large-scale high-throughput screens.

3.5.4. *lin-53* and *rbbp-5* act in parallel pathways

Combinatorial RNAi against *lin-53* and *rbbp-5* increases the phenotype penetrance when compared to the single knockdown of either *lin-53* or *rbbp-5*. This raises the question whether *lin-53* and *rbbp-5* act in the same or in parallel pathways, or whether a double knockdown of *lin-53* and *rbbp-5* has a synergistic effect. Animals on *lin-53* _CON_ *rbbp-5* RNA display a phenotype penetrance of 36.4% compared to 19% on *lin-53* RNAi and 24% on *rbbp-5* RNAi alone. Thus, the phenotype penetrance observed on combinatorial RNAi of *lin-53* and *rbbp-5* does not exceed the additive expectation of RNAi against either *lin-53* or *rbbp-5*, indicating that *lin-53* and *rbbp-5* do not interact synergistically. Co-knockdown of *lin-53* and *rbbp-5* increases the phenotype compared to RNAi against either *lin-53* or *rbbp-5*, indicating that *lin-53* and *rbbp-5* are not part of the same genetic pathway. Instead, *lin-53* _CON_ *rbbp-5* (RNAi) animals show a phenotype penetrance that only slightly deviates from the additive expectation of combined single RNAi effects, suggesting that *lin-53* and *rbbp-5* do not genetically interact, but are part of parallel cell-fate protecting pathways. In addition, triple depletion of *lin-53* and *rbbp-5* together with known genetic interactors of either *lin-53* or *rbbp-5* did not result in the enhancement of *gcy-5::gfp* induction efficiency in the germ line. Thus, based on single RNAi against *lin-53* and *rbbp-5* individually, double RNAi against *lin-53* _CON_ *rbbp-5*, and the absence of enhancers of *lin-53::rbbp-5* conjugated with known interactors of either *lin-53* or *rbbp-5*, it can be suggested that *lin-53* and *rbbp-5* act in parallel pathways.

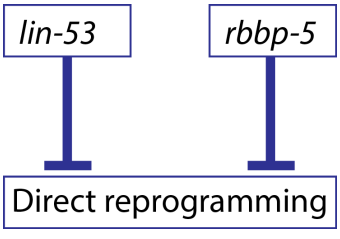

Figure 3.2.: ***lin-53* and *rbbp-5* appear to act in parallel pathways as reprogramming barriers.** RNAi experiments knocking down either *lin-53* or *rbbp-5* by themselves compared to combinatorial RNAi by conjugation against both, taken together with the apparent absence of shared genetic interactors, suggest that *lin-53* and *rbbp-5* act in parallel pathways as barriers to transdifferentiation.

3.5.5. Low hit rate of RNAi enhancer screen potentially due to focus on chromatin-related genes

lin-53 was co-depleted together with almost 800 chromatin-related genes to identify genetic interactors. Candidates from the primary screen were re-tested and compared to *lin-53*_CON_*Rluc* RNAi. Animals on *lin-53*_CON_*rbbp-5* RNAi showed significantly increased *unc-25::gfp* induction efficiency (Tukey's multiple comparisons test, $p \leq 0.05$), raising the question why there was only one candidate from the screen.
Due to the absence of an integrated line expressing *unc-30* under a heat shock promoter, an extrachromosomal line was used with a germ line transmission rate of about 50%. The induced expression of *unc-25::gfp* upon knockdown of *lin-53* and overexpression of *unc-30* can only be observed in the progeny of parental animals that were subjected to RNAi. Since only a subset of F1 animals would carry the transgenic array, weaker phenotypes might have been missed in the primary screen. Furthermore, on control RNAi 10 - 20% of animals showed germ line induction of the reporter *unc-25::gfp* upon overexpression of *unc-30*. Due to this high background, phenotypes with low penetrance might have been not detected.
From the enhancer screen for LIN-53 as a reprogramming barrier factor of germ line cells, one gene was detected out of 800 in total, resulting in a hit rate of 0.125%. In a previous whole-genome-screen overexpressing the ASE neuron TF CHE-1, which was performed in our lab (Ena Kolundzic, in revision), 160 new barrier factors out of 20,0000 were identified, that is, 0.8% of all tested genes were established as cell-fate protecting factors for germ cells. On the one hand, a focus on a pre-defined subset of genes increases the probability of identifying weak phenotypes that might otherwise be overlooked in a whole-genome screen, in which strong phenotypes dominate. On the other hand, limiting the screen to only 800 chromatin-related genes creates a bias that might have resulted in fewer candidate enhancers of LIN-53 as a reprogramming barrier, suggesting that by expanding the set of tested genes without pre-selection, more novel barrier factors might have been identified.

3.6. MRG-1 is a barrier factor to UNC-30 induced direct reprogramming

Originally, MRG-1 was identified as a reprogramming barrier in an automated screen using *hsp::che-1, gcy-5::gfp* transgenic background (Hajduskova et al., submitted for publication). By overexpressing *unc-30* under a heat shock promoter in animals on *mrg-1* RNAi, *unc-25::gfp* expression could be observed in the germ line, suggesting that MRG-1 has a general function safeguarding the cell fate. Thus, its knockdown permits the induction of varies new cell fates.

Using a commercial antibody, it was demonstrated that MRG-1 is localized in head neurons, the gut, and mainly the germ line, but interestingly, MRG-1 only partially co-localizes with LIN-53. The germ cell conversion observed in *mrg-1* (RNAi) animals

resembles that of PRC2 subunits, such as MES-4 or LIN-53 (Patel et al., 2012; Gaydos et al., 2012). However, co-knockdown of *mrg-1* and other PRC2 complex members, such as *mes-2*, *mes-3*, and *mes-6*, showed no obvious increase of *gcy-5::gfp* induction efficiency in the germ line when compared to single RNAi (Hajduskova et al., submitted for publication). The observation that MRG-1 and LIN-53 proteins only partially co-localize and the absence of synergism in germ cell conversion could indicate that *mrg-1* has PRC2-independent roles in protecting germ cells. Furthermore, *mrg-1* knockdown permits reprogramming without Notch signaling (Hajduskova et al., submitted for publication) in contrast to PRC2-mediated reprogramming (Seelk et al., 2016). The *gld-1 gld-2* double mutations combined with the mutant Notch receptor gene *glp-1* allows germ cell proliferation in the absence of Notch signaling (Kadyk, Kimble, 1998; Hansen et al., 2004; Seelk et al., 2016). In the *gld-1 gld-2 glp-1* triple mutant background depletion of PRC2 members is insufficient to permit germ cell reprogramming (Seelk et al., 2016), in contrast to knock down of *mrg-1* (Hajduskova et al. submitted for publication). Additionally, depletion of PRC2 members causes global loss of PRC2-mediated H3K27 methylation (Patel et al., 2012), which could not be observed in *mrg-1* (RNAi) animals. Global levels of H3K4 methylation are not affected in *mrg-1* depleted animals, which is in contrast to what has been observed upon knockdown of *rbbp-5* (Li, Kelly, 2011). Based on the distinctive effects of histone modification and the independence of Notch-signaling it has to be concluded that *mrg-1* does not genetically interact with the PRC2 complex to counteract germ cell reprogramming. Although overall H3K36 levels are not affected by knockdown of *mrg-1*, it is possible that the genomic distribution of H3K36 methylation is altered upon *mrg-1* RNAi, which in turn could affect gene repression. Interestingly, levels of H3K14ac are increased in *mrg-1* (RNAi) animals, which have been implicated as a DNA damage checkpoint in yeast and mouse (Wang et al., 2012). Recent findings indicated that MRG-1 and its ortholog MRG15 are involved in homologous pairing and chromosomal break repair (Hayakawa et al., 2010; Dombecki et al., 2011; Garcia, Olivia, 2008). Thus, it is possible that a reduction of MRG-1 levels lead to increased DNA damage. Decreased levels of H3K14ac might in turn lead to a reduced efficiency of H3K9 methylation, as it has been suggested previously (Alvarez, 2011), which causes a redistribution or lowering of repressive chromatin marks in the germ line. The exact mechanism of how MRG-1 levels affect histone modifications remain to be determined, but possibly MRG-1 associates with chromatin regulating complexes. The ortholog of MRG-1, MRG15, has been reported as being a component of the NuA4/Tip60 histone acetyltransferase (HAT) or mSin3A histone deacetylase (HDAC) complex (Chen et al., 2009; Yochum, Ayer, 2002; Doyon et al., 2004). In this regard it could be shown that MRG-1 interacts with the *C. elegans* homolog of yeast NuA4 subunit Eaf7 (ZK1127.3, Li, 2004), SIN-3, the ortholog of the Sin3 HDAC subunit, and the ortholog of human O-GlcNAc transferase (OGT) (Hajduskova et al., submitted for publication). Sin3 and OGT interact in mammalian cells and are thereby recruited to promoters of repressed genes (Yang et al., 2002). MRG-1 might therefore form a complex with OGT-containing Sin3 HDAC. Contrary to this reasoning, it has to be considered that OGT-1 was originally identified as repressive chromatin regulator belonging to the Polycomb group (PcG) class (Ingham, 1984), whereas it has also been suggested that OGT-1 can be part of his-

tone acetyl transferase complexes (Hoe, Nicholas, 2014). One of the strongest identified interactors of MRG-1 was the H3K9 methyltransferase SET26 (Hajduskova et al. submitted for publication, Greer et al. (2014)). Developmental defects are seen in animals lacking NuRD and MEC complex subunit LET-418 (Mi2) (Greer et al., 2014; Erdelyi et al., 2017). Interestingly, the effect of *mrg-1* RNAi is increased in the *set-26* mutant background, whereas the *ogt-1* knockout leads only to slight reprogramming enhancement and *sin-3* mutants showed no increased conversion efficiency in germ cells (Hajduskova et al., submitted for publication). This suggests that the association of MRG-1 with OGT-1 and SET-26 counteracts germ cell reprogramming. However, the exact mechanism of how MRG-1 prevents reprogramming has yet to be determined.

3.7. Depletion of HSP-1 is insufficient for UNC-30 to induce *unc-25::gfp* in the epidermis

HSP-1 was identified in a similar manner as MRG-1 in an automated screen as a barrier for inducing ectopic expression of reporter genes in the epidermis upon overexpression of TFs CHE-1 or ELT-7. Epidermal reporters were shown to be lost while neuron or intestine gene expression was observed. However, cells positive for the respective reporter did not change morphologically into neuron or gut cells, indicating that additional barriers for complete cell conversion exist. Interestingly, overexpression of *unc-30* was not sufficient to induce the expression of GABA specific neuronal reporters in *hsp-1* (RNAi) animals (Hajduskova et al. submitted for publication). The fact that hypodermal cells are not undergoing a morphological transformation indicates that additional factors are required, as suggested by several reprogramming studies in different contexts and species (Onder et al., 2012; Wapinski et al., 2013; Brumbaugh, Hochedlinger, 2013; Luo et al., 2013; Gifford, Meissner, 2012).
ogt-1 was identified as a genetic interactor of *hsp-1* first in mixed double RNAi experiments when overexpressing *che-1*, which could be confirmed by using an *ogt-1* null (ok430) mutant (Hajduskova et al. submitted for publication). The *ogt-1* mutant does not show a phenotype. Overexpression of *elt-7* in an *ogt-1* mutant background on *hsp-1* RNAi significantly increases the induction of gut reporter in epidermis compared to WT background.
In *C. elegans* OGT-1 has been linked to insulin signaling pathways and lifespan regulation, whereas the human ortholog of OGT-1, O-GlcNAc transferase OGT, is involved in temperature and nutrient sensing (Hanover et al., 2005; Mondoux et al., 2011; Love et al., 2010; Radermacher et al., 2014). As previously mentioned, the *Drosophila* homolog of OGT-1 was originally described as a repressive chromatin regulator and being a member of the Polycomb group (PcG) class protein (Ingham, 1984). OGT-1, however, can also be part of histone acetyltransferase-containing protein complex termed NSL (Hoe, Nicholas (2014), as reviewed by Gambetta, Müller (2015)). Evidently, two members of the NSL complex, SUMV-1 and SUMV-2, are suggested to be involved in gene suppression in germ line and epidermis (Yücel et al., 2014; Cui et al., 2006). This led to the question of whether *hsp-1* interacts with the NSL complex. Combinatorial

RNAi was performed by generating RNAi plasmids containing two target sequences of distinct genes. Co-knockdown of *hsp-1* together with NSL complex members while either overexpressing *che-1* or *elt-7* led to significantly increased reporter induction efficiency, suggesting that *hsp-1* is either directly or indirectly involved in chromatin regulation. Interestingly, co-knockdown of *hsp-1* and *hat-1* decreased the *hsp-1* RNAi mediated effect, indicating that *hat-1* is required for ectopic cell fate induction in the epidermis. The observation that *hsp-1* knockdown leads to decreased levels of H4Kac supports this notion. However, suppression of H4K5,8,12, and 16 acetylation levels is insufficient to explain permissiveness of epidermal cells to ectopic cell fate induction, as H4Kac level are also decreased in animals on RNAi of NSL complex members *smuv-1*, *mys-2*, and *ogt-1*. Single RNAi against either one did not permit ectopic cell fate induction (Hajduskova et al., submitted for publication). Thus, further investigation will be required to elucidate the exact mechanism, by which hsp-1 counteracts the induction of ectopic cell fates. Double RNAi by conjugation is perfectly suited to perform large scale screen to identify more genetic interactors of *hsp-1*.

3.8. Transcription factor specificity of barrier factors HSP-1 and MRG-1

As mentioned before, a previous screen in our lab showed that RNAi against *mrg-1* permits the induction of *gcy-5::gfp* upon overexpression of *che-1* (Hajduskova et al, in revision), which could be recapitulated by overexpressing *unc-30* to induce ectopic expression of *unc-25::gfp* in the germ line. HSP-1 was also identified as a barrier factor against ectopic fate reporter induction in the epidermis, using a *hsp::che-1* or *hsp::elt-7* transgenic background (Hajduskova et al. submitted for publication), which could not be confirmed overexpressing *unc-30*. This could suggest that barrier factors are specific to certain transcription factors (TF), such as HSP-1 to the TF CHE-1 and ELT-7. It is an open question whether barrier factors are indeed general or specific to certain TFs. Cell fate protecting mechanisms could be universal for a given tissue. Thus, their depletion would permit the induction of any new cell fate. Alternatively, barrier factors could be specific to the induced cell fate. One thing to consider is the lineage relation of the starter cell to the target fate, in this example neurons, assuming that developmentally closely related cells may be easiest to be converted into each other, as depicted in the Waddington model (Masserdotti et al., 2016). Astrocytes that share a common origin with neurons (Kriegstein, Arturo, 2009) are efficiently converted into functional neurons by overexpression of one TF (Berninger et al., 2007; Heinrich et al., 2010; Heins et al., 2002), while mouse embryonic fibroblasts that are of non-ectodermal origin or hepatocytes require more than one factor (Marro et al., 2011; Vierbuchen et al., 2010) or additional chemical manipulation (Hu et al., 2015; Ladewig et al., 2012; Li et al., 2015; Liu et al., 2013; Zhang et al., 2015) for efficient direct reprogramming into neurons. However, CHE-1 and UNC-30 are both neuronal fate inducing TF, and *elt-7* overexpression led to the induction of intestine specific reporter in animals on *hsp-1* RNAi, suggesting that the lineage relation was not the decisive factor. One approach to increase the efficiency of

induced direct reprogramming of distinct tissues into GABAergic motor neurons would be the simultaneous overexpression of *unc-30* together with a proneural gene, such as *cnd-1* that encodes for a helix-loop-helix protein closely related to the vertebrate NeuroD transcription factor (Hallam et al., 2000), or *hlh-14*, which also encodes for a basic helix-loop-helix protein that is required for neuronal development in *C. elegans* (Frank et al., 2003).
Alternatively, the depletion of additional barrier factors might be required to enhance the efficiency of UNC-30 induced reprogramming. Comparison of phenotype in *mrg-1* (RNAi) animals overexpressing *che-1* shows that in addition to *gcy-5::gfp* expression, germ cells also change their morphology and the formation of neurite-like extensions has been observed (Hajduskova et al., in revision). In contrast, the morphology of epidermal cells did not change upon *che-1* overexpression in HSP-1 depleted animals (Hajduskova et al., unpublished). Furthermore, different starter tissues might be amenable to direct reprogramming to varying degrees. Our lab has performed a whole-genome RNAi screen using *hsp::che-1* transgenic lines (Ena Kolunzdic, in revision). Most of the phenotypes were observed in the germ line followed by the intestine, whereas other tissues, such as muscle and epidermis showed, less often ectopically expressed *gcy-5::gfp* (Ena Kolundzic, in revision), suggesting that the germ line is less restricted towards transdifferentiation and, by extension, more amenable to induced morphological transformation.
Additionally, it is possible that *mrg-1* is part of a feed-forward-loop, in which *mrg-1* upregulates other barrier factors. These secondary barrier factors are also knocked down upon RNAi against *mrg-1*, but can still partially repress reprogramming, thereby explaining why only a small subset of animals on *mrg-1* RNAi shows reporter induction in the germ line. *hps-1* on the other hand might not positively regulate other barrier factors, specifically those preventing the induction of morphological changes, and while the conversion efficiency could be increased by combinatorial RNAi by ′stitching′ against *hsp-1* and members of the NSL complex, neurite-like formations were not observed in the epidermis. Thus, a large-scale high-throughput enhancer screen for *hsp-1* would be required to investigate the epidermis fate protective mechanisms of HSP-1 with the aim to achieve full conversion of epidermal cells. A null mutation of *hsp-1* is lethal and previous methods of performing double RNAi, either by generating double RNAi plasmids or by mixing different RNAi plasmid expressing bacteria together, were not suitable to address this question. Double RNAi by conjugation now allows to perform whole-genome screens to identify *hsp-1* phenotype enhancers and thus is a valuable addition to the methodological arsenal used to decipher cell-fate protective mechanisms and thereby add to our ability to directly convert fully differentiated cells.

3.9. Outlook - testing results from iPSC studies in *C. elegans in vivo*

It could be demonstrated that the newly developed method of double RNAi by conjugation allows to combine two different RNAi plasmids in a single bacterial cell in a high-throughput approach, knocking down two target genes simultaneously and thereby

allowing to identify that depletion of RBBP-5 enhances the reprogramming efficiency in *lin-53* (RNAi) animals.

Since the initial *in vitro* studies of converting fibroblast into muscle cells (Davis et al., 1987) direct reprogramming has been very promising approach to develop new medical applications to replace dead non-regenerative tissue, such as neurons. Cell fate inducing transcription factors have been instrumental to convert differentiated cells *in vitro* and *in vivo* (reviewed in Gascón et al. (2016), but these attempts of transdifferentiation are often either inefficient or even ineffective. It is therefore imperative to identify the cell-fate protective mechanisms to enable the targeted and controlled conversion of differentiated cells.

With the original protocol Takahashi, Yamanaka (2006) could convert 1% of transfected cells into iPSCs. Qin et al. (2014) identified reprogramming barriers in distinct pathways, thereby demonstrating that the cell fate is protected by numerous mechanisms that also interact with each other in feed-forward loops. Toh et al. (2016) showed that by depleting five genes simultaneously, the conversion efficiency could be increased by several fold up to 80%. Both of these studies have demonstrated the importance of investigating genetic interactions to improve reprogramming efficiency and effectiveness.

Previous methods of performing double RNAi in *C. elegans* either suffered from very high false-negative results (double RNAi by mixing) or were not suitable for large-scale high-throughput screens (double RNAi by ′stitching′). To study genetic interactions Lehner et al. (2006) used a set of mutants that were combined with RNAi to test in total 65,000 gene pairs to investigate signaling pathways that are mutated in human diseases. Ceron et al. (2007) used a similar approach to identify synthetic interactors of the Rb-related gene *lin-35*. Both studies required the availability of mutants for the gene of interest. Double RNAi by conjugation now allows to study genetic interactions of essential genes. By creating a donor RNAi strain, the target gene can be combined with RNAi against a pre-defined set of genes and genetic interactions can be studied at a large scale and in a high-throughput manner.

The transient repression of the p53-p21 pathway greatly increases iPSC reprogramming efficiency (Rasmussen et al., 2014). Knock down of p53 *in vivo* also improved the conversion rate of MEFs into functional dopaminergic neurons (Jiang et al., 2015; Liu et al., 2014), which suggests that there are common barriers of iPSC generation and direct reprogramming. Perhaps other roadblocks identified *in vitro*, such as members of the ubiquitin-proteaosome (e. g. Fbxw7; (Buckley et al., 2012)) or metalloproteases (e. g. members of the ADAM family; (Qin et al., 2014)) could also be common barrier factors to *in vivo* direct reprogramming. Double RNAi by conjugation allows to integrate data from iPSC generation into the *in vivo* model system *C. elegans* to advance and complete our understanding of cell-fate protective mechanisms in order to enhance direct reprogramming efficiency and effectiveness and make it applicable as medical treatment.

4. Material and Methods

4.1. Material

4.1.1. Antibiotics

Table 4.1.: Used antibiotics

Name of antibiotic	Stock concentration	Company
Ampicillin	100 mg/ml	Carl Roth GmbH + Co. KG
Carbenicillin	50 mg/ml	Carl Roth GmbH + Co. KG
Chloramphenicol	20 mg/ml	Carl Roth GmbH + Co. KG
Tetracycline	12.5 mg/ml	Carl Roth GmbH + Co. KG

4.1.2. Antibiodies

Table 4.2.: Used antibodies

Name	target	Mono-/Polyclonal; Species	Company
	Primary Antibodies		
PA8	Anti-trimethyl-Histone H3K27)	poly; rabbit	Millipore
PA9	Anti H3K27me3	mono; mouse	Dr. Hiroshi Kimura; Graduate School of Frontier Biosciences Osaka University
PA10	anti H3K36me2	mono; mouse	Dr. Hiroshi Kimura; Graduate School of Frontier Biosciences Osaka University
PA24	anti-H3K9me3	poly; rabbit	Abcam
PA47	Anti-Histone H3K4me3 ab8580	poly; rabbit	Abcam
PA48	Anti-Histone H3 (acetyl K9) ab4441	poly; rabbit	Abcam

PA49	Anti-Histone H3 (acetyl K14) ab52946	mono; rabbit	Abcam
PA54	Anti-lin-53 C-term Tier 1	mono; guinea pig	Pineda
PA82	Anti-RIM	mono; mouse	Hybridoma Bank
PA105	Anti-H3K27me3 antibody (ab6002)	mouse mono	Abcam
PA114	Anti-H4K5,8,12,16ac	poly; rabbit	Diagnode
PA122	Anti-MRG-1	poly; rabbit	Novus bio
	Secondary Antibodies		
SA2	IgG-HRP	anti-mouse	Santa Cruz
SA4	IgG-HRP	anti-rabbit	Santa Cruz
SA7	AlexaFluor488 Goat	Anti-Mouse	Mol. Probes
SA8	AlexaFluor488 Goat	Anti-Rabbit	Mol. Probes
SA9	AlexaFluor568 Goat	Anti-Rabbit	Mol. Probes
SA10	AlexaFluor568 Goat	Anti-Mouse	Mol. Probes
SA11	AlexaFluor488 Goat	Anti-Guinea pig	Mol. Probes
SA12	AlexaFluor568 Goat	Anti-Guinea pig	Mol. Probes

4.1.3. Buffers, solutions, and media

Table 4.3.: Used buffers, solutions and media and their composition.

Name	**Composition**
APS (10 %)	1 g APS in 10 ml ddH2O
Bleaching solution	for 1 ml: 100 Âţl 14 % NaCl, 200 Âţl 4M NaOH, 700 Âţl ddH_2O
Blocking solution	1x PBS, 0.25 % Triton X-100, 0.2 % Gelatine, 0.04 % NaN3, ddH_2O
BO_3 buffer 50 mL	0.5 ml 1M H_3BO_3, 125 Âţl 4 N NaOH, 4 ml 25 % Triton X-100, ddH2O
Freezing solution (1 L)	5.8 g NaCl, 50 ml 1 M KH_2PO_4 (pH 6), 240 ml glycerol, ddH_2O; before usage: add 0.3 ml 1 M $MgSO_4$
2x Gibson Assembly Master Mix	405 Îijl isothermal start mix, 25Îijl 1 M DTT, 50 Îijl 10 mM dNTPs, 50 Îijl NAD+ (NEB #M0363S âĂŞ 10 U/Îijl), 31.25 Îijl Phusion High Fidelity DNA Polymerase (NEB #M0530S) âĂŞ 2 U/Îijl), 437.75 Îijl ddH_2O
Glycerol (50%)	50 ml glycerol (100%), 50 ml ddH_2O
Lysis buffer	50 mM KCl, 10 mM Tris (pH 8.3), 2.5 mM $MgCl_2$, 0.45% Tween-20, 0.01% Gelatin before usage: add 0.1 mg/ml of proteinase K
LB (Luria Bertani), (fluid medium) (1L), pH 7	25 g LB broth (Carl Roth GmbH + Co. KG), ddH_2O

LB^{Amp} medium (1 L)	25 g LB broth (Carl Roth GmbH + Co. KG), ddH2O, Ampicillin (100 µg/ml final concentration)
LB^{Amp} plates (1 L)	25 g LB broth (Carl Roth GmbH + Co. KG), 15 g Agar (Carl Roth GmbH + Co. KG), ddH_2O, Ampicillin (100 µg/ml final concentration)
$LB^{Amp+Tet}$ plates (1 L)	25 g LB broth (Carl Roth GmbH + Co. KG), 15 g Agar (Carl Roth GmbH + Co. KG), $ddH4_2O$, Ampicillin (100 µg/ml final concentration), Tetracycline (12.5 µg/ml final concentration)
$LB^{Amp+Tet+Cam}$ plates	25 g LB broth (Carl Roth GmbH + Co. KG), 15 g Agar (Carl Roth GmbH + Co. KG), ddH_2O, Ampicillin (100 µg/ml final concentration)
$LB^{Amp+Tet}$ plates (1 L)	25 g LB broth (Carl Roth GmbH + Co. KG), 15 g Agar (Carl Roth GmbH + Co. KG), $ddH4_2O$, Ampicillin (100 µg/ml final concentration), Tetracycline (12.5 µg/ml final concentration), Chloramphenicol (20 µg/mL final concentration)
LB^{Cam} plates	25 g LB broth (Carl Roth GmbH + Co. KG), 15 g Agar (Carl Roth GmbH + Co. KG), $ddH4_2O$, Chloramphenicol (20 µg/mL final concentration)
M9 buffer (1 L)	6.0 g Na2HPO4, 3 g KH_2PO_4, 5 g NaCl , 50 mg Gelatine, ddH_2O; before usage: add 1 ml 1 M $MgSO_4$
NGM (1 L)	3 g NaCl, 20 g Agar (Carl Roth GmbH + Co. KG), 2,5 g Peptone (Becton, Dickinson and Company), ddH_2O, after autoclaving add: 1 ml Cholesterol (5 mg/ml in 95% EtOH stock solution), 1 ml 1 M $MgSO_4$, 1 ml 1 M $CaCl_2$, 25 ml 1 M K_2PO_4, 1 ml fungizone (Amphotericin B 2.5 mg/ml stock)
NGM for RNAi (1 L)	3 g NaCl, 20 g Agar (Carl Roth GmbH + Co. KG), 2,5 g Peptone (Becton, Dickinson and Company), ddH_2O after autoclaving add: 1 ml Cholesterol (5 mg/ml in 95% EtOH), 1 ml 1 M MgSO_4, 1 ml 1 M $CaCl_2$, 25 ml 1 M K_2PO_4, 1 ml fungizone (Amphotericin B 2.5 mg/ml stock), 1 ml 1 M
PBS 10x (1 L)	81.9 g NaCl, 2 g KCl, 14.2 g Na_2HPO_4, 2 g KH_2PO_4, ddH_2O
PFA 4 % (100 mL)	4 g PFA, ddH_2O, 10N NaOH
PGT	1x PBS, 0.25 % Triton X-100, 0.1 % Gelatine, 0.04 % NaN_3, ddH_2O
RFB 2x	160 mM KCl, 40 mM NaCl, 20 mM EGTA, 10 mM Spermidine, ddH_2O
SDS-PAGE running buffer (1 l) 10x	0.13 M Tris-base, 0.95 M Glycine, 1 % SDS, ddH2O
SDS sample buffer 5x	300 mM Tris-HCl (pH 6.8), 50 % glycerol, 10 % SDS, 5 % 14.3 M β-2-mercaptoethanol, 0.1 % bromphenol blue, ddH2O
SOC (1L)	5 g yeast extract, 20 g tryptone, 0.5 g NaCl, 1.186 g KCl, ddH_2O before usage: add 10 ml 1 M $MgCl_2$, 10 ml 1 M $MgSO_4$, 20 ml 1 M glucose

Stripping Buffer	15 g Glycine, 1 g SDS, 10 ml Tween20, ddH_2O; adjust pH to 2,2
TAE-Buffer (50x, pH 8,5) (1 L)	242 g Tris base, 57.1 ml glacial acetic acid, 18.6 g EDTA ddH_2O
Tankblotbuffer	25 mM Tris, 192 mM glycine (pH 8,3), 20 % MeOH, 0,025-0,1 % SDS (optional), ddH_2O
TBS (pH 7,5) 1x	25 mM Tris, 150 mM NaCl, ddH_2O
TBST 1x	1x TBS, 0,1 % Tween20
TBST 3 % BSA	6 g BSA in 200 ml 1x TBST
TTE buffer	100 mM Tris (pH 7.4), 0.01 % Triton X-100, 1 mM EDTA (pH 8.0), ddH_2O
Washing solution	1x PBS, 0.25 % Triton X-100, ddH_2O
YT 2x (yeast tryptone) medium (1 L), pH 7.5	16 g tryptone, 10 g yeast extract, 5 g NaCl, ddH_2O

4.1.4. Bacterial strains

Table 4.4.: Used bacterial strains

Strain name	**Genotype**	**Usage**
Escherichia coli: OP50	uracil auxotroph E. coli bacteria	food source for *C. elegans*
Escherichia coli: MACH1	F- Φ80lacZÎŤM15 ΔlacX74 hsdR(rKâĂŞ, mK+) ΔrecA1398 endA1 tonA	transformation; express dsRNA
Escherichia coli: HT115	F- *mcrA*, *mcrB*, IN(rrnD-rrnE)1 rnc14::Tn10(DE3 lysogen: lavUV5 promoter -T7 polymerase	transformation; express dsRNA
Escherichia coli: EPI300	F- mcrA Δ(mrr-hsdRMS-mcrBC) Φ80dlacZΔM15 ΔlacX74 *recA1 endA1 araD139* Δ(*ara*,*leu*)7697 *gal*U *gal*Kλ$^-$ *rpsL nupG trfA dhfr*	electroporation
Escherichia coli: SW105	SW103 ΔgalK	recombineering

4.1.5. *Caenorhabditic elegans* strains

Table 4.5.: *C. elegans* strains. Strains that were generated during this study are marked with an asterisk (*).

Strain name	**Genotype**	**Usage**
BAT028*	*otIs305 [hsp-16.2p::che-1::3xHA, rol-6(su1006)], ntIs1 [gcy-5p::GFP,lin-15(+)] V*	transgenic worm with an ASE neuronal fate marker

BAT256*	*otIs355 [rab-3::NLS::TagRFP] IV*	pan-neuronal reporter strain
BAT278*	*juIs244 (ttr-39::mCherry, ttx-3::gfp)*	GABAergic fate reporter strain
BAT453	*hsp-16.2/4::unc-30::unc-54; rol-6 (su1006)*	*unc-30* expressed under heat shock promoter
BAT684	*juIs8 [unc-25::GFP]; barEx147 [hsp-16.2/4::unc-30]*	transgenic worm with GABA neuronal fate reporter
BAT668*	*juIs8 [unc-25::GFP]*	GABA fate reporter
BAT722*	*stIs10166 [dpy-7p::HIS-24::mCherry, unc-119(+)];wIs125 [hsp::elt-7]; rrIs1 [elt-2::lacZ::GFP]*	transgenic worm with gut reporter
BAT1139	*ogt-1(ok430) III.; wIs125 [hsp::elt-7]; rrIs1 [elt-2::lacZ::GFP]*	transgenic worm with *ogt-1* null mutation
BAT1202	*otIs355 [rab-3::NLS::TagRFP] IV; barEx147 [hsp-16.2/4::unc-30]; juIs8 [unc-25::GFP]*	transgenic worm with GABA and pan-neuronal fate reporter
MT1806	*lin-15A* (n767) X.	transgenic worm with deletion in *lin-15A*

4.1.6. Enzymes

Table 4.6.: Used enzymes

Name of enzyme	**Activation temperature**	**Concentration**	Company
Taq DNA polymerase	45 °C - 68 °C	5,000 units/ml	NEB
Q5 DNA polymerase	50 °C - 72 °C	2,000 units/ml	NEB
Proteinase K	37 °C - 60 °C	800 units/ml	NEB
T4 DNA Ligase	16 °C	400,000 units/ml	NEB
Antarctic phosphatase	37 °C	5,000 units/ml	NEB

4.1.7. Equipment

Table 4.7.: Used Equipment

Name of kit	**Model**	**Company**
Autoclave	6410	CISA
Centrifuge	Heraeus Pico 17	Thermo Scientific
Centrifuge	5430	Eppendorf
Centrifuge	5810R	Eppendorf

Electroporator	Eporator	Eppendorf
Electroporation cuvette	0.2 cm electrode gap Gene pulser	Biorad
Electrophoresis power supply	EV231	Consort
Fluorescent Stereomicroscope	M205 FA	Leica
Gel documentation system	Quantum ST4	PEQLAB
Gel electrophoresis apparatus	HU10W	Biostep
Heating block	Thermomixer® Compact	Eppendorf
Incubator (15°C)	Mir-554	Sanyo
Incubator (20°C)	Mir-153	Sanyo
Incubator (25°C)	KB 115	Binder
Incubator (32°C)	AL01-06-100	Advantage Lab
Incubator (37°C)	Steri-Cult 200	Forma Scientific
Incubator (37°C)	Innova® 44	New Brunswick Scientific
Luminescent Image Analyzer	ImageQuant™ LAS 4000	GE Healthcare
Magnetic Stirrer	RCT basic	IKA
Microscope (Imaging) + Camera	Axio Imager + Sensicam	Zeiss + PCO
PCR Thermocycler	T100	Bio-Rad
pH Meter	HI2211	Hanna Instruments
Pipettes	Research® plus	Eppendorf
Rotating wheel	SB3	Stuart®
Rotator	Mini gyro-rocker SSM3	Stuart®
Rotator	Sea-saw rocker SS24	Stuart®
Spectrophotometer	NanoDrop 200c	Thermo Scientific
Stereomicroscope	SMZ745	Nikon
Stereomicroscope	MVX10	Olympus
Transilluminator	UVT-28 M	Herolab
Vortex	RS-VF 10	Phoenix Instrument
Water bath	TW2	Julabo
Western Blot power supply	PowerPac™ HC	Bio-Rad

4.1.8. Kits

Table 4.8.: Used kits

Name of kit	**Company**
GeneJET PCR Purification Kit	Thermo Scientific
HiPure Plasmid Midiprep Kit	Invitrogen
InvisorbÂő Spin Plasmid Mini Two	Stratec molecular
MinEluteÂő Gel Extraction Kit (50)	Qiagen

4.1.9. Plasmids

Table 4.9.: Used plasmids. Plasmids that were taken from the lab collection are marked with an asterisk (*). All generated plasmids were sequenced with Sanger sequencing by Eurofins Genomics.

Plasmid name	Description	Generated
L4440*	Empty vector with ampicillin resistance	Addgene- L4440 was a gift from Andrew Fire (Addgene plasmid 1654)
pRK24	F plasmid	Addegene
dBT85*	*hsp-16.2::2xFLAG*	lab collection (Tursun lab)
dBT190*	*hsp-16.4::2xFLAG*	lab collection (Tursun lab)
dBT318	*hsp-16.2::unc-30::2xFLAG*	Gibson cloning
dBT319	*hsp-16.4::unc-30::2xFLAG*	Gibson cloning
dBT436	L4440::Cam	Gibson cloning
dBT537	L4440*::hsp-1::hcf-1*	Gibson cloning
dBT538	L4440*::hsp-1::sumv-1*	Gibson cloning
dBT539	L4440*::hsp-1::sumv-2*	Gibson cloning
dBT553	L4440*::hsp-1::wdr-5.1*	Gibson cloning
dBT654	L4440:*:hat-1::hsp-1*	Gibson cloning
dBT655	L4440*::lin-53::hsp-1*	Gibson cloning
dBT690	L4440::oriT::CamR	Gibson cloning
dBT840	L4440*::lin-53::oriT*	Gibson cloning
dBT843	L4440*::rbbp-5::lin-53::oriT*	Gibson cloning
dBT842	L4440*::gld-1::oriT*	Gibson cloning
dBT841	L4440*::oma-1::oriT*	Gibson cloning
dBT846	L4440*::rpn-12::oriT*	Gibson cloning
dBT844	L4440*::lin-9::oriT*	Gibson cloning
dBT845	L4440*::lin-15A::oriT*	Gibson cloning
dBT847	pRK24::kanR	Recombineering

4.1.10. Primers

Table 4.10.: Used primers and according annealing temperatures. These primers were generated by Eurofins Genomics.

Primer name	Sequence	Usage	Annealing temperature
	Primers for cloning		
oMK01 FWD	cgg tgg cgg ccg ctc tag aaA GGT GGT GAG GTT GGA CTT G	cloning *lin-15A*	67 °C (Q5)
oMK02 REV	cca tgg aac cgg tgg atc caC ACA GAA CTT TAG TGG CGC	cloning *lin-15A*	67 °C (Q5)

oMK03 FWD	tgg atc cac cgg ttc cat ggT GGA ATT CTG TCA ATG GCA AAG	cloning *rpn-10*	63 (Q5)	°C
oMK04 REV	ggg atc cac gcg tca cgt ggG AGC TCC ATC CAC ATC CAT TTG	cloning *rpn-10*	63 (Q5)	°C
oMK05 FWD	tgg atc cac cgg ttc cat ggA AAT CTT CTG GCT GTG TG	cloning *rpn-12*	59 (Q5)	°C
oMK06 REV	ggg atc cac gcg tca cgt ggT GCT AAA ACA ATG CAT CG	cloning *rpn-12*	59 (Q5)	°C
oMK21 FWD	tgg atc cac cgg ttc cat ggT GAC GCT ATC GAC GAA CAA C	cloning *gld-1*	65 (Q5)	°C
oMK22 REV	ggg atc cac gcg tca cgt ggA GTG AGA GTG GGG CTC TG	cloning *gld-1*	65 (Q5)	°C
oMK33 FWD	tgg atc cac cgg ttc cat ggC CGA ATG CAG AAA CCA GAA TC	cloning *oma-1*	64 (Q5)	°C
oMK34 REV	ggg atc cac gcg tca cgt ggG GCC AAG TTT CTA TGG GAC	cloning *oma-1*	64 (Q5)	°C
oMK35 FWD	tgg atc cac cgg ttc cat ggG GGA ATC AAT TAA CCG AGC	cloning *oma-2*	61 (Q5)	°C
oMK36 REV	ggg atc cac gcg tca cgt ggA AAC GGA CTG ATT GGA CG	cloning *oma-2*	61 (Q5)	°C
oBT271	gcg gcc gcg aag ttc cta tac ttt cta gag aat agg aac ttc GCAT GCC TGC AGG TCG ACT CTA GAG G	cloning *hsp-16.2*	72 (Q5)	°C
oBT272	gcg gcc gcg aag ttc cta tac ttt cta gag aat agg aac ttc CAA AAA CGG AAC GTT GAG CTG GAC GG	cloning *hsp-16.4*	66 (Q5)	°C
oBT517 FWD	cta gcg tcg acg gta ccg gtA TGG ATG ACA ATA CGG CC	cloning *unc-30*	62 (Q5)	°C
oBT518 REV	cgt cct tgt agt cga tat cAA GTG GTC CAC TGT ACT G	cloning *unc-30*	62 (Q5)	°C
oBT1135 FWD	taa act tgg tct gac agT TAC GCC CCG CCC TGC CA	cloning Cam	72 (Q5)	°C
oBT1137 REV	ttg ttt att ttt cta aat aca ACG TAA GAG GTT CCA ACT TTC ACC ATA ATG AAA TAA GAT CAC	cloning Cam	72 (Q5)	°C
oBT1263 FWD	ttc gag ctc cac cgc CCT GTG ACG GAA GAT CAC TTC	cloning Kan	65 (Q5)	°C
oBT1264 REV	gag ctc aaa atc ccg cAG CGC TTT TCC GCT GCA T	cloning Kan	65 (Q5)	°C
oBT1285 FWD	cca ccg gtt cca tgg GGC GCT CGG TCT TGC CTT	cloning oriT	72 (Q5)	°C
oBT1286 REV	cca cgc gtc acg tgg AGC GCT TTT CCG CTG CAT AAC	cloning oriT	72 (Q5)	°C

oBT1414 FWD	GAA GTT TTA AAT CAA TCT AAA GTA TAT ATG AGT AA ACT TGG TCT GAC AGt tat tag aaa aat tca tcc agc aga cg	cloning Kan into pRK24	60 °C (Q5)
oBT1415 REV	TGT ATT TAG AAA AAT AAA CAA ATA GG GGT TCC GCG CAC ATT TCC CCG AAA AGc gcg gaa ccc cta ttt gt tta ttt ttc	cloining Kan into pRK24	60 °C (Q5)
oBT2223 FWD	TGG ATC CAC CGG TTC CAT GGT TCG CAC GAA TCA AGT TAC	cloning *uri-1*	66 °C (Q5)
oBT2224 REV	TGA TAT CGA ATT CCT GCA GCT GCC TGG AAG CTC TGA ATT TAC	cloning *uri-1*	66 °C (Q5)
oBT2225 FWD	TGG ATC CAC CGG TTC CAT GGC GAC CTA CGT CTA CTT TG	cloining *F52H3.5*	65 °C (Q5)
oBT2226 REV	TGA TAT CGA ATT CCT GCA GCG ATT AAT CCT CTC CTG TTT TG	cloning *F52H3.5*	65 °C (Q5)
oBT2227 FWD	TGG ATC CAC CGG TTC CAT GGC CAC CAC GTG GAA TTC TTC	cloning *C41C4.8*	69 °C (Q5)
oBT2228 REV	TGA TAT CGA ATT CCT GCA GCC CGA TGT CGG ACC AAG TAG	cloning *C41C4.8*	69 °C (Q5)
oBT2239 FWD	tgg atc cac cgg ttc cat ggC AGC TTA CTG TAG AGT TGA G	cloning *smg-7*	59 °C (Q5)
oBT2240 REV	tga tat cga att cct gca gcC GAC TGA TTC GTC TAG ATT C	cloining *smg-7*	59 °C (Q5)
oBT2241 FWD	tgg atc cac cgg ttc cat ggC TCG TAA TGA CAC ATG CG	cloning *lin-53*	61 °C (Q5)
oBT2242 REV	tga tat cga att cct gca gcG AGA AAT CGC TGA TCT TGG	cloning *lin-53*	61 °C (Q5)
oBT2391 FWD	tgg atc cac cgg ttc cat ggC TCG TAA TGA CAC ATG CG	cloning *lin-53*	61 °C (Q5)
oBT2392 REV	tga tat cga att cct gca gcG AGA AAT CGC TGA TCT TG	cloning *lin-53*	61 °C (Q5)
oBT2393 FWD	tgg atc cac cgg ttc cat ggC CGC CGA ACT ATG GAA ATT AAC	clonning *hat-1*	64 °C (Q5)
oBT2394 REV	tga tat cga att cct gca gcC TTT TCC CGA AAC CAG AAC	cloning *hat-1*	64 °C (Q5)
oBT2440 FWD	tgg atc cac cgg ttc cat ggA GAA TCT GCC AAA ATG TC	cloning *lin-8*	57 °C (Q5)
oBT2441 REV	ggg atc cac gcg tca cgt ggT TCG GAA AGT TGG AGA AAT ATG	cloning *lin-8*	57°C (Q5)
oBT2442 FWD	tgg atc cac cgg ttc cat ggT TGA CCC GAA ACT CAA GTC	cloning *lin-9*	62 °C (Q5)
oBT2443 REV	ggg atc cac gcg tca cgt ggA TAA GAA TTG CAT TCC AGC	cloning *lin-9*	62 °C (Q5)
oBT2444 FWD	tgg atc cac cgg ttc cat ggA GGT GGT GAG GTT GGA CTT G	cloning *lin-15A*	67 °C (Q5)

oBT2445 REV	tgg atc cac cgg ttc cat ggA GGT GGT GAG GTT GGA CTT G	cloning *lin-15A*	67 °C (Q5)
Primers for genotyping			
oBT40 FWD	cga gtc agt gag cga gga ag	genotyping L4440	61 °C (Taq)
oBT165 REV	CGA CGT TGT AAA ACG ACG G	genotyping L4440	57 °C (Taq)
oBT2169 FWD	gag ttt cag cag gcc gcc cag	genotyping oriT	67 °C (Taq)
oBT2170 REV	gac gag caa ggc aag acc gag c	genotyping oriT	67 °C (Taq)
oBT2235 REV	GTC CAA TGGA GAG TGT TCA GAT TC	genotyping *hcf-1*	58 °C (Taq)
oBT2236 REV	CTC TGT TGA AAG ACA CTG CTG AC	genotyping *wdr-5.1*	58 °C (Taq)
oBT2237 REV	CTT CGC TGG GCC ATA TCT GTT G	genotyping *smg-1*	61 °C (Taq)
oBT2238 REV	CTC CAC ATT ACT ATT CGA CGG GC	genotyping *smg-2*	60 °C (Taq)
oBT2476 REV	GGA TGG AAC CTG TGG CCT TG	genotyping *lin-8*	62 °C (Taq)
oBT2477 REV	GCA GAA TAG AAG AAC TCG CAC ATG	genotyping *lin-9*	59 °C (Taq)
oBT2478 REV	GGA GAC GGT TTA CTG AGA GAC C	genotyping *lin-15A*	60 °C (Taq)
oBT2479 REV	CGA TCC GAA GAC ACC ATC ATG C	genotyping *lin-53*	61 °C (Taq)
oBT2605 REV	CGA TGA AGA GAA CAA CGC GCA TC	genotyping *rpn-10*	62 °C (Taq)
oBT2606 REV	GGA GCA TGT GGA AGT CGG AC	genotyping *rpn-12*	61 °C (Taq)
oBT2661 REV	CTT GCA TCC AGT GTC CTG CTC	genotyping *gld-1*	61 °C (Taq)
oBT2662 REV	CAC TCT CAG CAT GGA CGA TGG	genotyping Rluc	61 °C (Taq)
oBT2947 REV	CCA AGC GAC ACA TTT CAG AG	genotyping *rbbp-5*	57 °C (Taq)
oBT3223 REV	GGT TTC TGC TTC TTC TGG ACT G	genotyping *set-2*	58 °C (Taq)
oBT3224 REV	GTT GCT CTC TGC TTC CGC TG	genotyping *dpy-30*	62 °C (Taq)
Primers for sequencing			

oBT206 FWD	ccg aac aac att tgc tct a	sequencing L4440	52 °C (Taq)
oBT207 REV	gga ctt aga agt cag agg ca	sequencing L4440	56 °C (Taq)
oBT259 REV	aag tca gag gcac ggg cgc gag atg	sequencing L4440	68 °C (Taq)
oBT521 FWD	GCC AAA GGA CCC AAA GGT ATG	sequencing *unc-30*	59 °C (Taq)
oBT522 FWD	TGA AGA CAT GGT GCA TCG AC	sequencing *unc-30*	58 °C (Taq)
oBT523 FWD	GCA CCA TTA ACC CAC AAT CC	sequencing *unc-30*	57 °C (Taq)
oBT524 FWD	GAG AAG AAA TCG CCG TCT GG	sequencing *unc-30*	59 °C (Taq)
oBT525 FWD	CTT CTT GCC AGA CAT CAT CTT G	sequencing *unc-30*	56 °C (Taq)
oBT526 FWD	GAT TCC AAT GTC TCC AAC GAC G	sequencing *unc-30*	59 °C (Taq)
oBT527 FWD	GAG GAC GCG AGT CAA ATC TG	sequencing *unc-30*	59 °C (Taq)

4.1.11. RNAi clones

Table 4.11.: RNAi clones. Descriptions taken from wormbase.org

Gene name	**Description**	**Derrived from**
Renilla luciferase	control	M. Hajduskova (Tursun lab)
lin-53	histone-chaperone LIN-53	Tursun et al. (2011)
rpn-10	proteasome Regulatory Particle	Chromatin sub-library
rpn-12	proteasome Regulatory Particle	Chromatin sub-library
rbbp-5	RetinoBlastoma protein Binding Protein	Chromatin sub-library
oma-2	Oocyte MAturation defective	Chromatin sub-library
gld-1	defective in Germ Line Developmen	Chromatin sub-library
mex-3	Muscle EXcess	Chromatin sub-library
lin-8	synthetic multivulva (synMuv) gene	Ahringer library
lin-9	synthetic multivulva (synMuv) gene	Ahringer library
lin-15A	synthetic multivulva (synMuv) gene	Ahringer library
hsp-1	Heat Shock Protein	Chromatin sub-library
ogt-1	O-linked GlcNAc Transferase	Ahringer library

4.2. Methods

4.2.1. Preparation of Plates

In the laboratory *C. elegans* is cultured on solid media that are seeded with bacteria as their food source. The added supplements to the media depent on the type of experiment.

4.2.1.1. Preparation of Nematode Growth Medium (NGM) Plates seeded with OP50 bacteria

NGM plates were prepared by pouring 7 mL of NGM (tab. 4.3) into a 6 cm petri dish. The plates dried O/N at RT. Dry plates were seed with 0.5 mL of OP50 (tab. 4.4) O/N culture. The plates were left to try O/N at RT for up to two days. Plates were stored at 4ÂřC.
The bacteria strain used as food source is the E. coli strain OP50 that is uracil autotroph. Thus, their growth is limited by the amount of uracil provided in the plate medium within peptone. The bacteria cannot overgrow the plates.
OP50 cultures were prepared by adding colonies obtained from a streak plate into 500 mL 2YT medium (tab. 4.3). The inoculated medium was incubated at 37 °C O/N while shaking at 130 rpm.

4.2.1.2. Preparation of 6-well RNAi plates seeded with RNAi bacteria

To prepare 6-well RNAi plates 3.5 mL NGM (tab. 4.3) was poured into each well. The 6-well plates were left to dry at RT for two days. Dried plates were seeded with 150 ÂţL of bacterial O/N culture and left to dry for up to two days at RT. The plates were stored at 4 °C.
Double stranded RNA (dsRNA) producing bacteria (tab. 4.4) HT115 were used for RNAi experiments. To induce the production of dsRNAs IPTG was added to the medium. The produced dsRNAs are taken up by the worm and are the building block for the gene silencing RNAi machinery.
The bacteria cultures were prepared by inoculating LB+Amp medium (tab. 4.3) from streaks from $LB^{+Amp+Tet}$ plates. The inoculated medium was incubated at 37 °C O/N while shaking at 130 rpm.

4.2.2. Worm specific methods

4.2.2.1. Maintenance and storage of *C. elegans*

Worm strains containing a heat shock construct were kept at 15 °C on NGM plates seeded with OP50 bacteria and propagated using standard procedures (Brenner, 1974). To maintain worms, a small chunk of a worm containing plate was cut out and placed upside down on a fresh plates seeded with OP50 bacteria.Alternatively, worms could be picked with a so called 'worm pick', consisting of a platinum wire attached to a glass pipette, and transferred to a fresh plate. Extrachromosol arrays in worms are only transmitted to some of the offspring. Worms carrying extrachromosol arrays were handpicked

by phenotypic inspection under the microscope looking for the selection marker in order to maintain the population. As an example for the worm strain BAT1202 (tab 4.5) only worms that showed a rolling movement due to a defect in cuticle collagen were picked and transferred to a fresh plate.

In order to maintain N2 males, N2 males were cross-fertilized with N2 hermaphrodytes on a weekly basis. Self-fertilized hermaphrodytes themselfes lead to a low frequency of male progeny (0.1 %).

Males of another genotype than N2 were generated by crossing N2 males with hermaphrodytes of the genotype of interest. The resulting male progreny was maintained by back crossing them with hermaphrodytes of the same genotype weekly.

4.2.2.2. Worm lysis

To break down peptide bonds and to free nucleic acids 1U of proteinase K (tab.4.6) to 10 U of lysis solution (tab. 4.3). Worms were transferred into lysis solution. A single worm was transferred into a PCR tube containing 20 ÂţL of lysis solution (if more worms were lyses, the volume of lysis solution was increased accordingly). The worm containing lysis solution was incubated at -80 °C for at least 30 minutes. This freeze-crack steps helps to break up the rigid cuticle of the worm to liberate the DNA. In the next step the frozen PCR tubes were placed into a thermocycler using the following program:

Table 4.12.

Temperature	**Time**	**Process**
60 °C	60 minutes	Activation of proteinase K
95 °C	30 minutes	Heat inactivation of proteinase K
12 °C	∞	Storage

4.2.2.3. Harvesting worms

Worms were harvested by washing off 6 cm plates with M9 buffer (tab.4.3) and transferred to 1.5 mL Eppendorf tubes. The worms were pelleted at 30 g and washed three times with 800 ÂţL of M9 buffer to remove OP50 bacteria. Harvested worms were then used in experiments such as RNAi or immuno stainings.

4.2.2.4. Synchronizing worms

Worms were washed of from plats containing many L1 larvae, but were not starved. The worms were collected in 1.5 mL Eppendorf tubes and allowed to settle for two minutes to separate the worms by size. After inspecting the Eppendorf tube under the microscope the upper layer, containing L1 larvae, was taken off and transferred into a new 1.5 mL Eppendorf tube. The worms were spinned down at 30 g for 1 minute, washed three times

with M9 buffer and transferred to a fresh plate containing OP50 bacteria. The plate was left at 15 °C until further usage.

4.2.2.5. Freezing worms for long term storage

Worms can be stored for long term at -80 °C. Starved plates containing plenty of L1 larvae were washed off and transferred into 1.5 mL Eppendorf tubes. The worms were spinned down at 30 g for 1 minute and washed three times with M9 buffer (tab.4.3). The M9 buffer was taken off and 2 mL of a 1:1 mixture of M9 buffer and freezing solution (tab. 4.3) was added and then transferred into a Cryo tube. To ensure slow freezing the cryo tube was placed into a Styrofoam box and kept for at least 24 h at -80 °C. After about 1 day the cryo tube was moved out from Styrofoam box and stored at -80 °C.

4.2.2.6. Transgenic crosses

Animals were mated by placing 6 to 8 males with 5 hermaphrodytes on a 6 cm plate containing a drop of OP50 to ensure that the worms would meet.
In the subsequent generation one would look for paternally or maternally expressed inherited markers. Crossing was carried out to introduce the GABA specific marker *unc-25::gfp* and pan-neuronal marker *rab-3::rfp* into strains carrying *hsp-16.2/4::unc-30; rol-6 (su1006)* (tab.4.5, BAT453). First, N2 males from the male stock (section 4.2.2.1) were first crossed with worms carrying *gcy-5::gfp* (BAT668, tab. 4.5). Males carrying *gcy-5::gfp* were then mated with transgenic worms carrying *hsp-16.2/4::unc-30, ttr-39::mCherry*. In the F1 generation animals that showed unc-25::gfp as well the rolling movement were singled out and allowed to reproduce. About 20 - 50 F2 animals were singled out to homozygous the GABA marker (unc-25::gfp) and the rolling movement indicating that the animals are carrying hsp-16.2/4::unc-30. Worms were singled out until the population was homozygous for markers.

Crossing was carried out to introduce ogt-1 mutant background (tab. 4.5, RB653) into worms carrying hsp::elt-7, elt-2::lacZ::gfp, rol-6 (tab. 4.5, BAT722). First, N2 males from male stock (section 4.2.2.1) were crossed with worms hsp::elt-7, elt-2::lacZ::gfp (tab. 4.5, BAT722). The male progeny from this strain was crossed into the ogt-1 mutant background (tab. 4.5, RB653). The F1 generation is heterozygous for both the marker and the mutation. Several F1 hermaphrodytes expressing the marker (GFP/GFP or GFP/+) were singled out and allowed to reproduce. About 50 F2 animals showing the marker were singled out to homozygous the marker as well as the mutation. The F2 mother animal was lysed in lysis buffer (tab. 4.3) as soon eggs had been layed on the plate and genotyped for the mutation (section 4.2.2.7). Worms were singled out until they were homozygous for both the marker and the mutation.

4.2.2.7. Genotyping

To genotype worms 2 ÂţL of worm lysate (section 4.2.2.2) was used as template for PCR (section 4.2.3.1) The mutation ogt-1 (ok430) is a deletion. Thus, it was possible

to confirm the mutation by the correct band size on an agarose gel (section 4.2.3.3). In addition a WT lysate was used as a negative control in the same PCR.

4.2.2.8. Antibody stainings

4.2.2.8.1. Antibody staining by reduction and oxidation method

Using the Reduction and Oxidation method worms were treated as previously described (**?**). Worms were resuspended in 2x RFB (tab. 4.3) + 2 % formaldehyde in 1.5 mL Eppendorf tubes, followed by three freeze-thaw-cycles. The worms were then fixed for 30 minutes at 25 °C. Each sample was washed once in TTE buffer (tab. 4.3) and incubated in TTE buffer + β-Mercaptoethanol at 37 °C for 4 h. Afterwards the samples were washed once with BO_3 buffer (tab. 4.3) and incubated in BO_3 + 10 mM DTT at 37 °C for 15 minutes. The samples were washed again with BO_3 buffer and then incubated in BO_3 + 0.3 % H_2O_2 for 15 minutes. The samples were washed for the third time with BO_3 buffer and then blocked with blocking solution (tab. 4.3) at 25 °C for 30 minutes. After blocking primary antibodies (tab. 4.2) were added to the worm samples and incubated at 4 °C O/N. The samples were washed five times in washing solution (tab. 4.3). Secondary antibodies (tab. 4.2) were added to the samples and incubated at 4 °C O/N in the dark, followed by five washing steps in washing solution. Samples were mounted in DAPI-containing mounting medium and imaged under Zeiss fluorescent microscope (tab. 4.7).

4.2.2.8.2. Antibody staining using slide crack method

Using the slide crack method (**?**) worms were subjected to freeze-crack using two SuperFrost Plus slides. Worms were carefully put in between two slides to form a slide sandwich and incubated for 30 minuts on dry ice. The worms were cracked by quickly opening the slide sandwich and immediately immersed in cold methanol or PFA and incubated for 5 minutes at RT. The worms were washed with 1x PBS (tab. 4.3) and blocking solution was added. The samples were incubated for 30 minutes at 25 °C. The subsequent steps were similar as the Reduction and Oxidation method.

4.2.3. Molecular Biology Methods

4.2.3.1. Polymerase Chain Reaction (PCR)

Polymerase chain reaction was used to amply the DNA fragment of interest. Specific primers were used to ensure that only the fragment of interest was amplified. The primers and their annealing temperatures are listed in table 4.10. The following reactions and programs were used for different PCRs.

4.2.3.1.1. NEB Taq Polymerase PCR (colony PCR)

5 Îijl 10x ThermoPol Reaction Buffer, 0.5 Îijl 10 mM dNTPs, 0.5 Îijl 10 ÎijM Forward Primer, 0.5 Îijl, 0.5 Îijl 10 ÎijM Reverse Primer, 2 Îijl Template DNA (bacterial culture), 0.125 Îijl Taq DNA Polymerase, ad Nuclease-free water until 50 ÂţL total volume is reached.

Table 4.13.

Temperature	Time	Process
95 °C	10 minutes	Initial denaturation
34 cycles		
95 °C	30 seconds	Denaturation
table 4.10	30 seconds	primer hybridization
68 °C	2 - 3 min depending on fragment length	Elongation
68 °C	5 min	Final elongation
12 °C	∞	Storage

4.2.3.1.2. NEB Q5 Polymerase PCR (cloning)

10 Îijl 5x Q5 Reaction Buffer, 1 Îijl 10 mM dNTPs, 2.5 Îijl 10 ÎijM Forward Primer, 2.5 Îijl 10 ÎijM Reverse Primer, 2 Îijl Template DNA, 0.5 Îijl Q5 High-Fidelity DNA Polymerase, ad 50 Îijl Nuclease-free water

Table 4.14.

Temperature	Time	Process
98 °C	30 seconds	Initial denaturation
34 cycles		
98 °C	10 seconds	Denaturation
table 4.10	30 seconds	primer hybridization
72 °C	1 - 3 min depending on fragment length	Elongation
68 °C	2 min	Final elongation
8 °C	∞	Storage

4.2.3.2. Colony PCR

Colony PCR was performed to identify bacterial colonies carrying the plasmid of interest after a performed transformation. Bacterial colonies were inoculated in 100 ÂţL LB_{Amp} medium (tab. 4.3) at 37 °C and 700 rpm for 2 hours. Of that culture 1 ÂţL was used as template for PCR (section 4.2.3.1). The DNA from positive colonies was isolated (section 4.2.3.7) and send for sequencing (Eurofins Genomics).

4.2.3.3. Gel electrophoresis

To analyze DNA bands and plasmids by their size, agarose gel electrophoresis was used. Agarose gels (1 %) in 1x TAE buffer were prepared with ethidium bromide (0.5 Âţg/mL

final concentration). TAE (1x) was also used as a running buffer. DNA samples were loaded with 6x loading dye. By applying 100 V over 30 minutes DNA fragments were separated by size. The Generuler 1 kb Plus DNA ladder (0.1 µg/mL) from Thermo Scientific was used as a marker.

4.2.3.4. DNA purification/Gel extraction

DNA samples were purified using GeneJET PCR Purification Kit from Thermo Scientific (tab. 4.8) according to manufacturer's instructions.
Alternatively DNA fragments were purified using gel extraction. The DNA fragments were visualized using UV light in 1 % agarose gels, cut out and collected in 1.5 mL Eppendorf tubes. The DNA containing agarose gel pieces were treated according to manufacturer's instructions using the QIAquick Gel Extraction Kit from QIAGEN (tab. 4.8).
DNA concentrations were measured using Nanodrop (tab. 4.7).

4.2.3.5. Molecular cloning

Molecular cloning was used to generate desired DNA sequences and amplify them. For RNAi experiments the plasmid L4440 was used.

4.2.3.5.1. Cloning using Restriction Enzymes

4.2.3.5.2. Gibson Cloning

The NEBuilder® Assembly Tool (http://nebuilder.neb.com) was used to design specific primers to amplify DNA fragments with overhangs (homology arms).
The vector DNA was digested with specific restriction enzymes (tab. 4.6). The insert DNA fragments were amplified (section 4.2.3.1.2) using the specific primers designed for Gibson cloning (tab. 4.10). All plasmids are listed in table 4.9.

The amplified fragments were combined with vector and 2x Gibson Mastermix (tab. 4.3) were combined in one reaction tube and incubated at 50 °C for 1 hour. The Gibson ligation was used for transformation (section 4.2.3.6).
The correct amount of vector and insert DNA added to the Gibson reaction were calculated as follows:

- vector: 0.1 pmol, insert 0.03 pmol

- $ng = \frac{(pmol \times bp \times 650)}{1000}$

4.2.3.6. Transformation in *Escherichia coli*

Free DNA is transferred into competent bacterial cells during transformation. For this study, three different types of competent cells were used for transformation experiments, the E. coli strains MACH1, HT115, and EPI300 (tab. 4.4).

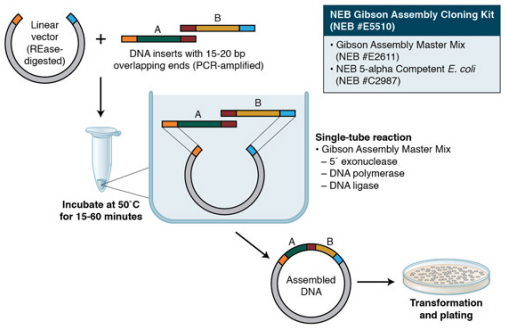

Figure 4.1.: Gibson Assembly Workflow modified from https://www.neb.com/applications/cloning-and%20synthetic-biology/dna-assembly-and%20cloning/gibson-assembly

4.2.3.6.1. Chemical transformation

Competent E. coli bacterial cells were transformed with ligation reaction (section 4.2.3.5.1) or Gibson reaction (section 4.2.3.5.2) using heat shock. The cells were thawed on ice (50 µL per reaction) and 2 ÂţL ligation/Gibson reaction was added for transformation of MACH1 cells, while 1 µL of isolated plasmid (1-100 ng) was added to HT115 bacterial cells.
The solution of bacterial cells and ligation mix were incubated for 30 minutes. Then the sample was heat shocked at 42 °C for 30 seconds (MACH1) or 90 seconds (HT115) in order to make the bacterial membrane more permeable for DNA fragment. After the heat shocks were immediately transferred on ice for 2 minutes and 250 µL of SOC medium (tab. 4.3) was added. The samples were incubated at 37 °C for 1 hour while shaking at 700 rpm in order to let the cells recover. The transformed cells were then plated on LB^{Amp} plates (MACH1) or on $LB^{Amp+Tet}$ plates (HT115) O/N at 37 °C. As a negative controll ddH2O was added to the competent bacteria cells and then treated as as described above.

4.2.3.6.2. Electroporation

A single colony of electrocompetent bacteria strains SW105 and EPI300 (tab. 4.4) were inoculated in 10 mL LB O/N at 32 °C (SW105) or 37ÂřC (EPI300). It is important to keep the temperature for SW105 under 32 °C to prevent the activation of the heat inducible λ Red recombinase. Of the overnight culture 500 µL were taken to inoculate 50 mL LB. The cultures were grown until a $OD_{600} = 0.4$ - 0.6 and then transferred on ice for 20 minutes. The bacteria cells were harvested in pre-cooled falcon tubes for 15 minutes at 4000 rpm at 4 °C. The cells were washed with ice-cold ddH2O. The cells were harested again for 15 minutes at 4000 rpm at 4 °C and all the supernatant was taken off except 1 mL. The pelleted cells were resuspended and immediately used for electroporation.
Aliquots of 100 µL were prepared in 1.5 mL Eppendorf tubes and to each aliquot 50 - 100 ng of plasmid DNA were pipetted. The sample was transferred to pre-chilled electroporate cuvettes. (tab. 4.7) and electroporated at 2.5 kV at an active constant time mode (time constant 4.8 - 5.4 seconds). After electroporation 900 µL of LB were

added immediately and the cells were incubated for 1 hour at 37 °C while shaking at 700 rpm. Afterwards 1:10 and 1:000 dilutions were plated on LB^{CamR} plates O/N at 32 °C (SW105) or 37 °C (EPI300).

4.2.3.7. Plasmid isolation from *Escherichia coli*

Single colonies of bacteria containing the plasmids of interest were used to inoculate 2 mL LB^{Amp} (tab.
reftab:buffer) O/N at 37 °C while shaking at 130 rpm. The plasmids of interest were isolated using the Invisorb Spin Plasmid Mini Two (250) Kit (Stratec, tab. 4.8) according to the manufacturer's specifications.
The DNA concentration was measured using the NanoDrop ND-1000 Spectrphotometer (tab. 4.7).

4.2.3.8. Bacterial Recombination

To heat activate the λ Red recombinasae in the SW105 containing the plasmid pRK24 (tab.4.9) a single colony was taken from LB_{Cam} plate (section) and inoculated O/N at 32 °C. The next day 500 µwere used to inoculate 50 mL LB_{Cam} starter culture and grown until OD_{600} = 0.4 - 0.6 in flasks. The OD_{600} was measured using the NanoDrop ND-1000 Spectrophotometer (tab. 4.7). The water bath was heated up to 42 °C (tab. 4.7). The flasks were incubated at 42 °C while gentle shaking for 20 minutes. Then the flasks were transferred to ice for 20 minutes. The bacteria were harvested for 15 minutes at 4000 rpm at 4 °C, washed twice with 12.5 % glycerol (tab. 4.3) and pelleted again. All supernatant was taken off except for 1 mL and 100 µL aliquots were prepared. At this point aliquots could be shock frozen with liquid Nitrogen and kept for up to 4 weeks. The PCR product containing the recombineering cassette for Kanamycin (200 ng) was electroporated into SW105+pRK24 as described before (section 4.2.3.8). As a negative control water was added to SW105+pRK24 and treated otherwise the same. After electroporation cells were incubated for 3 hours at RT and then plated on LB^{Kan} plates at 32 °C for 36 h.

4.2.4. Protein biochemical work

4.2.4.1. SDS-page

In a 1.5 mL Eppendorf tube 25 L4 animals were collected. The animals were washed three times. After the last washing step 1M SDS sample buffer (see 4.3) was added. The proteins are charged negatively with SDS allowing therefore to seperate them according to their molecular weight by applying an electric force field across the polyacrylamid gel (Shapiro, 1967; Laemmli, 1970). The samples were placed in a thermomixer to cook at 95 °C for 10 minutes followed by a freeze-crack step at -80 °C O/N. The samples were stored at -20 °C until usage.

4.2.4.1.1. Preparation of polyacrylamid gels

Each gel consists of two layers: In the upper layer the proteins are concentrated (stacking gel) before entering into the lower layer in which they are seperated based on their mass (separating gel).

Table 4.15.: **Prepared mixes for pouring gels.** All components are combined to pour the separating and the stacking gel. APS and TEMED have to be added last right before pouring the gel. The pH of the Tris buffer (asterisk (*)) for the stacking gel is 8.8, while a pH of 6.8 is used for the separating gel.

Components	**Separating gel**		**Stacking gel**
	7.5 %	10 %	5 %
1.5 M Tris (pH 8.8/6.8)	1.5 mL	1.5 mL	250 µL
Acrylamide: Bis 30 % 37.5:1	1.5 mL	2 mL	500 µL
20 % SDS	30 µL	30 µL	15 µL
ddH2O	2.9 mL	2.4 mL	2.2 mL
10 % APS	60 µL	60 µL	30 µL
TEMED	5 µL	5 µL	3 µL

First the separating gel (see tab. 4.15) was poured into casting. The choice of percentage of the separating gel depends on the protein that is to be detected. After the separating gel had solidified it was overlaid with with the stacking gel (see tab. 4.15). The wells are inserted and the gel is left to polymerize. The polymerized gels can be stored in Saran wrap at 4 °C for about a week.

4.2.4.1.2. Electrophoresis

Before starting the gel, samples have to be denatured by cooking them at 96 °C for 5 minutes and spinning them down at 17,000 g for 10 minutes. Of each sample 20 ÂţL was loaded on the gel. The PageRuler Prestained Protein ladder from Thermo Scientific was used as a marker. SDS sample buffer (see tab. 4.3) was used to load free wells in order that all samples run equally through the gel.
The loaded SDS gel are placed in tank containing SDS running buffer (see tab. 4.3). An electric force field is applied. The negatively charged proteins move through the gel towards the positive charge at a constant current of 10 mA in the stacking gel. Once the samples pass into the separating gel the current is upregulated to 20 mA. As soon as the bromophenol blue dye has reached the bottom of the gel the run is terminated.

4.2.4.2. Western blotting

Proteins that were separated based on their mass during Electrophoresis are now transferred from the polyacrylamide gel to a nitrocellulose membrane (**?**) and detected by using specific antibodies.

4.2.4.2.1. Wet transfer of proteins and blocking of membrane

First the SDS page gel containing the samples and the nitrocellulose membrane were equilibrated in 1x tank blot buffer (see tab. 4.3) for 5 minutes. Afterwards all components were assembled in a cassette from the postive to the negative pole in the following order: fiber pad, filter paper, nitrocellulose membrane, SDS page gel, filter paper, and a fiber pad. All components are kept in 1x tank blot buffer during assembly. The cassette is transfered to a tank containing 1x tank blot buffer and by applying a constant voltage of 100 V for 1h, ionic interactions lead to the adherence of proteins to the membrane. The transfer buffer has to be cooled down during transfer. Subsequently the nitrocellulose membrane containing the protein is transfered into 3 % BSA dissolved in 1x TBST (see tab. 4.3) for 1h while shaking at RT.

4.2.4.2.2. Immunological detection

The blocked nitrocellulose membrane contained probed proteins was incubated for 1 to 2 h at RT with primary antibody. The primary antibody was diluted in 3 % BSA dissolved in 1x TBST (see tab. 4.3) according the instruction of the manufacture. Subsequently the membrane was washed three times in 1x TBST for 10 minutes each. Afterwards a specific secondary antibody was added, diluted 1:10,000 in 3 % BSA dissolved in 1x TBST, and incubated for two hours at RT, followed by three washing steps in 1x TBST. All incubation and washing steps are conducted while gently shaking the membrane. The secondary antibody is coupled to horseradish peroxidase (HRP), which is used to produce a chemiluminescent signal in relation to the amount of protein.
To visualize the protein the blot was exposed to Lumi-Light Western blotting substrate from Sigma Aldrich. The Luminscent Imaga Analyzer detected the chemiluminescent signal using the ImagaQuant LAS4000 software.

4.2.5. RNAi interference

RNA interference describes the process in which dsRNA is cleaved into short interfering RNAs (siRNAs) that target sequence specific messenger RNAs (mRNAs), form a complex (RISC) that leads to degradation of its bound mRNA and thus to the down regulation of gene expression. This process was first described in *C. elegans* and can be used to target specific mRNAs to knock down the expression of a gene of interest to investigate its function through the analysis of the resulting phenotypes (Fire et al., 1998).
RNAi experiments were performed by feeding worms with dsRNA producing bacteria (tab. 4.4: HT115) using standard procedure (Timmons et al., 2001). In HT115 bacteria the RNAse III gene is interrupted by the Tn10-transposon, which contains a tetracycline-resistant gene. HT115 cells are transformed with the L4440 plasmid (tab. 4.9) containing a sequence targeting the gene of interest. Because they are modified to express the T7 RNA polymerase from an Isopropyl-β-D-1-thiogalactopyranoside (IPTG) inducible promoter, IPTG is added to the NGM medium for RNAi experiments (tab.4.3) to induce the production of dsRNA to cause a knock-down of the target gene in worms that take up these bacteria.

4.2.5.1. P0 RNAi-screen

For a P0 RNAi screen, L1 worms were harvested as described before (section 4.2.2.3) and plated onto 6-well RNAi plates containing RNAi bacteria to knock down a particular gene of interest. The worms were grown at 15 °C until they reached L3 - L4 stage and then heat shocked at 37 °C for 30 minutes. Immediately afterwards the plates were moved to 25 °C and incubated for 18 - 24 h until scoring. The heat shock activated the expression of the terminal selector gene UNC-30 (*hsp-16.2/4::unc-30*). The worms were screened under fluorescent dissecting scope (tab. 4.7) to detect ectopical expression of the fate reporters *unc-25::gfp* and *rab-3::tRFP*. The obtained data were analysed using a Paired Student's t test to determine statistical significance.

4.2.5.2. F1 RNAi-screen

For F1 RNAi screen, 7 - 15 synchronized L4 worms (section 4.2.2.4) were plated onto 6-well RNAi plate containing RNAi bacteria to knock down a particular gene of interest. The worms were grown at 15 °C until the F1 generation reached L4 status. At this point the plates were heat shocked for 30 minutes at 37 °C and then immediately moved to 25 °C for 18 to 24 h to induce the ubiquitously express the TF UNC-30 (*hsp-16.2/4::unc-30*). Worms expressing the fate reporters *unc-25::gfp* and/or *rab-3::tRFP* were scored under the fluorescent dissecting scope. The obtained data were analyse (paired Student's t-test).

4.2.5.3. Fluorescent Microscopy

To image worms a fluorescent microscope was used (Axio Imager 2, Zeiss) equipped with a digital camera (Sensicam, PCO). The worms were transferred onto 3 % agar pads placed on a glass slide and immobilized with sodium azide (20 mM). Sodium azide paralyzes the worms by interrupting the electron transport chain. A cover slip was placed on the agar pad and the worms were imaged using the Axio Imager 2 (tab. 4.7). The pictures were processed using the open source software MicroManager 1.4 (https://www.micro-manager.org/).

Bibliography

Alder Matthew N, Dames Shale, Gaudet Jeffrey, Mango Susan E. Gene silencing in Caenorhabditis elegans by transitive RNA interference. // RNA. 2003. 9, 1. 25–32.

Andersen Erik C, Lu Xiaowei, Horvitz HR. C. elegans ISWI and NURF301 antagonize an Rb-like pathway in the determination of multiple cell fates. // Development. 2006. 133, 14. 2695–704.

Ankeny RA. The natural history of Caenorhabditis elegans research. // Nat. Rev. Genet. 2001. 2, 6. 474–9.

Asikainen S, Vartiainen S, Lakso M, Neuroreport Nass R. Selective sensitivity of Caenorhabditis elegans neurons to RNA interference // Neuroreport. 2005.

Avery L, Wasserman S. Ordering gene function: the interpretation of epistasis in regulatory hierarchies. // Trends Genet. 1992. 8, 9. 312–6.

CRISPR provides acquired resistance against viruses in prokaryotes. // . 2007. 315, 5819. 1709–1712.

Baumeister Ralf, Ge Liming. The worm in us - Caenorhabditis elegans as a model of human disease. // Trends Biotechnol. 2002. 20, 4. 147–8.

Berninger B, Costa MR, âĂę Koch U of. Functional properties of neurons derived from in vitro reprogrammed postnatal astroglia // Journal of âĂę. 2007.

Bhavsar Rital B, Tsonis Panagiotis A. Exogenous Oct-4 inhibits lens transdifferentiation in the newt Notophthalmus viridescens. // PLoS ONE. 2014. 9, 7. e102510.

Boone Charles, Bussey Howard, Andrews Brenda J. Exploring genetic interactions and networks with yeast. // Nat. Rev. Genet. 2007. 8, 6. 437–49.

Bossinger Olaf, Fukushige Tetsunari, Claeys Myriam, Borgonie Gaetan, D McGhee, James. The apical disposition of the Caenorhabditis elegans intestinal terminal web is maintained by LET-413. // Dev. Biol. 2004. 268, 2. 448–56.

Brenner S. The genetics of Caenorhabditis elegans. // Genetics. 1974. 77, 1. 71–94.

Bric Anka, Miething Cornelius, Bialucha Carl U, Scuoppo Claudio, Zender Lars, Krasnitz Alexander, Xuan Zhenyu, Zuber Johannes, Wigler Michael, Hicks James, W McCombie, Richard, Hemann Michael T, Hannon Gregory J, Powers Scott, Lowe Scott W. Functional identification of tumor-suppressor genes through an in vivo RNA interference screen in a mouse lymphoma model. // Cancer Cell. 2009. 16, 4. 324–35.

Bridges BA, Foster PL, Timms AR. Effect of endogenous carotenoids on "adaptive" mutation in Escherichia coli FC40. // Mutat. Res. 2001. 473, 1. 109–19.

Brumbaugh Justin, Hochedlinger Konrad. Removing reprogramming roadblocks: Mbd3 depletion allows deterministic iPSC generation. // Cell Stem Cell. 2013. 13, 4. 379–81.

Brummelkamp Thijn R, Bernards René, Agami Reuven. A system for stable expression of short interfering RNAs in mammalian cells. // Science. 2002. 296, 5567. 550–3.

Buckley Shannon M, Beatriz Aranda-Orgilles,, Strikoudis Alexandros, Apostolou Effie, Loizou Evangelia, Kelly Moran-Crusio,, Farnsworth Charles L, Koller Antonius A, Dasgupta Ramanuj, Silva Jeffrey C, Stadtfeld Matthias, Hochedlinger Konrad, Chen Emily I, Aifantis Iannis. Regulation of pluripotency and cellular reprogramming by the ubiquitin-proteasome system. // Cell Stem Cell. 2012. 11, 6. 783–98.

Calixto A, Chelur D, Topalidou I, Chen X, methods Chalfie M. Enhanced neuronal RNAi in C. elegans using SID-1 // Nature methods. 2010.

Ceron Julian, Rual Jean-François, Chandra Abha, Dupuy Denis, Vidal Marc, Heuvel Sander. Large-scale RNAi screens identify novel genes that interact with the C. elegans retinoblastoma pathway as well as splicing-related components with synMuv B activity. // Bmc Dev Biol. 2007. 7, 1. 30.

Chalfie M, Tu Y, Euskirchen G, Ward WW, Prasher DC. Green fluorescent protein as a marker for gene expression. // Science. 1994. 263, 5148. 802–5.

Chen Di, Riddle Donald L. Function of the PHA-4/FOXA transcription factor during C. elegans post-embryonic development. // BMC Dev. Biol. 2008. 8, 1. 26.

Chen Jiekai, Liu He, Liu Jing, Qi Jing, Wei Bei, Yang Jiaqi, Liang Hanquan, Chen You, Chen Jing, Wu Yaran, Guo Lin, Zhu Jieying, Zhao Xiangjie, Peng Tianran, Zhang Yixin, Chen Shen, Li Xuejia, Li Dongwei, Wang Tao, Pei Duanqing. H3K9 methylation is a barrier during somatic cell reprogramming into iPSCs. // Nat. Genet. 2013. 45, 1. 34–42.

Chen Meizhen, Masumi Takano-Maruyama,, M Pereira-Smith, Olivia, Gaufo Gary O, Tominaga Kaoru. MRG15, a component of HAT and HDAC complexes, is essential for proliferation and differentiation of neural precursor cells. // J. Neurosci. Res. 2009. 87, 7. 1522–31.

Choi J, Costa ML, Mermelstein CS, Chagas C, Holtzer S, Holtzer H. MyoD converts primary dermal fibroblasts, chondroblasts, smooth muscle, and retinal pigmented epithelial cells into striated mononucleated myoblasts and multinucleated myotubes. // Proc. Natl. Acad. Sci. U.S.A. 1990. 87, 20. 7988–92.

Cinar Hediye N, Richards Keri L, Oommen Kavita S, Newman Anna P. The EGL-13 SOX domain transcription factor affects the uterine pi cell lineages in Caenorhabditis elegans. // Genetics. 2003. 165, 3. 1623–8.

Ciosk Rafal, Michael DePalma,, Priess James. Translational Regulators Maintain Totipotency in the Caenorhabditis elegans Germline // Science. 2006. 311, 5762. 851–853.

Cirillo LA, CE McPherson,, P EMBO âĂę, Bossard. Binding of the wingedâĂŘhelix transcription factor HNF3 to a linker histone site on the nucleosome // The EMBO âĂę. 1998.

Cirillo LA, Lin FR, Cuesta I, Friedman D, cell Jarnik M. Opening of compacted chromatin by early developmental transcription factors HNF3 (FoxA) and GATA-4 // Molecular cell. 2002.

Cong Le, Ran FA, Cox David, Lin Shuailiang, Barretto Robert, Habib Naomi, Hsu Patrick D, Wu Xuebing, Jiang Wenyan, Marraffini Luciano A, Zhang Feng. Multiplex genome engineering using CRISPR/Cas systems. // Science. 2013. 339, 6121. 819–23.

Cui Mingxue, Kim EB, Han Min. Diverse chromatin remodeling genes antagonize the Rb-involved SynMuv pathways in C. elegans. // PLoS Genet. 2006. 2, 5. e74.

Davis RL, Weintraub H, Lassar AB. Expression of a single transfected cDNA converts fibroblasts to myoblasts. // Cell. 1987. 51, 6. 987–1000.

Deneris Evan S, Hobert Oliver. Maintenance of postmitotic neuronal cell identity. // Nat. Neurosci. 2014. 17, 7. 899–907.

Detwiler MR, Reuben M, Li X, Rogers E, Lin R. Two zinc finger proteins, OMA-1 and OMA-2, are redundantly required for oocyte maturation in C. elegans. // Dev. Cell. 2001. 1, 2. 187–99.

Dhawan S, Georgia S, Tschen S, Fan G, cell Bhushan A. Pancreatic Îš cell identity is maintained by DNA methylation-mediated repression of Arx // Developmental cell. 2011.

Di Tullio Alessandro, Vu Manh Thien P, Schubert Alexis, Castellano Giancarlo, Månsson Robert, Graf Thomas. CCAAT/enhancer binding protein alpha (C/EBP(alpha))-induced transdifferentiation of pre-B cells into macrophages involves no overt retrodifferentiation. // Proc. Natl. Acad. Sci. U.S.A. 2011. 108, 41. 17016–21.

Djabrayan Nareg J, Dudley Nathaniel R, Sommermann Erica M, Rothman Joel H. Essential role for Notch signaling in restricting developmental plasticity. // Genes Dev. 2012. 26, 21. 2386–91.

Doitsidou Maria, Poole Richard J, Sarin Sumeet, Bigelow Henry, Hobert Oliver. C. elegans mutant identification with a one-step whole-genome-sequencing and SNP mapping strategy. // PLoS ONE. 2010. 5, 11. e15435.

Dombecki Carolyn R, Chiang Ason C, Kang Hyun-Joo J, Bilgir Ceyda, Stefanski Nicholas A, Neva Bryan J, Klerkx Elke P, Nabeshima Kentaro. The chromodomain protein MRG-1 facilitates SC-independent homologous pairing during meiosis in Caenorhabditis elegans. // Dev. Cell. 2011. 21, 6. 1092–103.

Doyon Yannick, Selleck William, Lane William S, Tan Song, Côté Jacques. Structural and functional conservation of the NuA4 histone acetyltransferase complex from yeast to humans. // Mol. Cell. Biol. 2004. 24, 5. 1884–96.

Dresbach T, Qualmann B, Kessels MM, Garner CC, Gundelfinger ED. The presynaptic cytomatrix of brain synapses. // Cell. Mol. Life Sci. 2001. 58, 1. 94–116.

Eitoku M, Sato L, Senda T, Horikoshi M. Histone chaperones: 30 years from isolation to elucidation of the mechanisms of nucleosome assembly and disassembly. // Cell. Mol. Life Sci. 2008. 65, 3. 414–44.

Erdelyi Peter, Wang Xing, Suleski Marina, Wicky Chantal. A Network of Chromatin Factors Is Regulating the Transition to Postembryonic Development in Caenorhabditis elegans. // G3 (Bethesda). 2017. 7, 2. 343–353.

Evans MJ, Kaufman MH. Establishment in culture of pluripotential cells from mouse embryos. // Nature. 1981. 292, 5819. 154–6.

Evans TC, Crittenden SL, Kodoyianni V, Kimble J. Translational control of maternal glp-1 mRNA establishes an asymmetry in the C. elegans embryo. // Cell. 1994. 77, 2. 183–94.

Fay David S, Yochem John. The SynMuv genes of Caenorhabditis elegans in vulval development and beyond. // Dev. Biol. 2007. 306, 1. 1–9.

Fedorov Yuriy, Anderson Emily M, Birmingham Amanda, Reynolds Angela, Karpilow Jon, Robinson Kathryn, Leake Devin, Marshall William S, Khvorova Anastasia. Off-target effects by siRNA can induce toxic phenotype. // RNA. 2006. 12, 7. 1188–96.

Feinberg Evan H, Hunter Craig P. Transport of dsRNA into cells by the transmembrane protein SID-1. // Science. 2003. 301, 5639. 1545–7.

Fire A, Xu S, Montgomery MK, Kostas SA, Driver SE, Mello CC. Potent and specific genetic interference by double-stranded RNA in Caenorhabditis elegans. // Nature. 1998. 391, 6669. 806–11.

Firnhaber C, Hammerlund M. Neuron-specific feeding RNAi in C. elegans and its use in a screen for essential genes required for GABA neuron function // PLoS genetics. 2013.

Frank CA, Baum Paul D, Garriga Gian. HLH-14 is a C. elegans achaete-scute protein that promotes neurogenesis through asymmetric cell division. // Development. 2003. 130, 26. 6507–18.

Frederick Anokye-Danso,, Anyanful Akwasi, Sakube Yasuji, Kagawa Hiroaki. Transcription factors GATA/ELT-2 and forkhead/HNF-3/PHA-4 regulate the tropomyosin gene expression in the pharynx and intestine of Caenorhabditis elegans. // J. Mol. Biol. 2008. 379, 2. 201–11.

Fukushige Tetsunari, Krause Michael. The myogenic potency of HLH-1 reveals widespread developmental plasticity in early C. elegans embryos. // Development. 2005. 132, 8. 1795–805.

Gambetta Maria C, Müller Jürg. A critical perspective of the diverse roles of O-GlcNAc transferase in chromatin. // Chromosoma. 2015. 124, 4. 429–42.

Garcia Sandra N, Olivia Pereira-Smith,. MRGing chromatin dynamics and cellular senescence. // Cell Biochem. Biophys. 2008. 50, 3. 133–41.

Gascón Sergio, Masserdotti Giacomo, Russo Gianluca L, Götz Magdalena. Direct Neuronal Reprogramming: Achievements, Hurdles, and New Roads to Success. // Cell Stem Cell. 2017. 21, 1. 18–34.

Gascón Sergio, Murenu Elisa, Masserdotti Giacomo, Ortega Felipe, Russo Gianluca L, Petrik David, Deshpande Aditi, Heinrich Christophe, Karow Marisa, Robertson Stephen P, Schroeder Timm, Beckers Johannes, Irmler Martin, Berndt Carsten, Angeli José P P, Conrad Marcus, Berninger Benedikt, Götz Magdalena. Identification and Successful Negotiation of a Metabolic Checkpoint in Direct Neuronal Reprogramming. // Cell Stem Cell. 2016. 18, 3. 396–409.

Gaydos Laura J, Rechtsteiner Andreas, Egelhofer Thea A, Carroll Coleen R, Strome Susan. Antagonism between MES-4 and Polycomb repressive complex 2 promotes appropriate gene expression in C. elegans germ cells. // Cell Rep. 2012. 2, 5. 1169–77.

Gifford Casey A, Meissner Alexander. Epigenetic obstacles encountered by transcription factors: reprogramming against all odds. // Curr. Opin. Genet. Dev. 2012. 22, 5. 409–15.

Gilleard JS, JD McGhee,. Activation of hypodermal differentiation in the Caenorhabditis elegans embryo by GATA transcription factors ELT-1 and ELT-3. // Mol. Cell. Biol. 2001. 21, 7. 2533–44.

Ginsberg Michael, Schachterle William, Shido Koji, Rafii Shahin. Direct conversion of human amniotic cells into endothelial cells without transitioning through a pluripotent state. // Nat Protoc. 2015. 10, 12. 1975–85.

Gore Athurva, Li Zhe, Fung Ho-Lim L, Young Jessica E, Agarwal Suneet, Jessica Antosiewicz-Bourget,, Canto Isabel, Giorgetti Alessandra, Israel Mason A, Kiskinis Evangelos, Lee Je-Hyuk H, Loh Yuin-Han H, Manos Philip D, Montserrat Nuria, Panopoulos Athanasia D, Ruiz Sergio, Wilbert Melissa L, Yu Junying, Kirkness Ewen F, Izpisua Belmonte Juan C, Rossi Derrick J, Thomson James A, Eggan Kevin,

Daley George Q, Goldstein Lawrence S, Zhang Kun. Somatic coding mutations in human induced pluripotent stem cells. // Nature. 2011. 471, 7336. 63–7.

Greer Eric L, E Beese-Sims, Sara, Brookes Emily, Spadafora Ruggero, Zhu Yun, Rothbart Scott B, David Aristizábal-Corrales,, Chen Shuzhen, Badeaux Aimee I, Jin Qiuye, Wang Wei, Strahl Brian D, Colaiácovo Monica P, Shi Yang. A histone methylation network regulates transgenerational epigenetic memory in C. elegans. // Cell Rep. 2014. 7, 1. 113–26.

Gupta Pratyush, Leahul Lindsay, Wang Xin, Wang Chris, Bakos Brendan, Jasper Katie, Hansen Dave. Proteasome regulation of the chromodomain protein MRG-1 controls the balance between proliferative fate and differentiation in the C. elegans germ line. // Development. 2015. 142, 2. 291–302.

Gurdon J. B. The developmental capacity of nuclei taken from intestinal epithelium cells of feeding tadpoles. // J Embryol Exp Morphol. 1962. 10. 622–40.

Hallam S, Singer E, Waring D, Jin Y. The C. elegans NeuroD homolog cnd-1 functions in multiple aspects of motor neuron fate specification. // Development. 2000. 127, 19. 4239–52.

Hanna Jacob H, Saha Krishanu, Jaenisch Rudolf. Pluripotency and cellular reprogramming: facts, hypotheses, unresolved issues. // Cell. 2010. 143, 4. 508–25.

Hanover John A, Forsythe Michele E, Hennessey Patrick T, Brodigan Thomas M, Love Dona C, Ashwell Gilbert, Krause Michael. A Caenorhabditis elegans model of insulin resistance: altered macronutrient storage and dauer formation in an OGT-1 knockout. // Proc. Natl. Acad. Sci. U.S.A. 2005. 102, 32. 11266–71.

Hansen Dave, Laura Wilson-Berry,, Dang Thanh, Schedl Tim. Control of the proliferation versus meiotic development decision in the C. elegans germline through regulation of GLD-1 protein accumulation. // Development. 2004. 131, 1. 93–104.

Harlow ML, Ress D, Stoschek A, Marshall RM, UJ McMahan,. The architecture of active zone material at the frog's neuromuscular junction. // Nature. 2001. 409, 6819. 479–84.

Haslbeck Veronika, Eckl Julia M, Kaiser Christoph J, Papsdorf Katharina, Hessling Martin, Richter Klaus. Chaperone-interacting TPR proteins in Caenorhabditis elegans. // J. Mol. Biol. 2013. 425, 16. 2922–39.

Hayakawa Tomohiro, Zhang Fan, Hayakawa Noriyo, Ohtani Yasuko, Shinmyozu Kaori, Nakayama Jun-ichi, Andreassen Paul R. MRG15 binds directly to PALB2 and stimulates homology-directed repair of chromosomal breaks. // J. Cell. Sci. 2010. 123, Pt 7. 1124–30.

Heinrich Christophe, Blum Robert, Gascón Sergio, Masserdotti Giacomo, Tripathi Pratibha, Sánchez Rodrigo, Tiedt Steffen, Schroeder Timm, Götz Magdalena, Berninger

Benedikt. Directing astroglia from the cerebral cortex into subtype specific functional neurons. // PLoS Biol. 2010. 8, 5. e1000373.

Heins N, Malatesta P, Cecconi F, Nature âĂę Nakafuku M. Glial cells generate neurons: the role of the transcription factor Pax6 // Nature âĂę. 2002.

Hillier Ladeana W, Coulson Alan, Murray John I, Bao Zhirong, Sulston John E, Waterston Robert H. Genomics in C. elegans: so many genes, such a little worm. // Genome Res. 2005. 15, 12. 1651–60.

Hodgkin J, Doniach T. Natural variation and copulatory plug formation in Caenorhabditis elegans. // Genetics. 1997. 146, 1. 149–64.

Hoe Matthew, Nicholas Hannah R. Evidence of a MOF histone acetyltransferase-containing NSL complex in C. elegans. // Worm. 2014. 3, 4. e982967.

Holmberg Johan, Perlmann Thomas. Maintaining differentiated cellular identity. // Nat. Rev. Genet. 2012. 13, 6. 429–39.

Hörmanseder Eva, Simeone Angela, Allen George E, Bradshaw Charles R, Figlmüller Magdalena, Gurdon John, Jullien Jerome. H3K4 Methylation-Dependent Memory of Somatic Cell Identity Inhibits Reprogramming and Development of Nuclear Transfer Embryos. // Cell Stem Cell. 2017. 21, 1. 135–143.e6.

Horn Thomas, Sandmann Thomas, Fischer Bernd, Axelsson Elin, Huber Wolfgang, Boutros Michael. Mapping of signaling networks through synthetic genetic interaction analysis by RNAi. // Nat. Methods. 2011. 8, 4. 341–6.

Horner MA, Quintin S, Domeier ME, Kimble J, Labouesse M, Mango SE. pha-4, an HNF-3 homolog, specifies pharyngeal organ identity in Caenorhabditis elegans. // Genes Dev. 1998. 12, 13. 1947–52.

Hu E, Tontonoz P, Spiegelman BM. Transdifferentiation of myoblasts by the adipogenic transcription factors PPAR gamma and C/EBP alpha. // Proc. Natl. Acad. Sci. U.S.A. 1995. 92, 21. 9856–60.

Hu W, Qiu B, Guan W, Wang Q, Wang M, Li W, cell Gao L stem. Direct conversion of normal and Alzheimer's disease human fibroblasts into neuronal cells by small molecules // Cell stem cell. 2015.

Hussein Samer M, Batada Nizar N, Vuoristo Sanna, Ching Reagan W, Autio Reija, Närvä Elisa, Ng Siemon, Sourour Michel, Hämäläinen Riikka, Olsson Cia, Lundin Karolina, Mikkola Milla, Trokovic Ras, Peitz Michael, Brüstle Oliver, P Bazett-Jones, David, Alitalo Kari, Lahesmaa Riitta, Nagy Andras, Otonkoski Timo. Copy number variation and selection during reprogramming to pluripotency. // Nature. 2011. 471, 7336. 58–62.

Hwang Woong Y, Fu Yanfang, Reyon Deepak, Maeder Morgan L, Tsai Shengdar Q, Sander Jeffry D, Peterson Randall T, Yeh J-R Joanna R, Joung JK. Efficient genome editing in zebrafish using a CRISPR-Cas system. // Nat. Biotechnol. 2013. 31, 3. 227–9.

Ieda Masaki, Fu Ji-Dong D, Paul Delgado-Olguin,, Vedantham Vasanth, Hayashi Yohei, Bruneau Benoit G, Srivastava Deepak. Direct reprogramming of fibroblasts into functional cardiomyocytes by defined factors. // Cell. 2010. 142, 3. 375–86.

Ingham PW. A gene that regulates the bithorax complex differentially in larval and adult cells of Drosophila. // Cell. 1984. 37, 3. 815–23.

Jackson Aimee L, Linsley Peter S. Recognizing and avoiding siRNA off-target effects for target identification and therapeutic application. // Nat Rev Drug Discov. 2010. 9, 1. 57–67.

Jarriault Sophie, Schwab Yannick, Greenwald Iva. A Caenorhabditis elegans model for epithelial-neuronal transdifferentiation. // Proc. Natl. Acad. Sci. U.S.A. 2008. 105, 10. 3790–5.

Jayakody Sujatha A, Anai Gonzalez-Cordero,, Ali Robin R, Pearson Rachael A. Cellular strategies for retinal repair by photoreceptor replacement. // Prog Retin Eye Res. 2015. 46. 31–66.

Jellinger KA, Bancher C. Neuropathology of Alzheimer's disease: a critical update. // J. Neural Transm. Suppl. 1998. 54. 77–95.

Jenner P, Olanow CW. Understanding cell death in Parkinson's disease. // Ann. Neurol. 1998. 44, 3 Suppl 1. S72–84.

Jiang H, Xu Z, Zhong P, Ren Y, Nature âĂę Liang G. Cell cycle and p53 gate the direct conversion of human fibroblasts to dopaminergic neurons // Nature âĂę. 2015.

Jin Y, Hoskins R, Horvitz HR. Control of type-D GABAergic neuron differentiation by C. elegans UNC-30 homeodomain protein. // Nature. 1994. 372, 6508. 780–3.

Jinek Martin, Chylinski Krzysztof, Fonfara Ines, Hauer Michael, Doudna Jennifer A, Charpentier Emmanuelle. A programmable dual-RNA-guided DNA endonuclease in adaptive bacterial immunity. // Science. 2012. 337, 6096. 816–21.

Kadyk LC, Kimble J. Genetic regulation of entry into meiosis in Caenorhabditis elegans. // Development. 1998. 125, 10. 1803–13.

Kagias Konstantinos, Ahier Arnaud, Fischer Nadine, Jarriault Sophie. Members of the NODE (Nanog and Oct4-associated deacetylase) complex and SOX-2 promote the initiation of a natural cellular reprogramming event in vivo. // Proc. Natl. Acad. Sci. U.S.A. 2012. 109, 17. 6596–601.

Kamath RS, Ahringer J. Genome-wide RNAi screening in Caenorhabditis elegans // Methods. 2003.

Kamath RS, M Martinez-Campos,, Zipperlen P, Fraser AG, Ahringer J. Effectiveness of specific RNA-mediated interference through ingested double-stranded RNA in Caenorhabditis elegans. // Genome Biol. 2001. 2, 1. RESEARCH0002.

Katherine McJunkin,, Mazurek Anthony, Premsrirut Prem K, Zuber Johannes, Dow Lukas E, Simon Janelle, Stillman Bruce, Lowe Scott W. Reversible suppression of an essential gene in adult mice using transgenic RNA interference. // Proc. Natl. Acad. Sci. U.S.A. 2011. 108, 17. 7113–8.

Kawamura Teruhisa, Suzuki Jotaro, Wang Yunyuan V, Menendez Sergio, Morera Laura B, Raya Angel, Wahl Geoffrey M, Izpisúa Belmonte Juan C. Linking the p53 tumour suppressor pathway to somatic cell reprogramming. // Nature. 2009. 460, 7259. 1140–4.

Kiefer Julie C, Smith Pliny A, Mango Susan E. PHA-4/FoxA cooperates with TAM-1/TRIM to regulate cell fate restriction in the C. elegans foregut. // Dev. Biol. 2007. 303, 2. 611–24.

Kimble J, Hirsh D. The postembryonic cell lineages of the hermaphrodite and male gonads in Caenorhabditis elegans. // Dev. Biol. 1979. 70, 2. 396–417.

Kragl M, Knapp D, Nacu E, Khattak S, Nature Maden M. Cells keep a memory of their tissue origin during axolotl limb regeneration // Nature. 2009.

The glial nature of embryonic and adult neural stem cells. // . 2009. 32. 149–184.

Kulessa H, Frampton J, Graf T. GATA-1 reprograms avian myelomonocytic cell lines into eosinophils, thromboblasts, and erythroblasts. // Genes Dev. 1995. 9, 10. 1250–62.

Ladewig J, Mertens J, Kesavan J, Doerr J, Nature âĂę Poppe D. Small molecules enable highly efficient neuronal conversion of human fibroblasts // Nature âĂę. 2012.

Ladewig Julia, Koch Philipp, Brüstle Oliver. Leveling Waddington: the emergence of direct programming and the loss of cell fate hierarchies. // Nat. Rev. Mol. Cell Biol. 2013. 14, 4. 225–36.

Lederberg J, Tatum EL. Gene recombination in Escherichia coli. // Nature. 1946. 158, 4016. 558.

Systematic mapping of genetic interactions in Caenorhabditis elegans identifies common modifiers of diverse signaling pathways. // . 2006. 38, 8. 896–903.

Li Hongyuan, Liu Xin, Wang Dan, Su Liangping, Zhao Tingting, Li Zhongwei, Lin Cong, Zhang Yu, Huang Baiqu, Lu Jun, Li Xiaoxue. O-GlcNAcylation of SKN-1 modulates the lifespan and oxidative stress resistance in Caenorhabditis elegans. // Sci Rep. 2017. 7. 43601.

Li Tengguo, Kelly William G. A role for Set1/MLL-related components in epigenetic regulation of the Caenorhabditis elegans germ line. // PLoS Genet. 2011. 7, 3. e1001349.

Li X, Zuo X, Jing J, Ma Y, Wang J, Liu D, Zhu J, cell Du X stem. Small-molecule-driven direct reprogramming of mouse fibroblasts into functional neurons // Cell stem cell. 2015.

Liang Jiancong, Wan Ma, Zhang Yi, Gu Peili, Xin Huawei, Jung Sung Y, Qin Jun, Wong Jiemin, Cooney Austin J, Liu Dan, Songyang Zhou. Nanog and Oct4 associate with unique transcriptional repression complexes in embryonic stem cells. // Nat. Cell Biol. 2008. 10, 6. 731–9.

Liu ML, Zang T, Zou Y, Chang JC, Nature âĂę Gibson JR. Small molecules enable neurogenin 2 to efficiently convert human fibroblasts into cholinergic neurons // Nature âĂę. 2013.

Liu XinJian, Huang Qian, Li Fang, Li Chuan-Yuan Y. Enhancing the efficiency of direct reprogramming of human primary fibroblasts into dopaminergic neuron-like cells through p53 suppression. // Sci China Life Sci. 2014. 57, 9. 867–75.

Love Dona C, Krause Michael W, Hanover John A. O-GlcNAc cycling: emerging roles in development and epigenetics. // Semin. Cell Dev. Biol. 2010. 21, 6. 646–54.

Loyola Alejandra, Almouzni Genevieve. Histone chaperones, a supporting role in the limelight. // Biochim. Biophys. Acta. 2004. 1677, 1-3. 3–11.

Luo Min, Ling Te, Xie Wenbing, Sun He, Zhou Yonggang, Zhu Qiaoyun, Shen Meili, Zong Le, Lyu Guoliang, Zhao Yun, Ye Tao, Gu Jun, Tao Wei, Lu Zhigang, Grummt Ingrid. NuRD blocks reprogramming of mouse somatic cells into pluripotent stem cells. // Stem Cells. 2013. 31, 7. 1278–86.

Ma Natalie J, Moonan Daniel W, Isaacs Farren J. Precise manipulation of bacterial chromosomes by conjugative assembly genome engineering. // Nat Protoc. 2014. 9, 10. 2285–300.

Maki Nobuyasu, Rinako Suetsugu-Maki,, Tarui Hiroshi, Agata Kiyokazu, Katia Del Rio-Tsonis,, Tsonis Panagiotis A. Expression of stem cell pluripotency factors during regeneration in newts. // Dev. Dyn. 2009. 238, 6. 1613–6.

Mali P, Yang L, Esvelt KM, Aach J, âĂę Guell M. RNA-guided human genome engineering via Cas9 // âĂę. 2013.

Mango SE, Lambie EJ, Kimble J. The pha-4 gene is required to generate the pharyngeal primordium of Caenorhabditis elegans. // Development. 1994. 120, 10. 3019–31.

Marro S, Pang ZP, Yang N, Tsai MC, Qu K, cell Chang HY stem. Direct lineage conversion of terminally differentiated hepatocytes to functional neurons // Cell stem cell. 2011.

Masserdotti Giacomo, Gascón Sergio, Götz Magdalena. Direct neuronal reprogramming: learning from and for development. // Development. 2016. 143, 14. 2494–510.

Meacham Corbin E, Ho Emily E, Dubrovsky Esther, Gertler Frank B, Hemann Michael T. In vivo RNAi screening identifies regulators of actin dynamics as key determinants of lymphoma progression. // Nat. Genet. 2009. 41, 10. 1133–7.

Min Kyoengwoo, Kang Junsu, Lee Junho. A modified feeding RNAi method for simultaneous knock-down of more than one gene in Caenorhabditis elegans. // BioTechniques. 2010. 48, 3. 229–32.

Mondoux Michelle A, Love Dona C, Ghosh Salil K, Fukushige Tetsunari, Bond Michelle, Weerasinghe Gayani R, Hanover John A, Krause Michael W. O-linked-N-acetylglucosamine cycling and insulin signaling are required for the glucose stress response in Caenorhabditis elegans. // Genetics. 2011. 188, 2. 369–82.

Cell lineage and fate determination. // . 1998.

Nasu Akira, Ikeya Makoto, Yamamoto Takuya, Watanabe Akira, Jin Yonghui, Matsumoto Yoshihisa, Hayakawa Kazuo, Amano Naoki, Sato Shingo, Osafune Kenji, Aoyama Tomoki, Nakamura Takashi, Kato Tomohisa, Toguchida Junya. Genetically matched human iPS cells reveal that propensity for cartilage and bone differentiation differs with clones, not cell type of origin. // PLoS ONE. 2013. 8, 1. e53771.

Norris Adam, Gracida Xicotencatl, Calarco John. CRISPR-mediated genetic interaction profiling identifies RNA binding proteins controlling metazoan fitness // Elife. 2017. 6. e28129.

Onder Tamer T, Kara Nergis, Cherry Anne, Sinha Amit U, Zhu Nan, Bernt Kathrin M, Cahan Patrick, Marcarci BO, Unternaehrer Juli, Gupta Piyush B, Lander Eric S, Armstrong Scott A, Daley George Q. Chromatin-modifying enzymes as modulators of reprogramming. // Nature. 2012. 483, 7391. 598–602.

Paddison Patrick J, Caudy Amy A, Bernstein Emily, Hannon Gregory J, Conklin Douglas S. Short hairpin RNAs (shRNAs) induce sequence-specific silencing in mammalian cells. // Genes Dev. 2002. 16, 8. 948–58.

Park In-Hyun H, Zhao Rui, West Jason A, Yabuuchi Akiko, Huo Hongguang, Ince Tan A, Lerou Paul H, Lensch MW, Daley George Q. Reprogramming of human somatic cells to pluripotency with defined factors. // Nature. 2008. 451, 7175. 141–6.

Pasi CE, Dereli-Öz A, Negrini S, Friedli M, Fragola G, Lombardo A, Van Houwe G, Naldini L, Casola S, Testa G, Trono D, Pelicci PG, Halazonetis TD. Genomic instability in induced stem cells. // Cell Death Differ. 2011. 18, 5. 745–53.

Patel Tulsi, Tursun Baris, Rahe Dylan P, Hobert Oliver. Removal of Polycomb repressive complex 2 makes C. elegans germ cells susceptible to direct conversion into specific somatic cell types. // Cell Rep. 2012. 2, 5. 1178–86.

Payman Samavarchi-Tehrani,, Golipour Azadeh, David Laurent, Sung Hoon-Ki K, Beyer Tobias A, Datti Alessandro, Woltjen Knut, Nagy Andras, Wrana Jeffrey L. Functional genomics reveals a BMP-driven mesenchymal-to-epithelial transition in the initiation of somatic cell reprogramming. // Cell Stem Cell. 2010. 7, 1. 64–77.

Perrimon Norbert, Ni Jian-Quan Q, Perkins Lizabeth. In vivo RNAi: today and tomorrow. // Cold Spring Harb Perspect Biol. 2010. 2, 8. a003640.

Petrella Lisa N, Wang Wenchao, Spike Caroline A, Rechtsteiner Andreas, Reinke Valerie, Strome Susan. synMuv B proteins antagonize germline fate in the intestine and ensure C. elegans survival. // Development. 2011. 138, 6. 1069–79.

Phillips GR, Huang JK, Wang Y, Tanaka H, Shapiro L, Zhang W, Shan WS, Arndt K, Frank M, Gordon RE, Gawinowicz MA, Zhao Y, Colman DR. The presynaptic particle web: ultrastructure, composition, dissolution, and reconstitution. // Neuron. 2001. 32, 1. 63–77.

Premsrirut Prem K, Dow Lukas E, Kim Sang Y, Camiolo Matthew, Malone Colin D, Miething Cornelius, Scuoppo Claudio, Zuber Johannes, Dickins Ross A, Kogan Scott C, Shroyer Kenneth R, Sordella Raffaella, Hannon Gregory J, Lowe Scott W. A rapid and scalable system for studying gene function in mice using conditional RNA interference. // Cell. 2011. 145, 1. 145–58.

Qin Han, Blaschke Kathryn, Wei Grace, Ohi Yuki, Blouin Laure, Qi Zhongxia, Yu Jingwei, Yeh Ru-Fang F, Hebrok Matthias, Miguel Ramalho-Santos,. Transcriptional analysis of pluripotency reveals the Hippo pathway as a barrier to reprogramming. // Hum. Mol. Genet. 2012. 21, 9. 2054–67.

Qin Han, Diaz Aaron, Blouin Laure, Lebbink Robert J, Patena Weronika, Tanbun Priscilia, M LeProust, Emily, T McManus, Michael, Song Jun S, Miguel Ramalho-Santos,. Systematic identification of barriers to human iPSC generation. // Cell. 2014. 158, 2. 449–461.

Quintin S, Michaux G, L McMahon,, Gansmuller A, Labouesse M. The Caenorhabditis elegans gene lin-26 can trigger epithelial differentiation without conferring tissue specificity. // Dev. Biol. 2001. 235, 2. 410–21.

Radermacher Pablo T, Myachina Faina, Bosshardt Fritz, Pandey Rahul, Mariappa Daniel, Müller H-Arno J A, Lehner Christian F. O-GlcNAc reports ambient temperature and confers heat resistance on ectotherm development. // Proc. Natl. Acad. Sci. U.S.A. 2014. 111, 15. 5592–7.

Rasmussen MA, Holst B, Tümer Z, reports Johnsen MG cell. Transient p53 suppression increases reprogramming of human fibroblasts without affecting apoptosis and DNA damage // Stem cell reports. 2014.

Richard Jai P, Zuryn Steven, Fischer Nadine, Pavet Valeria, Vaucamps Nadège, Jarriault Sophie. Direct in vivo cellular reprogramming involves transition through discrete, non-pluripotent steps. // Development. 2011. 138, 8. 1483–92.

Transorganogenesis and transdifferentiation in C. elegans are dependent on differentiated cell identity. // . 2016. 420, 1. 136–147.

Riddle Misty R, Weintraub Abraham, Nguyen Ken C, Hall David H, Rothman Joel H. Transdifferentiation and remodeling of post-embryonic C. elegans cells by a single transcription factor. // Development. 2013. 140, 24. 4844–9.

Roignant Jean-Yves Y, Carré Clément, Mugat Bruno, Szymczak Dimitri, Lepesant Jean-Antoine A, Antoniewski Christophe. Absence of transitive and systemic pathways allows cell-specific and isoform-specific RNAi in Drosophila. // RNA. 2003. 9, 3. 299–308.

Rosenmund Christian, Rettig Jens, Brose Nils. Molecular mechanisms of active zone function. // Curr. Opin. Neurobiol. 2003. 13, 5. 509–19.

Rubin GM, Yandell MD, Wortman JR, Gabor Miklos GL, Nelson CR, Hariharan IK, Fortini ME, Li PW, Apweiler R, Fleischmann W, Cherry JM, Henikoff S, Skupski MP, Misra S, Ashburner M, Birney E, Boguski MS, Brody T, Brokstein P, Celniker SE, Chervitz SA, Coates D, Cravchik A, Gabrielian A, Galle RF, Gelbart WM, George RA, Goldstein LS, Gong F, Guan P, Harris NL, Hay BA, Hoskins RA, Li J, Li Z, Hynes RO, Jones SJ, Kuehl PM, Lemaitre B, Littleton JT, Morrison DK, Mungall C, PH O'Farrell,, Pickeral OK, Shue C, Vosshall LB, Zhang J, Zhao Q, Zheng XH, Lewis S. Comparative genomics of the eukaryotes. // Science. 2000. 287, 5461. 2204–15.

Seelk Stefanie, Irene Adrian-Kalchhauser,, Hargitai Balázs, Hajduskova Martina, Gutnik Silvia, Tursun Baris, Ciosk Rafal. Increasing Notch signaling antagonizes PRC2-mediated silencing to promote reprograming of germ cells into neurons. // Elife. 2016. 5.

Sieburth D, Ch'ng QL, Dybbs M, Nature Tavazoie M. Systematic analysis of genes required for synapse structure and function // Nature. 2005.

Sindhu Camille, Payman Samavarchi-Tehrani,, Meissner Alexander. Transcription factor-mediated epigenetic reprogramming. // J. Biol. Chem. 2012. 287, 37. 30922–31.

Sommermann Erica M, Strohmaier Keith R, Maduro Morris F, Rothman Joel H. Endoderm development in Caenorhabditis elegans: the synergistic action of ELT-2 and -7 mediates the specificationâĘŠdifferentiation transition. // Dev. Biol. 2010. 347, 1. 154–66.

Sonnhammer EL, Durbin R. Analysis of protein domain families in Caenorhabditis elegans. // Genomics. 1997. 46, 2. 200–16.

Sulston JE, Horvitz HR. Post-embryonic cell lineages of the nematode, Caenorhabditis elegans. // Dev. Biol. 1977. 56, 1. 110–56.

Sulston JE, Schierenberg E, White JG, Thomson JN. The embryonic cell lineage of the nematode Caenorhabditis elegans. // Dev. Biol. 1983. 100, 1. 64–119.

T McManus, Michael, Petersen Christian P, Haines Brian B, Chen Jianzhu, Sharp Phillip A. Gene silencing using micro-RNA designed hairpins. // RNA. 2002. 8, 6. 842–50.

T Sandoval-Guzmán,, Wang H, Khattak S, cell Schuez M stem. Fundamental differences in dedifferentiation and stem cell recruitment during skeletal muscle regeneration in two salamander species // Cell stem cell. 2014.

Takahashi Kazutoshi, Yamanaka Shinya. Induction of pluripotent stem cells from mouse embryonic and adult fibroblast cultures by defined factors. // Cell. 2006. 126, 4. 663–76.

Takahashi Maiko, Iwasaki Hideki, Inoue Hideshi, Takahashi Kenji. Reverse genetic analysis of the Caenorhabditis elegans 26S proteasome subunits by RNA interference. // Biol Chem. 2002. 383, 7-8. 1263–6.

Tapscott SJ, Davis RL, Thayer MJ, Cheng PF, Weintraub H, Lassar AB. MyoD1: a nuclear phosphoprotein requiring a Myc homology region to convert fibroblasts to myoblasts. // Science. 1988. 242, 4877. 405–11.

Thomas CM, Smith CA. Incompatibility group P plasmids: genetics, evolution, and use in genetic manipulation. // Annu. Rev. Microbiol. 1987. 41. 77–101.

Thomson JA, J Itskovitz-Eldor,, Shapiro SS, Waknitz MA, Swiergiel JJ, Marshall VS, Jones JM. Embryonic stem cell lines derived from human blastocysts. // Science. 1998. 282, 5391. 1145–7.

Timmons L, Court DL, Fire A. Ingestion of bacterially expressed dsRNAs can produce specific and potent genetic interference in Caenorhabditis elegans. // Gene. 2001. 263, 1-2. 103–12.

Tocchini Cristina, Keusch Jeremy J, Miller Sarah B, Finger Susanne, Gut Heinz, Stadler Michael B, Ciosk Rafal. The TRIM-NHL protein LIN-41 controls the onset of developmental plasticity in Caenorhabditis elegans. // PLoS Genet. 2014. 10, 8. e1004533.

Toh Cheng-Xu Delon X, Chan Jun-Wei W, Chong Zheng-Shan S, Wang Hao F, Guo Hong C, Satapathy Sandeep, Ma Dongrui, Goh Germaine Y, Khattar Ekta, Yang Lin, Tergaonkar Vinay, Chang Young-Tae T, Collins James J, Daley George Q, Wee Keng B, Farran Chadi A, Li Hu, Lim Yoon-Pin P, Bard Frederic A, Loh Yuin-Han H. RNAi Reveals Phase-Specific Global Regulators of Human Somatic Cell Reprogramming. // Cell Rep. 2016. 15, 12. 2597–607.

Tursun Baris, Patel Tulsi, Kratsios Paschalis, Hobert Oliver. Direct conversion of C. elegans germ cells into specific neuron types. // Science. 2011. 331, 6015. 304–8.

Unhavaithaya Y, Shin TH, Miliaras N, Lee J, Cell Oyama T. MEP-1 and a homolog of the NURD complex component Mi-2 act together to maintain germline-soma distinctions in C. elegans // Cell. 2002.

Vierbuchen Thomas, Ostermeier Austin, Pang Zhiping P, Kokubu Yuko, Südhof Thomas C, Wernig Marius. Direct conversion of fibroblasts to functional neurons by defined factors. // Nature. 2010. 463, 7284. 1035–41.

Waddington C. H. The strategy of the genes. A discussion of some aspects of theoretical biology. 1957.

Wang Tim, Wei Jenny J, Sabatini David M, Lander Eric S. Genetic screens in human cells using the CRISPR-Cas9 system. // Science. 2014. 343, 6166. 80–4.

Wang Yu, Kallgren Scott P, Reddy Bharat D, Kuntz Karen, Luis López-Maury,, Thompson James, Watt Stephen, Ma Chun, Hou Haitong, Shi Yang, Yates John R, Bähler Jürg, J O'Connell, Matthew, Jia Songtao. Histone H3 lysine 14 acetylation is required for activation of a DNA damage checkpoint in fission yeast. // J. Biol. Chem. 2012. 287, 6. 4386–93.

Wapinski Orly L, Vierbuchen Thomas, Qu Kun, Lee Qian Y, Chanda Soham, Fuentes Daniel R, Giresi Paul G, Ng Yi H, Marro Samuele, Neff Norma F, Drechsel Daniela, Martynoga Ben, Castro Diogo S, Webb Ashley E, Südhof Thomas C, Brunet Anne, Guillemot Francois, Chang Howard Y, Wernig Marius. Hierarchical mechanisms for direct reprogramming of fibroblasts to neurons. // Cell. 2013. 155, 3. 621–35.

Ward S, Carrel JS. Fertilization and sperm competition in the nematode Caenorhabditis elegans. // Dev. Biol. 1979. 73, 2. 304–21.

Weintraub H, Tapscott SJ, Davis RL, Thayer MJ, Adam MA, Lassar AB, Miller AD. Activation of muscle-specific genes in pigment, nerve, fat, liver, and fibroblast cell lines by forced expression of MyoD. // Proc. Natl. Acad. Sci. U.S.A. 1989. 86, 14. 5434–8.

Wilmut I, Schnieke AE, J McWhir,, Kind AJ, Campbell KH. Viable offspring derived from fetal and adult mammalian cells. // Nature. 1997. 385, 6619. 810–3.

Winston William M, Molodowitch Christina, Hunter Craig P. Systemic RNAi in C. elegans requires the putative transmembrane protein SID-1. // Science. 2002. 295, 5564. 2456–9.

Xie Huafeng, Ye Min, Feng Ru, Graf Thomas. Stepwise reprogramming of B cells into macrophages. // Cell. 2004. 117, 5. 663–76.

Yang Xiaoyong, Zhang Fengxue, Kudlow Jeffrey E. Recruitment of O-GlcNAc transferase to promoters by corepressor mSin3A: coupling protein O-GlcNAcylation to transcriptional repression. // Cell. 2002. 110, 1. 69–80.

Yochum Gregory S, Ayer Donald E. Role for the mortality factors MORF4, MRGX, and MRG15 in transcriptional repression via associations with Pf1, mSin3A, and Transducin-Like Enhancer of Split. // Mol. Cell. Biol. 2002. 22, 22. 7868–76.

Yoshida Yoshinori, Yamanaka Shinya. Recent stem cell advances: induced pluripotent stem cells for disease modeling and stem cell-based regeneration. // Circulation. 2010. 122, 1. 80–7.

Yu Junying, Vodyanik Maxim A, Kim Smuga-Otto,, Jessica Antosiewicz-Bourget,, Frane Jennifer L, Tian Shulan, Nie Jeff, Jonsdottir Gudrun A, Ruotti Victor, Stewart Ron, Slukvin Igor I, Thomson James A. Induced pluripotent stem cell lines derived from human somatic cells. // Science. 2007. 318, 5858. 1917–20.

Yücel Duygu, Hoe Matthew, Llamosas Estelle, Kant Sashi, Jamieson Callum, Young Pamela A, Crossley Merlin, Nicholas Hannah R. SUMV-1 antagonizes the activity of synthetic multivulva genes in Caenorhabditis elegans. // Dev. Biol. 2014. 392, 2. 266–82.

Yuzyuk T, Fakhouri THI, Kiefer J, cell Mango SE. The Polycomb Complex Protein mes-2/E(z) Promotes the Transition from Developmental Plasticity to Differentiation in C. elegans Embryos // Developmental cell. 2009.

Zhang L, Yin JC, Yeh H, Ma NX, Lee G, cell Chen XA stem. Small molecules efficiently reprogram human astroglial cells into functional neurons // Cell stem cell. 2015.

Zhao Yang, Yin Xiaolei, Qin Han, Zhu Fangfang, Liu Haisong, Yang Weifeng, Zhang Qiang, Xiang Chengang, Hou Pingping, Song Zhihua, Liu Yanxia, Yong Jun, Zhang Pengbo, Cai Jun, Liu Meng, Li Honggang, Li Yanqin, Qu Xiuxia, Cui Kai, Zhang Weiqi, Xiang Tingting, Wu Yetao, Zhao Yiding, Liu Chun, Yu Chen, Yuan Kehu, Lou Jinning, Ding Mingxiao, Deng Hongkui. Two supporting factors greatly improve the efficiency of human iPSC generation. // Cell Stem Cell. 2008. 3, 5. 475–9.

Zhong Mei, Niu Wei, Lu Zhi J, Sarov Mihail, Murray John I, Janette Judith, Raha Debasish, Sheaffer Karyn L, Lam Hugo Y, Preston Elicia, Slightham Cindie, Hillier LaDeana W, Brock Trisha, Agarwal Ashish, Auerbach Raymond, Hyman Anthony A, Gerstein Mark, Mango Susan E, Kim Stuart K, Waterston Robert H, Reinke Valerie, Snyder Michael. Genome-wide identification of binding sites defines distinct functions for Caenorhabditis elegans PHA-4/FOXA in development and environmental response. // PLoS Genet. 2010. 6, 2. e1000848.

Zhou Qiao, Brown Juliana, Kanarek Andrew, Rajagopal Jayaraj, Melton Douglas A. In vivo reprogramming of adult pancreatic exocrine cells to beta-cells. // Nature. 2008. 455, 7213. 627–32.

Zhu J, Fukushige T, JD McGhee,, Rothman JH. Reprogramming of early embryonic blastomeres into endodermal progenitors by a Caenorhabditis elegans GATA factor. // Genes Dev. 1998. 12, 24. 3809–14.

Zuryn Steven, Ahier Arnaud, Portoso Manuela, White Esther R, Morin Marie-Charlotte C, Margueron Raphaël, Jarriault Sophie. Transdifferentiation. Sequential histone-modifying activities determine the robustness of transdifferentiation. // Science. 2014. 345, 6198. 826–9.

A. Appendix

Table A.1.: Conjugation attempts in liquid medium in 2 mL Eppendorf tubes combining overnight cultures of donor and recipient at 32 °C. Donor strain SW105(pRK24-kan; *hsp-1*); recipient strain: HT115(*ogt-1*)

Total amount donor and recipient	Ratio D:R	Ratio of dilution	Incubation	Plating 1:10	Plating 1:100	Conjugation
20	1 to 1	1 to 5	1h	no	no	0/8
20	1 to 10	1 to 5	1h	no	no	0/8
21	1 to 3	1 to 5	1h	no	no	0/8
50	5 to 1	1 to 1	1h	no	no	0/8
99	1 to 3	0	1h	yes	no	0/8
100	1 to 1	0	1h	no	no	0/8
100	1 to 1	2 to 1	1h	no	no	0/8
100	5 to 1	0	1h	ND	ND	ND
100	1 to 1	0	1h	yes	no	0/8
100	1 to 10	0	1h	yes	no	0/8
200	1 to 1	0	1h	yes	no	0/8
200	1 to 1	0	1h	yes	no	0/8
200	1 to 10	1 to 1	1h	yes	no	0/8
200	1 to 10	1 to 1	1h	yes	no	0/8
500	1 to 3	1 to 1	1h	yes	yes	0/8
500	3 to 1	1 to 1	1h	yes	yes	0/8
1000	1 to 5	0	1h	yes	yes	0/8
1000	5 to 1	0	1h	yes	yes	0/8
1000	5 to 1	0	1h	ND	ND	ND
200	1 to 1	0	2h	yes	no	0/8
200	1 to 1	0	2h	yes	no	0/8
200	1 to 10	1 to 1	2h	yes	no	0/8
200	1 to 10	1 to 1	2h	yes	no	0/8
1000	5 to 1	0	2h	ND	ND	ND
100	1 to 5	1 to 1	ON	no	no	0/8
200	1 to 10	1 to 1	ON	yes	no	0/8
20	1 to 10	1 to 50	ON	yes	yes	0/8
10	1 to 5	1 to 100	ON	yes	no	0/8
200	10 to 1	1 to 1	ON	no	no	0/8
20	10 to 1	1 to 50	ON	yes	no	0/8
100	5 to 1	1 to 1	ON	no	no	0/8
10	5 to 1	1 to 100	ON	no	no	0/8

Table A.2.: Conjugation in liquid medium in 20 mL Falcon tubes O/N at 32 °C. Donor and recipient cultures in stationary phase. Mixtures were plated on $LB^{Amp+Tet+Cam}$ plates and then streaked out.

Total amount donor and recipient	Ratio D:R	Ratio of added LB medium	Ratio of added LB-AKC medium	Incubation	Plating 1:10	Plating 1:100	Conjugation
100	5 to 1	1 to 10	0	ON	yes	yes	0/8
200	1 to 1	1 to 5	0	ON	no	no	0/8
200	1 to 1	1 to 5	0	ON	yes	yes	0/8
200	1 to 10	1 to 5	0	ON	yes	yes	ND
200	1 to 10	1 to 5	0	ON	yes	yes	0/8
200	1 to 10	1 to 5	0	ON	NA	yes	0/8
200	1 to 5	1 to 5	0	ON	NA	yes	0/8
200	10 to 1	1 to 5	0	ON	NA	no	0/8
200	5 to 1	1 to 5	0	ON	NA	yes	0/8
210	1 to 3	1 to 5	0	ON	NA	yes	ND
210	3 to 1	1 to 5	0	ON	NA	no	0/8
1000	5 to 1	0	0	1h	no	no	0/8
200	1 to 1	0	1 to 5	ON	no	no	0/8
200	1 to 1	0	1 to 5	ON	no	no	0/8
200	1 to 10	0	1 to 5	ON	yes	yes	0/8
200	1 to 10	0	1 to 5	ON	no	no	0/8
100	5 to 1	0	1 to 10	ON	no	no	0/8

Table A.3.: Conjugation of SW105 (pRK24-kan) with HT115 (*ogt-1*) on solid LB agar plates, incubated O/N at 32 °C. Mixture resulted in colonies. Donor and recipient plasmid detected by PCR.

Total amount donor and recipient [µL]	Ratio D:R	Incubation	Plating 1:10	Plating 1:100	Conjugation	PCR confirmation donor	PCR confirmation recipient
1000	5 to 1	ON	yes	yes	8/8	8/8	8/8

Table A.4.: Conjugation in liquid medium. Donor SW105 (pRK24-kan; *hsp-1*) and recipient HT115 (*ogt-1*) were grown until OD_{600} = 0.5. and mixed in 1.5 mL Eppendorf tubes, diluted with either LB or SOC medium, incubated at 32 °C for 2 to 8h and subsequently plated and streaked out on $LB^{Amp+Tet+Cam}$ plates.

Total amount donor and recipient [µL]	Ratio D:R	Ratio dilution with LB [µL]	Ratio dilution with SOC [µL]	Incu-bation [hours]	Pla-ting 1:10	Con-jugation
50	1 to 5	1:1	0	2h	no	0/8
50	5 to 1	1:1	0	2h	no	0/8
50	1 to 10	1:1	0	2h	yes	0/8
50	10 to 1	1:1	0	2h	no	0/8
50	1 to 5	0	1:1	2h	yes	0/8
50	5 to 1	0	1:1	2h	no	0/8
50	1 to 10	0	1:1	2h	yes	0/8
50	10 to 1	0	1:1	2h	no	0/8
50	1 to 5	1:1	0	4h	yes	0/8
50	5 to 1	1:1	0	4h	no	0/8
50	1 to 10	1:1	0	4h	yes	0/8
50	10 to 1	1:1	0	4h	no	0/8
50	1 to 5	0	1:1	4h	yes	0/8
50	5 to 1	0	1:1	4h	no	0/8
50	1 to 10	0	1:1	4h	yes	0/8
50	10 to 1	0	1:1	4h	no	0/8
50	1 to 5	1:1	0	6h	yes	0/8
50	5 to 1	1:1	0	6h	no	0/8
50	1 to 10	1:1	0	6h	yes	0/8
50	10 to 1	1:1	0	6h	no	0/8
50	1 to 5	0	1:1	6h	yes	0/8
50	5 to 1	0	1:1	6h	no	0/8
50	1 to 10	0	1:1	6h	yes	0/8
50	10 to 1	0	1:1	6h	no	0/8
50	1 to 5	1:1	0	8h	yes	0/8
50	5 to 1	1:1	0	8h	yes	0/8
50	1 to 10	1:1	0	8h	yes	0/8
50	10 to 1	1:1	0	8h	no	0/8
50	1 to 5	0	1:1	8h	yes	0/8
50	5 to 1	0	1:1	8h	yes	0/8
50	1 to 10	0	1:1	8h	yes	0/8
50	10 to 1	0	1:1	8h	no	0/8

Table A.5.: Conjugation in liquid medium. Donor SW105 (pRK24-kan; *hsp-1*) and recipient HT115 (*ogt-1*) were grown until $OD_{600} = 0.5$. and mixed in 1.5 mL Eppendorf tubes, diluted with either LB or SOC medium, incubated at 32 °C for 2 to 8h and subsequently plated and streaked out on $LB^{Amp+Tet+Cam}$ plates.

Total amount donor and recipient [µL]	Ratio D:R	Incubation [hours]	Plating 1:10	Conjugation
100	1 to 5	2h	yes	0/8
100	5 to 1	2h	no	0/8
100	1 to 10	2h	no	0/8
100	10 to 1	2h	no	0/8
100	1 to 1	2h	no	0/8
100	1 to 5	4h	yes	0/8
100	5 to 1	4h	no	0/8
100	1 to 10	4h	yes	0/8
100	10 to 1	4h	no	0/8
100	1 to 1	4h	yes	0/8
100	1 to 5	6h	yes	0/8
100	5 to 1	6h	no	0/8
100	1 to 10	6h	yes	0/8
100	10 to 1	6h	no	0/8
100	1 to 1	6h	yes	0/8
100	1 to 5	8h	yes	0/8
100	5 to 1	8h	yes	0/8
100	1 to 10	8h	yes	0/8
100	10 to 1	8h	yes	0/8
100	1 to 1	8h	yes	0/8

Table A.6.: Donor and recipient culture were grown until late exponential phase and mixted on LB agar plate, incubated at 32 °C O/N. Subsequently the mixture was plated and resulting colonies were streaked out.

Donor	Donor OD600	Recipient	Recipient OD600	Ratio donor to recipient	Incubation time	Colonies 1:10	colonies 1:100	streak out of single colonies
SW105	0.91	*ogt-1*	0.84	1:1	on	1000	20	1/8
						1000	5	0/8
						1000	9	0/8
						>1000	500	0/8
						OG	500	2/8
						OG	1000	1/8

Table A.7.: Conjugation on solid LB agar using two different host strains, SW105 and HT115, that are mixed with *ogt-1*, incubated at 32 °C O/N and plated on $LB^{Amp+Tet+Cam}$ plates. Donor and recipient strain were grown until exponential phase.

Donor	Donor OD600	Recipient	Recipient OD600	Ratio donor to recipient	added LB to conjugate volume ratio	colonies 1:100	streak out of single colonies
SW105	0.5	*ogt-1*	0.75	1:1	0	>20	0/8
					2:1	>100	0/8
					1:1	>100	0/8
					1:2	>500	0/8
H1	0.64	*ogt-1*	0.75	1:1	0	10	-
					2:1	12	-
					1:1	50	3/8
					1:2	50	0/8

Table A.8.: Conjugation of SW105 with HT115 on solid LB agar plates, incubated at 32 °C O/N, plated on $LB^{Amp+Tet+Cam}$ plates. Mixtures were diluted with LB medium in increasing amounts.

Donor	Donor OD600	Recipient	Recipient OD600	Ratio donor to recipient	added LB	colonies 1:100	streak out of single colonies
SW105	0.53	*ogt-1*	0.83	1:1	1:1	30	0/8
					1:2	50	1/8
					1:3	50	0/8
					1:4	50	0/8
					1:5	50	1/8

Table A.9.: Conjugation on solid LB agar of SW105(pRK24-kan; *hsp-1*) with HT115 (*ogt-1*), incubated at 32 °C O/N or for 1h, then plated on $LB^{Amp+Tet+Cam}$ plates.

Donor	Donor OD600	Recipient	Recipient OD600	Ratio donor to recipient	added LB	Incubation time	colonies 1:10	colonies 1:100	streak out of single colonies
SW105	0.86	*ogt-1*	1.15	1:1	1:2	on	ND	0	0/0
					1:3			1000	0/8
					1:5			30	1/8
					1:8			100	0/8
					1:10			1000	0/8
SW105	0.97	*ogt-1*	1.15	1:1	1:1	1h	0	ND	0/0
					1:5		0		0/0
					1:8		0		0/0
					1:10		0		0/0

Table A.10.: Conjugation of SW105 (pRK24-kan; *hsp-1*) with HT115(*ogt-1*) at different ratios, testing whether an overabundance of donor or recipient increases the conjugation success rate. Incubation O/N at 32 °C, streaked on $LB^{Amp+Tet+Cam}$ plates.

Donor	Donor OD600	Recipient	Recipient OD600	Ratio donor to recipient	colonies 1:100	colonies 1:1000	streak out of single colonies
SW105	0.92	*ogt-1*	1.01	10:1	0	0	0/8
				1:10	50	0	0/8
				5:1	2	0	2/2
				1:5	50	8	0/8

Table A.11.: Conjugation of SW105 (pRK24-kan; *hsp-1*) with HT115(*ogt-1*) on LB agar plates containing either Ampicillin, Kanamycin, Chloramphenicol or without antibiotic. Donor and recipient were combined at a ratio of 5:1 and incubated O/N at 32 °C. MIxtures were streaked on $LB^{Amp+Tet+Cam}$ plates.

Donor	Donor OD600	Recipient	Recipient OD600	Ratio donor to recipient	Ratio added LB	Medium	colonies 1:1000	streak out of single colonies
					1:1	LB agar	50	0/8
					1:2	LB agar	100	1/16
SW105	0.74	*ogt-1*	1.01	5:1		LB Amp	0	0/0
					1:1	1/2		
						LB Kan	0	0/0
						1/2		
						LB Chl	0	0/0
						1/2		
					1:1	LB agar	0	0/0
					1:2	LB agar	20	1/8
H1	0.96	*ogt-1*	1.01	5:1		LB Amp	20	0/8
					1:1	1/2		
						LB Kan	0	0/0
						1/2		
						LB Chl	0	0/0
						1/2		

Table A.12.: Conjugation on LB agar plates incubated O/N at 37°C. Subsequent antibiotic selection on $LB^{Amp+Tet+Cam}$. Increase of dilution does not yield a better conjugation success rate.

Donor	Donor OD600	Recipient	Recipient OD600	Ratio donor to recipient	Ratio added LB	colonies 1:1000	streak out of single colonies
					1:2	0	0/8
SW105	0.93	*ogt-1*	0.95	5:1	1:5	0	0/8
					1:10	2	0/8
					1:2	0	0/8
H1	0.75	*ogt-1*	0.95	5:1	1:5	1	1/1
					1:10	8	0/8

Table A.13.: Comparative conjugation of using pRK24 (unmodified) in "original" donor strain, in SW105 as well as pRK24-kan after recombineering. Incubation for 1h or O/N at 32°C. Plating and subsequent streak out on $LB^{Amp+Tet+Chl}$ plates.

Donor	Donor OD600	Recipient	Recipient OD600	Ratio donor to recipient	Incubation time	streak out of single colonies
pRK24 (original)	0.96	sg41	0.84	5:1	1h	8/8
					on	8/8
SW105 (pRK24-amp)	0.76	sg41	0.84	5:1	1h	8/8
					on	8/8
SW105(pRK24-kan)	0.81	ogt-1	1.13	5:1	1h	ND
					on	8/8

Table A.14.: Conjugation of newly generated donor strain EPI300 (pRK24-kan; *hsp-1*) at different growth phases. Conjuguation 1h or O/N at 37ÂřC on LB agar plates. Antibiotic selection on $LB^{Amp+Tet+Cam}$ plates.

Donor		Donor OD600	Recipient	Recipient OD600	Ratio donor to recipient	Incubation time	streak out of single colonies
EPI300 dBT462)	(pRK24-kan;	0.83	*ogt-1*	0.7	5:1	on	8/8
EPI300 dBT462)	(pRK24-kan;	1.2	*ogt-1*	0.7	5:1	on	8/8
EPI300 dBT462)	(pRK24-kan;	0.94	*ogt-1*	1.25	5:1	1h	1/8
EPI300 dBT462)	(pRK24-kan;	0.94	*ogt-1*	1.25	5:1	on	8/8

Table A.15.: Conjugation of overnight cultures in exponential phase, incubated for 1h at 37°C, plated and subsequently streaked out on $LB^{Amp+Tet+Cam}$.

Donor	Donor OD600	Recipient	Recipient OD600	Ratio Donor to Recipient	Incubation time	streak out of single colonies	PCR confirmation donor	PCR confirmation recipient
hsp-1	2.03	*smuv-1*	3.42	5:1	1 h	8/8	8/8	8/8
		ogt-1	3.39					
hsp-1	1.33	ogt-1	1.87	5:1	1 h	16/16	NA	3/3
		smuv-1	2.4					
		smuv-2	2.48					
		wdr-5.1	2.09					

Table A.16.: Conjugation of bacterial cultures either in exponential or in stationary growth phase cultures, incubated for 1h at 37°C, plated and subsequently streaked out on $LB^{Amp+Tet+Cam}$.

Donor	Donor OD600	Recipient	Recipient OD600	Ratio Donor to Recipient	Incubation time	streak out of single colonies	PCR confirmation donor	PCR confirmation recipient
lin-53	0.6 1.2	*utx-1*	0.57 1.73	5:1	1 h	8/8 8/8	4/4 4/4	4/4 4/4

Table A.17.: Conjugation in 96-well plates of donor EPI300(pRK24-kan; *lin-53*) with recipient HT115(*ogt-1*) incubated for 1h at 37 °C.

Row	Donor	OD600 donor	Recipient	OD600 recipient	Volume donor : recipient [µL]	LB-Carb-Tet-Chl plate streak out
A C	*lin-53*	4.1	*utx-1*	3.1	20:5	2/12 4/12
F H	*lin-53*	14.1	*utx-1*	3.1	5:5	11/12 12/12

Affidavit

Erklärung über die selbstständige Abfassung meiner Dissertation

Hiermit erkläre ich, Marlon Kazmierczak, Matrikel-Nr: 522580, dass ich die vorliegende Dissertation selbstständig und ohne Benutzung anderer als der angegebenen Hilfsmittel angefertigt habe.
Die aus fremden Quellen direkt oder indirekt übernommenen Gedanken sind als solche kenntlich gemacht.
Die Dissertation wurde bisher in gleicher oder ähnlicher Form keiner anderen Prüfungsbehörde vorgelegt oder veröffentlicht.

Berlin, den 18.07.2018

Acknowledgments

I would like to thank all people that helped me with my dissertation.

First of all I would like to thank Dr. Baris Tursun for giving me this interesting topic, for the excellent professional support, as well as providing great ideas for solving many issues in the lab and writing the thesis.
I also would like to thank Prof. Dr. Thomas Sommer, Prof. Dr. Ann Ehrenhofer-Murray, Dr. Baris Tursun, Prof. Dr. Ana Pombo, and Prof. Dr. Uwe Ohler for being part of my PhD committee.
I would like to thank my whole lab for the great support, the atmosphere, and occasional laughter.
Thanks also to Dr. Anna Reid, Nida ul Fatima, Samuel Katz, and Valentina Grigorieva for proof-reading and helpful suggestions while writing the thesis.
Ich möchte mich bei meiner Familie und meinen Freunden für die Unterstützung während der Doktorarbeit bedanken.